Spring 1-1-2015

Aerosol Health Impact Source Attribution Studies with the CMAQ Adjoint Air Quality Model

Matthew Douglas Turner
University of Colorado at Boulder, mattdturner@gmail.com

Aerosol Health Impact Source Attribution Studies with the CMAQ Adjoint Air Quality Model

by

M. D. Turner

B.S., Drexel University, 2009

M.S., Drexel University, 2009

A thesis submitted to the

Faculty of the Graduate School of the

University of Colorado in partial fulfillment

of the requirements for the degree of

Doctor of Philosophy

Department of Mechanical Engineering

2015

This thesis entitled:
Aerosol Health Impact Source Attribution Studies with the CMAQ Adjoint Air Quality Model
written by M. D. Turner
has been approved for the Department of Mechanical Engineering

_____

Prof. Daven Ker Henze

_____

Prof. Jana Milford

Date _____

The final copy of this thesis has been examined by the signatories, and we find that both the content and the form meet acceptable presentation standards of scholarly work in the above mentioned discipline.

Turner, M. D. (Ph.D., Air Quality Modeling)

Aerosol Health Impact Source Attribution Studies with the CMAQ Adjoint Air Quality Model

Thesis directed by Prof. Daven Ker Henze

Fine particulate matter ($PM_{2.5}$) is an air pollutant consisting of a mixture of solid and liquid particles suspended in the atmosphere. Knowledge of the sources and distributions of $PM_{2.5}$ is important for many reasons, two of which are that $PM_{2.5}$ has an adverse effect on human health and also an effect on climate change. Recent studies have suggested that health benefits resulting from a unit decrease in black carbon (BC) are four to nine times larger than benefits resulting from an equivalent change in $PM_{2.5}$ mass. The goal of this thesis is to quantify the role of emissions from different sectors and different locations in governing the total health impacts, risk, and maximum individual risk of exposure to BC both nationally and regionally in the US. We develop and use the CMAQ adjoint model to quantify the role of emissions from all modeled sectors, times, and locations on premature deaths attributed to exposure to BC. From a national analysis, we find that damages resulting from anthropogenic emissions of BC are strongly correlated with population and premature death. However, we find little correlation between damages and emission magnitude, suggesting that controls on the largest emissions may not be the most efficient means of reducing damages resulting from BC emissions. Rather, the best proxy for locations with damaging BC emissions is locations where premature deaths occur. Onroad diesel and nonroad vehicle emissions are the largest contributors to premature deaths attributed to exposure to BC, while onroad gasoline emissions cause the highest deaths per amount emitted. Additionally, emissions in fall and winter contribute to more premature deaths (and more per amount emitted) than emissions in spring and summer. From a regional analysis, we find that emissions from outside each of six urban areas account for 7% to 27% of the premature deaths attributed

to exposure to BC within the region. Within the region encompassing New York City and Philadelphia, reductions in emissions from large industrial combustion sources that are not classified as EGUs (i.e., non-EGU) are estimated to have up to triple the benefits per unit emission of reductions to onroad diesel sectors, and provide similar benefits per unit of reduced emission to that of onroad gasoline emissions in the region. While a majority of vehicle emission controls that regulate PM focus on diesel emissions, our analysis shows the most efficient target for stricter controls is actually onroad gasoline emissions. From an analysis of the health impacts of BC emissions on specific demographic populations, we find that emissions in the southern half of the US tend to disproportionally affect persons with a below high school education and persons below 50% of the poverty level. Analysis of national risk (independent of population and mortality rates) shows that the largest risks are associated with drier climates, due to the increased atmospheric lifetime resulting from less wet removal of aerosols. Lastly, analysis of the impacts of BC emissions on maximum individual risk shows that contributions to maximum individual risk are weakly to strongly correlated with emissions (R^2 ranging from 0.23 in the San Joaquin Valley to 0.93 in the Dallas region). Overall, this thesis shows the value of high-resolution, adjoint-based source attribution studies for determining the locations, seasons, and sectors that have the greatest estimated impact on human health in air quality models.

Acknowledgements

The works presented in this paper were funded through NASA Applied Sciences Program under grant number NNX09AN77G. In addition to the funding, this work would not have been possible without the help and support of many people. I would first like to thank my research advisors, Professor Daven Henze, and Professor Amir Hakami for their support and guidance throughout the entire project, especially during the adjoint development. I would also like to thank Professors Jana Milford, Michael Hannigan, and Peter Hamlington for being on my defense committee. I also thank all of the collaborators on the adjoint development project, including but not limited to: Shunliu Zhao, Jaroslav Resler, Gregory Carmichael, Charles Stanier, Jaemeen Baek, Adrian Sandu, Armistead Russell, Athanasios Nenes, Gill-Ran Jeong, Shannon Capps, Rob Pinder, Sergey Napelenok, Jesse Bash, Peter Percell, Tianfeng Chai, Havala Pye, and Daewon Byun. Finally, I would like to thank my wife Megan for her understanding, encouragement, and support throughout my PhD.

Contents

Tables

Table

Figures

Figure

Chapter 1

Introduction

1.1 Motivation and Objectives

Fine particulate matter ($PM_{2.5}$) is an air pollutant consisting of a suspended mixture of solid and liquid particles that are less than 2.5 μm in diameter. Knowledge of the sources and distributions of $PM_{2.5}$ is important for many reasons, two of which are that $PM_{2.5}$ has an adverse effect on human health (e.g., Krewski et al. [2009]; WHO [2006]; Pope et al. [2002]; Katanoda et al. [2011]; Lepeule et al. [2012]; Kazuhiko et al. [2011]; Puett et al. [2009]; Gauderman et al. [2002]; Cohen et al. [2004]), and $PM_{2.5}$ also has an effect on climate change (e.g., Bauer and Menon [2012]; Bond [2007]; Jacobson [2010]; Bond et al. [2013]; Anenberg et al. [2012]; Shindell et al. [2012]). Since its inception in 1970, the US Environmental Protection Agency (EPA) has been tasked with the protection of human health and the environment. Title I of the Clean Air Act dictates that the EPA is in charge of setting National Ambient Air Quality Standards (NAAQS) for air pollutants that may endanger public health or welfare. In addition to the development of NAAQS, the EPA evaluates the cost and effectiveness of emissions control policies and monitors NAAQS exceedences. One major aspect of this process is the use of air quality models to estimate current and future distributions of $PM_{2.5}$.

Many atmospheric chemical transport models (CTM) can simulate the distribution and fate of aerosols. However, these models contain considerable uncertainty. There are several different methods to decrease uncertainty in the models, such as developing a better

understanding of physical processes, using data assimilation techniques to constrain the models with observations [Bergamaschi et al., 2009; Kurokawa et al., 2009; Zhu et al., 2013; Chai et al., 2009; Henze et al., 2009], and using an ensemble of models to obtain robust results [Mallet and Sportisse, 2006; Stevenson et al., 2006; van Noije et al., 2006; Koch et al., 2009]. These approaches allow the use of air quality models for understanding source-receptor relationships. Quantifying the role of emissions from different sectors and different locations in governing the total health impacts is critical towards developing effective control strategies.

This project focuses on elucidating the sources of aerosols that have an adverse human health impact through the development and application of adjoint sensitivity modeling. This thesis addresses the following research objectives:

(1) Develop the adjoint of aerosol microphysics for the CMAQ adjoint model.

(2) Use adjoint sensitivity analysis to attribute both national and regional-scale health impacts to emissions from specific locations, seasons, and sectors to facilitate more effective air quality control strategies.

(3) Investigate potential disparities of health impacts for different population demographics.

(4) Examine the impacts of emissions on maximum individual risk in the US.

This project results in the first adjoint air quality model that includes an adjoint of aerosol size distribution, improving the overall utility of the CMAQ model. Accounting for the particle size distribution is important for both health and climate concerns, as it is associated with the particles' origin, their transport in the atmosphere, and the degree to which they are inhaled into the respiratory system [WHO, 2006].

This project begins with the development of an adjoint model of the CMAQ chemical transport model, which provides an efficient means of performing sensitivity analysis. As

opposed to forward sensitivity techniques, where sensitivities of all state variables with respect to a few parameters (inputs) are calculated, adjoint sensitivity analysis calculates the sensitivity of a single model response metric with respect to all sources [Sandu et al., 2005a]. For example, an adjoint model can provide sensitivities of premature deaths (through the use of the concentration response functions) with respect to emissions at a highly resolved spatial, temporal, and sectoral level. This tool can be used to determine the sensitivity of premature death in a region with respect to emissions throughout the modeled domain.

Here we present the background, model development, and initial applications for this thesis. Section 1.2 reviews background information on the health and climate effects of fine particulate matter. In Sections 1.2.7 and 1.2.8, we describe the CMAQ air quality model, as well as provide an introduction to adjoint models in Section 1.2.9. Exposure to $PM_{2.5}$ in ambient air has been shown to be a cause of various adverse health effects, such as cardiopulmonary disease and lung cancer [Krewski et al., 2009; WHO, 2006; Pope et al., 2002; Katanoda et al., 2011; Lepeule et al., 2012; Kazuhiko et al., 2011; Puett et al., 2009; Gauderman et al., 2002; Cohen et al., 2004], leading to an estimated 130,000 premature deaths in 2005 in the US alone [Fann et al., 2012b]. Some studies have found associations of increased premature deaths and morbidity to concentrations of black carbon (BC) [Suh and Zanobetti, 2010; Adar et al., 2007; Peng et al., 2009; WHO, 2012; Power et al., 2011; Wilker et al., 2013; Grahame et al., 2014]. We thus consider applications of the CMAQ adjoint that quantify the impact of emissions in each and every grid cell on the health burden attributed to BC exposure from both national (Chapter 2) and regional (Chapter 3) studies, as well as the impacts on maximum individual risk and specific subsets of the population (Chapter 4). Lastly, Chapter 5 discusses some conclusions for the current work.

1.2 Background

In this section we give an overview of particulate matter and its effect on climate and human health. Section 1.2.1 discusses size distributions of particulate matter in addition to

some of the major sources of these particles. In section 1.2.2 we present a brief overview of the climate effects (direct, indirect, and semi-direct) of $PM_{2.5}$. Sections 1.2.3 and 1.2.4 discuss the short-term and long-term health effects of exposure to $PM_{2.5}$, in addition to discussing the national health burden attributed to exposure to $PM_{2.5}$. Section 1.2.5 continues the discussion of health effects by considering the monetary damage values for different $PM_{2.5}$ precursor emissions. In section 1.2.6, we present information about how emissions are calculated, in addition to some of the uncertainties in the development of emission inventories.

1.2.1 Particulate Matter

The size distribution of PM is divided into three main modes: coarse, accumulation, and nucleation. The coarse mode consists of particles with an aerodynamic diameter between 2.5 μm and 10 μm ($PM_{2.5-10}$). Particles in the coarse mode are mainly produced by the mechanical break-up of larger particles, have a shorter lifetime in the atmosphere than smaller particles, and usually settle back to the surface due to gravitational forces within minutes to hours. Examples of coarse mode particles are dust, sea salt, and plant and insect parts.

The accumulation mode consists of particles with an aerodynamic diameter between 0.1 μm and 2.5 μm ($PM_{0.1-2.5}$). Particles in the accumulation mode are usually formed through coagulation from particles in the nucleation mode. Particles in this mode have the longest lifetime in the atmosphere (days to weeks), and they do not typically coagulate to the coarse mode.

The nucleation mode consists of particles with an aerodynamic diameter less than 0.1 μm ($PM_{0.1}$). Particles in the nucleation mode can be directly emitted into the atmosphere, formed from condensation of vapors, and formed from nucleation of atmospheric species. Nucleation mode particles do not settle significantly by gravity. However, particles in this mode are short-lived in the atmosphere and usually coagulate to the accumulation mode. The combination of particles in the accumulation mode and nucleation mode is often referred

to as fine PM ($PM_{2.5}$). Ammonium sulfate and ammonium nitrate combine to account for about half of the average mass concentration of $PM_{2.5}$ in the US, with the rest of the mass concentration coming from carbonaceous aerosols, sodium, chloride, and water [Seinfeld and Pandis, 2006].

1.2.2 Effects of PM on Climate Change

Aerosols have direct, indirect, and semi-direct effects on radiative forcing. Radiative forcing is a perturbation in the radiative energy budget of the Earth caused by an external source [Myhre et al., 2013]. Aerosols have a direct radiative forcing because they both scatter and absorb solar and infrared radiation in the atmosphere [Myhre et al., 2013]. While aerosols in general can cause both a "cooling" and a "warming" effect in the atmosphere, the overall combination of both direct and indirect effects results in the cooling of the atmosphere [Myhre et al., 2013].

Indirect Effects Indirect radiative forcing from aerosols is caused by changes in cloud properties. Aerosols alter the efficiency at which liquid water, ice and mixed-phase clouds form and precipitate, which alters the properties of the clouds [Twomey, 1974]. There is a set amount of water available for clouds. The water can form large droplets within the clouds, which causes precipitation (a major removal mechanism for aerosols). The presence of cloud condensation nuclei in the atmosphere causes the water to condense onto the particles. This results in more, but smaller droplets in the clouds, which increases the cloud albedo [Twomey, 1974]. In addition to increasing the albedo, this effect tends to decrease the chance of precipitation. If precipitation is suppressed, this results in excess water remaining in the atmosphere [Albrecht, 1989].

Semi-Direct Effects While the indirect effects occur when aerosols alter cloud microphysics, absorbing aerosols (AA) near clouds have been thought to cause changes in cloud cover (semi-direct effect) [Hansen et al., 1997]. This is caused by the AA within or near clouds increasing the temperature around the clouds, promoting cloud evaporation.

A decrease in cloud cover increases the warming impacts of AA, due to the decrease in the amount of solar radiation that is reflected upward by the clouds (cloud albedo effect). Similar studies to Hansen et al. [1997] have shown that this semi-direct effect is enhanced due to a low-cloud feedback loop [Jacobson, 2002] in which the cloud loss increases the capacity for AA absorption.

Arctic Climate Effects In addition to the effects of atmospheric aerosol on radiative forcing, AA that is deposited on snow and ice in the arctic has a substantial effect on climate. The high contrast in albedo between BC and snow or ice on which it has deposited results in enhanced absorption of sunlight, which heats the Arctic atmosphere and leads to increased melting of snow and ice [Hansen, 2005]. The global mean surface temperature warming resulting from the radiative forcing of BC on snow is approximately three times more than an equal forcing of CO_2 [Flanner et al., 2007].

1.2.3 Health Effects of $PM_{2.5}$

Exposure to $PM_{2.5}$ in ambient air has been shown to be a cause of various adverse health effects, both short-term and long-term, as well as premature death. In 2009 the US EPA released the Integrated Science Assessment for Particulate Matter (PM ISA), which included a literature review of articles that analyzed the health impacts of exposure to PM [US EPA, 2009].

Short-Term Exposure In the 2009 PM ISA, articles discussing the effects of short-term exposure to $PM_{2.5}$ were analyzed, and a causal determination was made for various health effects. It was determined that short-term exposure to $PM_{2.5}$ has a causal relationship with cardiovascular effects and premature death, while short-term exposure to $PM_{2.5}$ is likely to have a causal relationship with respiratory effects.

Increases in $PM_{2.5}$ and sulfate have been shown to increase mortality in exposed populations, mainly owing to an increase in cardiovascular premature death. The Health Effects Institute (HEI) performed an extension of a previous American Cancer Society (ACS) study

and discovered significant increases in the relative risk of cardiopulmonary and lung cancer deaths, as well as deaths from all causes resulting from exposure to $PM_{2.5}$ [WHO, 2006].

Long-Term Exposure Long-term exposure to $PM_{2.5}$ has been shown to have a consistent association with an increased risk of cardiovascular premature death. For example, in an extended analysis of the Harvard Six Cities cohort that included an additional 11 years of follow-up and $PM_{2.5}$ data, Lepeule et al. [2012] found that a 10 $\mu g/m^3$ increase in $PM_{2.5}$ resulted in a 14% increased risk of all-cause death (95% CI: 7% to 22%), and a 26% increase in cardiovascular death (95% CI: 14% to 40%). Studies also suggest that long-term exposure to $PM_{2.5}$ is most strongly associated with premature death due to ischemic heart disease, dysrhythmias, heart failure, and cardiac arrest. For these causes of death, an increased $PM_{2.5}$ exposure of 10 $\mu g/m^3$ was associated with an 8-18% increase in death [Pope et al., 2004].

Component-Specific Health Effects Some studies have started focusing on species-specific $PM_{2.5}$ analyses for health impacts. One such study by Bell et al. [2009] analyzed source-specific effects of PM species on both CVD and respiratory diseases. The study found that BC and vanadium concentration increases resulted in the largest increase in health effect estimates for both CVD and respiratory effects. Bell et al. [2009] showed a 25.8% (95% CI: 4.4 to 47.2) increase in the risk estimate for cardiovascular disease per interquartile range increase in the fraction of BC to $PM_{2.5}$ mass. An increase in interquartile range in the fraction of BC to $PM_{2.5}$ mass was shown to cause a 511% (95% CI: 80.7 to 941) increase in the risk estimate for respiratory disease. Janssen et al. [2011] performed a review of four cohort studies that measured exposure to BC. They calculated a pooled effect relative risk value of 1.007 (95% CI: 1.004 to 1.009) for $PM_{2.5}$, and 1.05 (95% CI: 1.04 1.09) for BC. Grahame et al. [2014] performed a review of the health effects of exposure to BC and suggested that there is a causal relationship between exposure to BC and premature death. Such findings suggest that consideration of BC-related health impacts may be of importance.

1.2.4 Health Burden of Pollutant Exposure

As previously mentioned, exposure to ground-level $PM_{2.5}$ is associated with increased risk of premature death and morbidity. Many studies have estimated the public health burden attributed to exposure to $PM_{2.5}$. Cohen et al. [2005] used economic, meteorologic, and demographic data, as well as available $PM_{2.5}$ measurements in 304 cities, to estimate that 799,000 premature deaths globally were attributed to exposure to urban outdoor air pollution. Anenberg et al. [2010] used simulated global concentrations of $PM_{2.5}$ to estimate the global burden of premature death attributed to exposure to $PM_{2.5}$ from anthropogenic emissions. They estimated that anthropogenic $PM_{2.5}$ was associated with 3,721,000 global premature deaths annually. Of those premature deaths, 141,000 cardiopulmonary and lung cancer deaths occurred in North America. Fann et al. [2012b] used the CMAQ model in conjunction with observed concentration data to create spatially resolved annual mean $PM_{2.5}$ concentrations over the continental United States. Using this information, as well as the US EPA's BenMAP software, they estimated the total public health burden associated with $PM_{2.5}$ exposure for various risk estimates. They estimated that 130,000 to 320,000 (depending on the risk estimate used) premature deaths were attributed to $PM_{2.5}$ exposure. They also estimated an array of morbidity impacts, such as 62,000 hospital admissions related to cardiovascular problems. Caiazzo et al. [2013] used the CMAQ model to assess the health impacts of emission sectors in the US. They estimated 200,400 premature deaths due to exposure to $PM_{2.5}$ in the US in 2005 were attributed to combustion emissions, with EGUs being the largest contributor (52,200 premature deaths).

A concern with model-based estimates of exposure is model resolution [Li et al., 2015; Punger and West, 2013; Pisoni et al., 2010]. Punger and West [2013] analyzed the effect of grid resolution on estimates of the burden of $PM_{2.5}$ on premature death in the US. They found that coarse grid resolutions (>250 km) produce premature death estimates that are 30-40% lower than the estimates at 12-km resolution. They also found that simulations

performed at 36-km resolution resulted in premature death burdens 11% higher than at 12-km resolution. Additionally, Punger and West [2013] and Li et al. [2015] both showed that changes in model resolution have different impacts for exposure to different pollutants, with the greatest effect on health impact estimates related to exposure to BC.

1.2.5 Damages of Pollutant Exposure

When calculating damages associated with pollutant exposure, a value of a statistical life (VSL) is used to convert from premature deaths to a monetary value. Muller and Mendelsohn [2007] used an integrated assessment model to estimate the marginal damages associated with emitting an additional ton of pollution from approximately 10,000 sources in the US. They estimated that $PM_{2.5}$ emissions account for $17.4 billion of gross annual damages (GAD) per year. Muller et al. [2011] again used an integrated assessment model to estimate the gross damages for each industry in the US. They estimated that a total of $184 billion of gross external damages (GED). For both of these studies a fixed damage value was used throughout the domain.

Fann et al. [2009] examined how the location and source of an emission reduction influence the magnitude of the benefit per ton ($/ton) estimate for $PM_{2.5}$ reductions. Using a reduced-form air quality model, they modeled emission control strategies for each of nine urban areas. They showed that the $/ton for some pollutants are much higher than others. They also showed a large variability in $/ton estimates for the same pollutant across various sources and locations. Fann et al. [2012a] used the CAMx source apportionment photochemical model to estimate $PM_{2.5}$ benefit per ton estimates for seventeen sectors across the continental US. They estimated that the benefit per ton of reducing directly emitted $PM_{2.5}$ is an order of magnitude larger than reducing precursor emissions.

Additionally, in 2011 the US EPA released a report analyzing the benefits and costs of the Clean Air Act from 1990 to 2020 [US EPA, 2011]. They estimated that the efforts to meet the 1990 Clean Air Act Amendment are projected to cost about $65 billion annually.

However, the value of the improvements resulting from these efforts are estimated to reach approximately $2 trillion, with a majority of the benefits coming from premature death reduction (approximately $1.8 trillion of the $2 trillion total benefits). To achieve the highest benefit to cost ratio, it is necessary to determine the emissions to which stricter control strategies would yield the largest reduction in premature deaths associated with pollutant exposure.

1.2.6 Emissions and Uncertainty

When using atmospheric chemical transport models to evaluate air quality and climate issues, a vast array of input information is required, including emission profiles. However, emission inventories are subject to substantial levels of uncertainty, which limits the confidence that can be placed in results that are based on them. In the US, the National Emission Inventory (NEI) is a compilation of emission profiles from state, local, and tribal air agencies, as well as the emission information from EPA emission programs. NEI emission inventories include criteria air pollutants (CAPs), pollutants related to the implementation of NAAQS, as well as hazardous air pollutants (HAPs) that are associated with EPA's Air Toxics Program. CAPs include lead, carbon monoxide, nitrogen oxides, volatile organic compounds, sulfur dioxide, ammonia, and particulate matter. HAPs include 187 other pollutants, such as mercury, hydrochloric acid, and heavy metals. The emission sources are divided into categories: stationary sources are "point" or "nonpoint", mobile sources are either onroad (cars and trucks driven on roads) or non-road (locomotives, aircraft, marine, etc.).

Emissions for various sectors at various locations are calculated based on emission factors. An emission factor is a value that attempts to relate the quantity of a pollutant released to the activity that releases the pollutant. Emission factors are generally expressed as a weight of pollutant divided by a unit weight, volume, distance, or duration of the activity that is emitting the pollutant. In most cases, the emission factors are simply an average of

all available emission profile data. Emissions are then calculated by

$$E = A * EF * (1 - \frac{ER}{100}), \tag{1.1}$$

where E is the calculated emissions, A is the activity rate, EF is the emission factor, and ER is the overall emission reduction efficiency.

Power plant emission profiles tend to have very low uncertainty, with uncertainty estimates below 5% [Pouliot et al., 2012]. This is a result of the availability of a large number of detailed, hourly emission data that are a product of the continuous emissions monitoring system (CEMS). Mobile source inventories contain significant uncertainties with regard to the magnitude of CO and NO_x emissions, with uncertainty estimates of approximately 30% [Fujita et al., 2012]. Much of the mobile-source tailpipe emissions data are typically estimated based on procedures that are of a limited duration. The short-term tests may not accurately represent the emissions over longer time periods. Also, the effects of emission spikes that result from variability in engine loads are not accurately represented [Hallmark et al., 2002].

Emissions from nonpoint stationary sources (fugitive emissions, open biomass burning, etc.) have much larger uncertainties, with uncertainty estimates greater than 100% [He et al., 2011]. There are many causes for the high level of uncertainty in nonpoint stationary sources. The individual sources may be small and widely dispersed, or in the case of fugitive emissions, they may result from unknown sources. Additionally, in cases such as agricultural-related ammonia, biomass burning, and biogenic emissions, emissions may be from processes that contain inherent variability. For example, considerable uncertainties remain in determining the burned area for biomass burning. Also, many fires cannot be observed during the flaming stage due to obstruction in the satellite view (such as from cloud coverage) [Schroeder et al., 2008]. The use of observations to constrain emissions is thus an important, developing topic for aerosol modeling.

1.2.7 CMAQ Model

The air quality model currently used by the EPA is the CMAQ modeling system [Appel et al., 2007]. CMAQ is a three-dimensional Eulerian chemical transport model of gaseous and aerosol air pollution. CMAQ is developed to have multi-scale capabilities so that separate models are not required for urban scale and regional scale air quality modeling.

The CMAQ model consists of horizontal advection and diffusion, vertical advection and diffusion, gas-phase chemistry, aerosol microphysics, and cloud processes (including wet deposition and aqueous chemistry). In version 4.7.1 of the CMAQ model (the version that the adjoint is developed from), both the piecewise parabolic method (ppm) and global mass-conserving (yamo) advection schemes are supported. The yamo method uses the ppm scheme for horizontal advection and derives a vertical velocity component at each grid cell that satisfies the continuity equation using the driving meteorology model's density. This version of the model uses the ACM2 planetary boundary layer model [Pleim, 2007]. The ACM2 model is able to represent both the supergrid and subgrid-scale components of turbulent transport in the convective boundary layer.

CMAQ v4.7.1 allows the user to choose either the CB05 chemical mechanism or the SAPRC99 chemical mechanism. Some of the differences between the CB05 and SAPRC99 mechanisms are that they use a different scheme for condensing the organic chemistry, and the SAPRC99 mechanism has more detailed organic chemistry than CB05. The cloud process module includes aqueous chemistry and wet deposition. Wet deposition is calculated for both subgrid-scale convective clouds, as well as resolved clouds. The CMAQ aerosol module is detailed in the next section.

1.2.8 CMAQ Aerosol Module

CMAQ version 4.7.1 utilizes a new aerosol module called AERO5. The AERO5 module employs a modal approach to represent the size distribution of particulate matter [Binkowski

and Roselle, 2003; Mebust et al., 2003]. The particle size distribution is represented as a superposition of three lognormal sub-distributions, called modes: Aitken mode, accumulation mode, and coarse mode. In the default configuration, CMAQ estimates concentrations of aerosols in each of the three modes (e.g., ASO4I, ASO4J, ASO4K correspond to sulfate aerosol in the Aitken mode, accumulation mode, and coarse mode, respectively). All three modes are subject to wet and dry deposition, in addition to condensation.

The AERO5 modules solves the general dynamic equation for aerosols:

$$\begin{aligned}\frac{\partial}{\partial t}n(v,t) = \frac{1}{2}\int_0^v K(v-q,q)n(v-q,t)n(q,t)dq \\ - n(v,t)\int_0^\infty K(q,v)n(q,t)dq \\ - \frac{\partial}{\partial v}(I(v)n(v,t)) + J_0(v)\delta(v-vo) + S(v) + R(v)\end{aligned} \tag{1.2}$$

where the first term on the right hand side corresponds to the formation of particles of volume v from coagulation, the second term corresponds to the loss of particles of volume v, the third term corresponds to condensation and evaporation, the fourth term corresponds to the formation of particles of volume v by nucleation, $S(v)$ are sources, and $R(v)$ are removals (deposition). $n(v,t)$ is the particle number distribution, K is the coagulation coefficient, $I(v)$ is the condensation growth rate, and $J_0(v)$ is the nucleation rate. Equilibrium concentrations of inorganic aerosols are solved using ISORROPIA II [Fountoukis and Nenes, 2007].

While previous versions treated all secondary organic aerosol (SOA) as semi-volatile, the AERO5 module has the following four additional SOA processes:

(1) SOA formed by in-cloud oxidation from glyoxal and methyglyoxal.

(2) Enhancement of isoprene-derived SOA under acidic conditions.

(3) SOA originating from aromatic oxidation under low-NO_x conditions.

(4) Oligomerization of particle-phase semi-volatile organic material.

Previous versions of CMAQ considered coarse-mode particles to be dry and inert. Additionally, components in the coarse mode could not evaporate or condense. CMAQ version 4.7, however, allows semi-volatile aerosol components to condense and evaporate from the coarse mode and non-volatile sulfate to condense on the coarse mode. CMAQ version 4.7 also uses dynamic mass transfer to simulate the coarse mode. This is because particles in the coarse mode are often not in equilibrium with the gas-phase.

1.2.9 Adjoint Model

In contrast to forward model sensitivity analysis, adjoint modeling provides receptor-based sensitivities. The adjoint method has two main advantages: First, the adjoint model calculates sensitivities with respect to all model parameters simultaneously, requiring significantly less run time than forward model sensitivity analysis. Second, the computed gradient is numerically precise when using the adjoint model, whereas forward model perturbation methods are more subject to roundoff and truncation errors. While most adjoints of Eulerian chemical transport models [Sandu et al., 2005a] have been developed and used for inverse modeling of gas-phase species [Elbern et al., 2000; Martien and Harley, 2006], several studies have addressed aerosols [Hakami et al., 2005; Henze et al., 2007]. An adjoint of a fixed size aerosol model has been developed for a global coupled chemistry-aerosol model [Henze et al., 2007], and a box model adjoint of aerosol dynamics has been studied [Sandu et al., 2005b; Henze et al., 2004]. Hakami et al. [2005] applied the adjoint of the STEM-2k1 chemical transport model to constrain BC emissions during the Asian Pacific Regional Aerosol Characterization Experiment. Dubovik et al. [2008] developed the adjoint of the GOCART aerosol transport model to retrieve global aerosol source emissions from satellite observations. Huneeus et al. [2009] developed a simplified global aerosol model and its adjoint to optimize aerosol and aerosol precursor emissions using variational data assimilation. The new CMAQ aerosol adjoint is detailed in Section 2.7.1.1.

1.3 References

SD Adar, DR Gold, BA Coull, J Schwartz, PH Stone, and H Suh. Focused exposures to airborne traffic particles and heart rate variability in the elderly. Epidemiology, 18(1): 95–103, January 2007.

BA Albrecht. Aerosols, cloud microphysics, and fractional cloudiness. Science, 245(4923): 1227–1230, 1989.

SC Anenberg, LW Horowitz, DQ Tong, and JJ West. An estimate of the global burden of anthropogenic ozone and fine particulate matter on premature human mortality using atmospheric modeling. Environ. Health Perspect., 118(9):1189–1195, April 2010.

SC Anenberg, J Schwartz, D Shindell, M Amann, G Faluvegi, Z Klimont, G Janssens-Maenhout, L Pozzoli, R Van Dingenen, E Vignati, L Emberson, NZ Muller, JJ West, M Williams, V Demkine, WK Hicks, J Kuylenstierna, F Raes, and V Ramanathan. Global air quality and health co-benefits of mitigating near-term climate change through methane and black carbon emission controls. Environ. Health Perspect., 120(6):831–839, June 2012.

KW Appel, AB Gilliland, G Sarwar, and RC Gilliam. Evaluation of the Community Multiscale Air Quality (CMAQ) model version 4.5: Sensitivities impacting model performance part I - Ozone. Atmos. Environ., 41(40):9603–9615, 2007.

SE Bauer and S Menon. Aerosol direct, indirect, semidirect, and surface albedo effects from sector contributions based on the IPCC AR5 emissions for preindustrial and present-day conditions. J. Geophys. Res.: Atmos., 117:D01206, 2012.

ML Bell, K Ebisu, RD Peng, JM Samet, and F Dominici. Hospital admissions and chemical composition of fine particle air pollution. Am. J. Respir. Crit. Care Med., 179(12):1115–1120, June 2009.

P Bergamaschi, C Frankenberg, JF Meirink, M Krol, MG Villani, S Houweling, F Dentener, EJ Dlugokencky, JB Miller, and LV Gatti. Inverse modeling of global and regional CH4 emissions using SCIAMACHY satellite retrievals. J. Geophys. Res.: Atmos., 114(D22): D22301, 2009.

FS Binkowski and SJ Roselle. Models-3 Community Multiscale Air Quality (CMAQ) model aerosol component - 1. Model description. J. Geophys. Res.: Atmos., 108:–, 2003.

TC Bond. Can warming particles enter global climate discussions? Environ. Res. Letters, 2 (4), 2007.

TC Bond, SJ Doherty, DW Fahey, PM Forster, T Berntsen, BJ DeAngelo, MG Flanner, S Ghan, B Kärcher, and D Koch. Bounding the role of black carbon in the climate system: A scientific assessment. J. Geophys. Res.: Atmos., 118(11):5380–5552, 2013.

F Caiazzo, A Ashok, IA Waitz, SHL Yim, and SRH Barrett. Air pollution and early deaths in the United States. Part I: Quantifying the impact of major sectors in 2005. Atmos. Environ., 79(198-208), 2013.

T Chai, GR Carmichael, Y Tang, A Sandu, A Heckel, A Richter, and JP Burrows. Regional NOx emission inversion through a four-dimensional variational approach using SCIAMACHY tropospheric NO2 column observations. Atmos. Environ., 43(32):5046–5055, 2009.

AJ Cohen, HR Anderson, B Ostro, KD Pandey, M Krzyzanowski, N Kuenzli, K Gutschmidt, CA Pope, I Romieu, JM Samet, and KR Smith. Mortality impacts of urban air pollution. In Majid Ezzati, AD Lopez, A Rodgers, and C Murray, editors, Comparative Quantification of Health Risks: Global and Regional Burden of Disease Due to Selected Major Risk Factors, Vol. 2. World Health Organization, Geneva, 2004.

AJ Cohen, HR Anderson, B Ostro, KD Pandey, M Krzyzanowski, N Kunzli, K Gutschmidt, A Pope, I Romieu, JM Samet, and K Smith. The global burden of disease due to outdoor air pollution. J. Toxicol. Environ. Health, 68(13-14):1301–1307, 2005.

O Dubovik, T Lapyonok, YJ Kaufman, M Chin, P Ginoux, RA Kahn, and A Sinyuk. Retrieving global aerosol sources from satellites using inverse modeling. Atmos. Chem. Phys., 8(2):209–250, 2008.

H Elbern, H Schmidt, O Talagrand, and A Ebel. 4d-variational data assimilation with an adjoint air quality model for emission analysis. Environ. Modell. Softw., 15(6-7):539–548, 2000.

N Fann, CM Fulcher, and BJ Hubbell. The influence of location, source, and emission type in estimates of the human health benefits of reducing a ton of air pollution. Air Qual., Atmos. Health, 2(3):169–176, 2009. doi: 10.1007/s11869-009-0044-0.

N Fann, KR Baker, and CM Fulcher. Characterizing the PM2.5-related health benefits of emission reductions for 17 industrial, area and mobile emission sectors across the U.S. Environ. Int., 49(C):141–151, November 2012a.

N Fann, AD Lamson, SC Anenberg, K Wesson, D Risley, and BJ Hubbell. Estimating the national public health burden associated with exposure to ambient PM2.5 and ozone. Risk Analysis, 32(1):81–95, January 2012b.

MG Flanner, CS Zender, JT Randerson, and PJ Rasch. Present-day climate forcing and response from black carbon in snow. J. Geophys. Res.: Atmos., 112(D11), June 2007.

C Fountoukis and A Nenes. ISORROPIA II: A computationally efficient thermodynamic equilibrium model for K+–Ca 2+–Mg 2+–NH 4+–Na+–SO 4 2–NO 3–Cl–H 2 O aerosols. Atmos. Chem. Phys., 7(17):4639–4659, 2007.

EM Fujita, DE Campbell, B Zielinska, JC Chow, CE Lindhjem, A DenBleyker, GA Bishop, BG Schuchmann, DH Stedman, and DR Lawson. Comparison of the MOVES2010a, MOBILE6.2, and EMFAC2007 mobile source emission models with on-road traffic tunnel and remote sensing measurements. J. Air Waste Manage., 62(10):1134–1149, October 2012.

WJ Gauderman, F Gilliland, H Vora, E Avol, and D Stram. Association between air pollution and lung function growth in southern California children: Results from a second cohort. Am. J. Respir. Crit. Care Med., 166:76–84, June 2002.

TJ Grahame, R Klemm, and RB Schlesinger. Public health and components of particulate matter: The changing assessment of black carbon. J. Air Waste Manage., 64(6):620–660, May 2014.

A Hakami, DK Henze, JH Seinfeld, T Chai, Y Tang, GR Carmichael, and A Sandu. Adjoint inverse modeling of black carbon during the asian pacific regional aerosol characterization experiment. J. Geophys. Res.: Atmos., 110(D14301), 2005.

SL Hallmark, R Guensler, and I Fomunung. Characterizing on-road variables that affect passenger vehicle modal operation. Transport. Res. D-Tr. E., 7(2):81–98, 2002.

J Hansen. Efficacy of climate forcings. J. Geophys. Res.: Atmos., 110(D18):D18104, 2005.

J Hansen, M Sato, and R Ruedy. Radiative forcing and climate response. J. Geophys. Res.: Atmos., 102(D6):6831, March 1997.

M He, J Zheng, S Yin, and Y Zhang. Trends, temporal and spatial characteristics, and uncertainties in biomass burning emissions in the Pearl River Delta, China. Atmos. Environ., 45(24):4051–4059, August 2011.

DK Henze, JH Seinfeld, W Liao, A Sandu, and GR Carmichael. Inverse modeling of aerosol dynamics: Condensational growth. J. Geophys. Res.: Atmos., 109(D14), 2004.

DK Henze, A Hakami, and JH Seinfeld. Development of the adjoint of GEOS-Chem. Atmos. Chem. Phys., 7(9):2413–2433, 2007.

DK Henze, JH Seinfeld, and DT Shindell. Inverse modeling and mapping US air quality influences of inorganic PM 2.5 precursor emissions using the adjoint of GEOS-Chem. Atmos. Chem. Phys., 9(16):5877–5903, 2009.

N Huneeus, O Boucher, and F Chevallier. Simplified aerosol modeling for variational data assimilation. Geosci. Model Dev., 2(2):213–229, 2009.

MZ Jacobson. Control of fossil-fuel particulate black carbon and organic matter, possibly the most effective method of slowing global warming. J. Geophys. Res.: Atmos., 107(D19): 4410, 2002.

MZ Jacobson. Short-term effects of controlling fossil-fuel soot, biofuel soot and gases, and methane on climate, Arctic ice, and air pollution health. J. Geophys. Res.: Atmos., 115, 2010.

NAH Janssen, G Hoek, M Simic-Lawson, P Fischer, L van Bree, H ten Brink, M Keuken, RW Atkinson, HR Anderson, B Brunekreef, and FR Cassee. Black carbon as an additional indicator of the adverse health effects of airborne particles compared with PM10 and PM2. 5. Environ. Health Perspect., 119(12):1691–1699, August 2011.

K Katanoda, T Sobue, H Satoh, K Tajima, T Suzuki, H Nakatsuka, T Takezaki, T Nakayama, H Nitta, K Tanabe, and S Tominaga. An association between long-term exposure to ambient air pollution and mortality from lung cancer and respiratory diseases in japan. J. Epidemiol., 21(2):132–143, 2011.

I Kazuhiko, R Mathes, Z Ross, A Nádas, G Thurston, and T Matte. Fine particulate matter constituents associated with cardiovascular hospitalizations and mortality in New York City. Environ. Health Perspect., 119(4):467, April 2011.

D Koch, M Schulz, S Kinne, C McNaughton, JR Spackman, Y Balkanski, S Bauer, T Berntsen, TC Bond, O Boucher, M Chin, A Clarke, N De Luca, F Dentener, T Diehl, O Dubovik, R Easter, D W Fahey, J Feichter, D Fillmore, S Freitag, S Ghan, P Ginoux, S Gong, L Horowitz, T Iversen, A Kirkevag, Z Klimont, Y Kondo, M Krol, X Liu, R Miller, V Montanaro, N Moteki, G Myhre, JE Penner, J Perlwitz, G Pitari, S Reddy, L Sahu, H Sakamoto, G Schuster, JP Schwarz, O Seland, P Stier, N Takegawa, T Takemura, C Textor, JA van Aardenne, and Y Zhao. Evaluation of black carbon estimations in global aerosol models. Atmos. Chem. Phys., 9(22):9001–9026, 2009.

D Krewski, M Jerrett, RT Burnett, R Ma, E Hughes, Y Shi, MC Turner, CA Pope, G Thurston, EE Calle, MJ Thun, B Beckerman, P DeLuca, N Finkelstein, K Ito, DK Moore, KB Newbold, T Ramsay, Z Ross, H Shin, and B Tempalski. Extended follow-up and spatial analysis of the American Cancer Society study linking particulate air pollution and mortality. Technical Report HEI Research Report 140, Health Effects Institute, Boston, Mass., USA, 2009. URL `http://ephtracking.cdc.gov/docs/RR140-Krewski.pdf`.

J Kurokawa, K Yumimoto, I Uno, and T Ohara. Adjoint inverse modeling of NOx emissions over eastern China using satellite observations of NO2 vertical column densities. Atmos. Environ., 43(11):1878–1887, 2009.

J Lepeule, F Laden, D Dockery, and J Schwartz. Chronic exposure to fine particles and mortality: an extended follow-up of the Harvard Six Cities study from 1974 to 2009. Environ. Health Perspect., 120(7):965–970, July 2012.

Y Li, DK Henze, D Jack, and PL Kinney. The influence of air quality model resolution on health impact assessment for fine particulate matter and its components. Air Qual., Atmos. Health, 2015.

V Mallet and B Sportisse. Uncertainty in a chemistry-transport model due to physical parameterizations and numerical approximations: An ensemble approach applied to ozone modeling. J. Geophys. Res.: Atmos., 11(1), 2006.

PT Martien and RA Harley. Adjoint sensitivity analysis for a three-dimensional photochemical model: Implementation and method comparison. Environ. Sci. Technol., 40(8): 2663–2670, 2006.

MR Mebust, BK Eder, FS Binkowski, and SJ Roselle. Models-3 Community Multiscale Air Quality (CMAQ) model aerosol component - 2. Model evaluation. J. Geophys. Res.: Atmos., 108:–, 2003.

NZ Muller and R Mendelsohn. Measuring the damages of air pollution in the United States. J. Environ. Econ. Manage., 54(1):1–14, 2007.

NZ Muller, R Mendelsohn, and W Nordhaus. Environmental accounting for pollution in the United States economy. Am. Econ. Rev., 101(5):1649–1675, August 2011.

G Myhre, D Shindell, FM Bréon, W Collins, J. Fuglestvedt, J Huang, D Koch, JF Lamarque, D Lee, B Mendoza, T Nakajima, A Robock, G Stephens, T Takemura, and H Zhang. Climate Change 2013: The Physical Science Basis. Contribution of Working Group I to the Fifth Assessment Report of the Intergovernmental Panel on Climate Change, chapter Anthropogenic and Natural Radiative Forcing. Cambridge University Press, Cambridge, United Kingdom and New York, NY, USA, 2013.

RD Peng, ML Bell, AS Geyh, A McDermott, SL Zeger, JM Samet, and F Dominici. Emergency admissions for cardiovascular and respiratory diseases and the chemical composition of fine particle air pollution. Environ. Health Perspect., 117(6):957–963, February 2009.

E Pisoni, C Carnevale, and M Volta. Sensitivity to spatial resolution of modeling systems designing air quality control policies. Environ. Modell. Softw., 25(1):66–73, January 2010.

JE Pleim. A combined local and nonlocal closure model for the atmospheric boundary layer. Part I: Model description and testing. J. Appl. Meteorol., 46(9):1383–1395, September 2007.

CA Pope, RT Burnett, MJ Thun, EE Calle, D Krewski, K Ito, and GD Thurston. Lung cancer, cardiopulmonary mortality, and long-term exposure to fine particulate air pollution. J. Am. Med. Assoc., 287(9):1132–1141, 2002.

CA Pope, RT Burnett, GD Thurston, MJ Thun, EE Calle, D Krewski, and JJ Godleski. Cardiovascular mortality and long-term exposure to particulate air pollution - epidemiological evidence of general pathophysiological pathways of disease. Circulation, 109(1): 71–77, 2004.

G Pouliot, E Wisner, and D Mobley. Quantification of emission factor uncertainty. J. Air Waste Manage., 62(3):287–298, 2012.

MC Power, MG Weisskopf, and SE Alexeeff. Traffic-related air pollution and cognitive function in a cohort of older men. Environ. Health Perspect., 119(5):682–687, 2011.

RC Puett, JE Hart, JD Yanosky, C Paciorek, J Schwartz, H Suh, FE Speizer, and F Laden. Chronic fine and coarse particulate exposure, mortality, and coronary heart disease in the Nurses' Health Study. Environ. Health Perspect., 117(11):1697–1701, June 2009.

EM Punger and JJ West. The effect of grid resolution on estimates of the burden of ozone and fine particulate matter on premature mortality in the USA. Air Qual., Atmos. Health, 6(3):563–573, May 2013.

A Sandu, DN Daescu, GR Carmichael, and T Chai. Adjoint sensitivity analysis of regional air quality models. J. Comput. Phys., 204(1):222–252, 2005a.

A Sandu, W Liao, GR Carmichael, DK Henze, and JH Seinfeld. Inverse modeling of aerosol dynamics using adjoints: Theoretical and numerical considerations. Aerosol Sci. Technol., 39(8):677–694, 2005b.

W Schroeder, E Prins, L Giglio, I Csiszar, C Schmidt, J Morisette, and D Morton. Validation of GOES and MODIS active fire detection products using ASTER and ETM plus data. Remote Sensing of Environment, 112(5):2711–2726, 2008.

JH Seinfeld and SN Pandis. Atmospheric Chemistry and Physics: From Air Pollution to Climate Change. John Wiley & Sons, Inc., Hoboken, New Jersey, 2nd edition, 2006.

D Shindell, JCI Kuylenstierna, E Vignati, R Van Dingenen, M Amann, Z Klimont, SC Anenberg, NZ Muller, G Janssens-Maenhout, F Raes, J Schwartz, G Faluvegi, L Pozzoli, K Kupiainen, L Hoeglund-Isaksson, L Emberson, D Streets, V. Ramanathan, K Hicks, NTK Oanh, G Milly, M Williams, V Demkine, and D Fowler. Simultaneously mitigating near-term climate change and improving human health and food security. Science, 335(6065): 183–189, 2012.

S Stevenson, FJ Dentener, and MG Schultz. Multimodel ensemble simulations of present-day and near-future tropospheric ozone. J. Geophys. Res.: Atmos., 111(D08301), 2006.

HH Suh and A Zanobetti. Exposure error masks the relationship between traffic-related air pollution and heart rate variability. J. Occup. Environ. Med., 52(7):685–692, July 2010.

S Twomey. Pollution and planetary albedo. Atmos. Environ., 8(12):1251–1256, 1974.

US EPA. Integrated Science Assessment for Particulate Matter. Technical report, U.S. Environmental Protection Agency: National Center for Environmental Assessment, Washington, DC, December 2009. URL `http://www.epa.gov/ncea/pdfs/partmatt/Dec2009/PM_ISA_full.pdf`.

US EPA. Benefits and Costs of the Clean Air Act from 1990 To 2020. Technical report, U.S. Environmental Protection Agency: Office of Air and Radiation, March 2011. URL `http://www.epa.gov/cleanairactbenefits/prospective2.html`.

TPC van Noije, HJ Eskes, FJ Dentener, DS Stevenson, K Ellingsen, MG Schultz, O Wild, M Amann, CS Atherton, DJ Bergmann, I Bey, KF Boersma, T Butler, J Cofala, J Drevet, AM Fiore, M Gauss, DA Hauglustaine, LW Horowitz, ISA Isaksen, MC Krol, JF Lamarque, MG Lawrence, RV Martin, V Montanaro, JF Muller, G Pitari, MJ Prather, JA Pyle, A Richter, JM Rodriguez, NH Savage, SE Strahan, K Sudo, S Szopa, and M van Roozendael. Multi-model ensemble simulations of tropospheric no_2 compared with gome retrievals for the year 2000. Atmos. Chem. Phys., 6(10):2943–2979, 2006.

WHO. Health risks of particulate matter from long-range transboundary air pollution. Technical report, World Health Organization Regional Office of Europe, Copenhagen, 2006. URL `http://www.euro.who.int/__data/assets/pdf_file/0006/78657/E88189.pdf`.

WHO. Health effects of black carbon. Technical report, World Health Organization, European Centre for Environment and Health, Bonn Office, April 2012. URL `http://www.euro.who.int/__data/assets/pdf_file/0004/162535/e96541.pdf`.

EH Wilker, MA Mittleman, BA Coull, A Gryparis, ML Bots, J Schwartz, and D Sparrow. Long-term exposure to black carbon and carotid intima-media thickness: the Normative Aging Study. Environ. Health Perspect., 121(9):1061–1067, September 2013.

L Zhu, DK Henze, KE Cady Pereira, MW Shephard, M Luo, RW Pinder, JO Bash, and GR Jeong. Constraining US ammonia emissions using TES remote sensing observations and the GEOSChem adjoint model. J. Geophys. Res.: Atmos., 118(8):3355–3368, April 2013. doi: 10.1002/jgrd.50166.

Chapter 2

Differences Between Magnitudes and Health Impacts of BC Emissions Across the US Using 12km Scale Seasonal Source Apportionment

Matthew D. Turner[1], Daven K. Henze[1], Amir Hakami[2], Shunliu Zhao[2], Jaroslav Resler[3], Gregory R. Carmichael[4], Charles O. Stanier[4], Jaemeen Baek[4], Adrian Sandu[5], Armistead G. Russell[6a], Athanasios Nenes[6b], Gill-Ran Jeong[6b], Shannon L. Capps[6c,7], Rob W. Pinder[7], Sergey L. Napelenok[7], Jesse O. Bash[7], Peter B. Percell[8], and Tianfeng Chai[9]

[1]Mechanical Engineering Department, University of Colorado, Boulder, Colorado 80309, United States

[2]Department of Civil and Environmental Engineering, Carleton University, Ottawa, Ontario K1S 5B6, Canada

[3]Nonlinear Modeling, Institute of Computer Science, Prague 182 07, Czech Republic

[4]Department of Chemical and Biochemical Engineering, University of Iowa, Iowa City, Iowa 52242, United States

[5]Computer Science, Virginia Tech, Blacksburg, Virginia 24061, United States

[6a]School of Civil and Environmental Engineering, [6b]School of Earth and Atmospheric Sciences, and [6c]School of Chemical and Biomolecular Engineering, Georgia Tech, Atlanta, Georgia 30331, United States

[7]Atmospheric Modeling and Analysis Division, U.S. EPA, Research Triangle Park, North Carolina 27711, United States

[8]Department of Geosciences, University of Houston, Houston, Texas 77004, United States

[9]College of Computer, Mathematical, and Natural Sciences, University of Maryland, College Park, Maryland 20742, United States

2.1 Abstract

Recent assessments have analyzed the health impacts of $PM_{2.5}$ from emissions from different locations and sectors using simplified or reduced-form air quality models. Here we present an alternative approach using the adjoint of the Community Multiscale Air Quality (CMAQ) model, which provides source-receptor relationships at highly-resolved sectoral, spatial, and temporal scales. While damages resulting from anthropogenic emissions of BC are strongly correlated with population and premature death, we found little correlation between damages and emission magnitude, suggesting that controls on the largest emissions may not be the most efficient means of reducing damages resulting from anthropogenic BC emissions. Rather, the best proxy for locations with damaging BC emissions is locations where premature deaths occur. Onroad diesel and nonroad vehicle emissions are the largest contributors to premature deaths attributed to exposure to BC, while onroad gasoline emissions cause the highest deaths per amount emitted. Emissions in fall and winter contribute to more premature deaths (and more per amount emitted) than emissions in spring and summer. Overall, these results show the value of high-resolution source attribution for determining the locations, seasons, and sectors for which BC emission controls have the most effective health benefits.

2.2 Introduction

Exposure to fine particulate matter ($PM_{2.5}$) in ambient air has been shown to be a cause of various adverse health effects, such as cardiopulmonary disease and lung cancer [Krewski et al., 2009; WHO, 2006; Pope et al., 2002; Katanoda et al., 2011; Lepeule et al., 2012; Kazuhiko et al., 2011; Puett et al., 2009; Gauderman et al., 2002; Cohen et al., 2004], leading to an estimated 130,000 premature deaths in 2005 in the US alone [Fann et al., 2012b]. Recent work has focused on species-specific and source-specific analyses of $PM_{2.5}$ health impacts. Many studies have associated increased premature deaths with proximity to major roadways [Finkelstein et al., 2004; Finkelstein, 2005; Gehring et al., 2006; Wilker et al., 2013b]. Other studies have found associations of increased premature deaths and morbidity to concentrations of black carbon (BC) [Suh and Zanobetti, 2010; Adar et al., 2007; Peng et al., 2009; WHO, 2012; Power et al., 2011; Wilker et al., 2013a]. Bell et al. [2009] analyzed source-specific effects of $PM_{2.5}$ species on both cardiovascular and respiratory diseases and found that increases in concentrations of BC and Vanadium resulted in the largest increase in these diseases. Reviews of the health effects of exposure to BC have suggested that there is a causal relationship between exposure to BC and premature death [Janssen et al., 2011; Grahame et al., 2014]. There is additional interest in BC owing to potential near-term climate benefits of reductions of BC emissions [Bauer and Menon, 2012; Bond, 2007; Jacobson, 2010; Bond et al., 2013; Anenberg et al., 2012; Shindell et al., 2012].

Since studies implicate exposure to ambient $PM_{2.5}$ in causing a large number of premature deaths, it is further important to determine which emissions, in terms of both location and source sectors, have the largest effect on human health. Even if one assumes uniform toxicity per unit mass of $PM_{2.5}$, the health effects of emissions can vary greatly between locations and sectors, due to differences in spatial distributions of emissions and population. Muller et al. [2011] used a dispersion model to estimate air pollution damages (from both health and climate effects) associated with emissions of six gaseous or particulate pollutants

across a wide range of sectors and found that the utility sector contributes to the most air pollution damages in the US. Fann et al. [2012a] estimated the $PM_{2.5}$-related health benefits associated with emission reductions for 17 sectors across the US and found that the largest benefits-per-ton of emission reductions come from reducing directly emitted $PM_{2.5}$. Tainio et al. [2010] estimated that traffic accounts for approximately 30% of emissions of $PM_{2.5}$, yet exposure to traffic emissions account for approximately 50% of adverse health effects associated with exposure to $PM_{2.5}$ in Finland. Human health benefits-per-ton can also vary substantially across emissions from different locations and source sectors. Using a reduced-form air quality model to evaluate the benefits-per-ton estimates for the same pollutant across various sources and 9 urban areas, Fann et al. [2009] estimated benefits-per-ton estimates ranging from \$65,000/*ton* for carbon electric generating utility (EGU) and non-EGU emissions in Salt Lake City to \$2,500,000/*ton* for area source carbon emissions in Phoenix (2006\$).

While variability in emission damages across locations and sectors is clearly significant, incorporating this type of analysis into air quality control strategies is often hindered by the computational expense of quantifying damages for numerous sources. Previous works have used simplified, [Muller et al., 2011; Muller and Mendelsohn, 2009] reduced-form, or coarser models [Fann et al., 2009; Levy et al., 2009; Fann et al., 2012a] and considered a limited number of sources. An alternative approach is using adjoint modeling, which provides a means to analyze detailed source-receptor relationships at a highly-resolved sectoral, spatial, and temporal scale [Hakami et al., 2006; Lapina et al., 2014]. Koo et al. [2013] used adjoint modeling for evaluating $PM_{2.5}$ health impacts from the aviation sector in a global model, and other studies have applied this approach to evaluate $PM_{2.5}$ health impacts from a range of sectors at global [Li et al., 2015] and regional scales [Dedoussi and Barrett, 2014]. Pappin and Hakami [2013b] used adjoint modeling for estimation of premature death due to short-term exposure to gas-phase pollutants, and this approach has been further applied for estimation of ozone health impacts [Pappin and Hakami, 2013a; Mesbah et al., 2013; Zhao et al., 2013].

In this work, we introduce and apply a new CMAQ adjoint model to quantify the individual role of more than 10^6 emissions (13 sectors $\times$ 97,416 locations $\times$ 4 seasons) on premature deaths attributed to exposure to BC in the US at much lower computational cost than the more than 10^6 simulations that would be needed to obtain the same results without this tool.

2.3 Materials and Methods

2.3.1 Forward Model

BC concentrations are estimated using the Community Multiscale Air Quality (CMAQ) model v4.7.1 [Byun and Schere, 2006]. The modeling domain covers the continental US, northern Mexico, and southern Canada at a 12km × 12km resolution (396 × 246). The vertical domain consists of 24 terrain-following layers in sigma-pressure coordinates. Meteorological inputs were obtained from version 3.1 of the Weather Research Forecasting model (WRF) [US EPA, 2011; Skamarock et al., 2005]. Boundary conditions and initial condition profiles were obtained by running GEOS-Chem version 8.02.03 with a grid resolution of 2.0° × 2.5° (latitude × longitude) and 47 vertical layers [US EPA, 2012b].

We use anthropogenic emissions from version 2 of the 2008 National Emission Inventory (2008 NEI) [US EPA, 2013], Canada's 2006 inventory and Mexico's Phase III 2008 inventory. The 2008 NEI includes five sectors: nonpoint, point, nonroad mobile, onroad mobile, and fires. Biogenic emissions are obtained from the BEIS3.14 model [Pierce and Waldruff, 1991]. Wildfire emissions were calculated using the SMARTFIRE2 system [Ewer et al., 1999]. Sectoral emission profiles were obtained by running the Sparse Matrix Operator Kernel Emissions (SMOKE) modeling system [Coats and Houyoux, 1996] v3.5.1 for the following sectors: onroad mobile, nonroad mobile, fire, EGU, non-EGU, commercial marine, non-US point, dust, rail, non-point, non-US onroad, and non-US nonpoint and nonroad. The onroad mobile sector was further differentiated by fuel type based on the source classification code in SMOKE. The nonpoint sector (called "stationary area" in previous NEIs) includes sources such as residential heating, gas stations, dry cleaning, commercial cooking, etc. The non-EGU sector includes large industrial combustion sources that are not categorized as EGUs. The "non-US" sectors contain emission sources that are located outside of the continental US (i.e., Southern Canada and Northern Mexico).

We use CMAQ to estimate national premature deaths from exposure to BC using the

following health impact function [Anenberg et al., 2011]:

$$J = \sum_{i=1}^{N} M_i \cdot (1 - e^{-\beta \cdot C_{av,i}}) \tag{2.1}$$

where M_i is the 2010 gridded annual non-accidental premature deaths in the US for people age 30 or older, $C_{av,i}$ is the gridded annual average BC concentration, i is the grid cell index, N is the number of grid cells, and β is the concentration response factor. We use a concentration response factor of 0.005827 (response factor is calculated from the relative risk estimate presented in Krewski et al. [2009], 1.06 (1.04-1.08)). Mortality rates for 2004-2006 are from the Centers for Disease Control and National Center for Health Statistics [Abt, 2013. Bethesda, MD.]. Our linear approximation of this health impact function yields a high bias of approximately 15%.

2.3.2 Adjoint Model

In contrast to forward model sensitivity analysis, adjoint modeling provides receptor-based sensitivities. The adjoint method has two main advantages: First, the adjoint model calculates sensitivities with respect to all model parameters simultaneously, requiring significantly less run time than forward model sensitivity analysis. Second, the computed gradient is numerically precise when using the adjoint model, whereas forward model perturbation methods are more subject to roundoff and truncation errors. While most adjoints of Eulerian chemical transport models [Sandu et al., 2005a] have been developed and used for inverse modeling of gas-phase species [Elbern et al., 2000; Martien and Harley, 2006], several studies have addressed aerosols [Hakami et al., 2005; Henze et al., 2007]. An adjoint of a fixed size aerosol model has been developed for a global coupled chemistry-aerosol model [Henze et al., 2007], and a box model adjoint of aerosol dynamics has been studied [Sandu et al., 2005b; Henze et al., 2004]. Hakami et al. [2005] applied the adjoint of the STEM-2k1 chemical transport model to constrain BC emissions during the Asian Pacific Regional Aerosol

Characterization Experiment. Dubovik et al. [2008] developed the adjoint of the GOCART aerosol transport model to retrieve global aerosol source emissions from satellite observations. Huneeus et al. [2009] developed a simplified global aerosol model and its adjoint to optimize aerosol and aerosol precursor emissions using variational data assimilation.

Inclusion of aerosols in the existing CMAQ-ADJ [Hakami et al., 2007] results in the first coupled gas-aerosol, regional adjoint model to explicitly describe aerosol mass composition and size distribution (see Supporting Information for adjoint development details). For this project, the receptor function of interest is national premature death attributed to BC exposure (Equation 2.1). The adjoint model calculates the sensitivity of this function with respect to emissions at highly-resolved scales. The resulting sensitivities quantify the effects of location, time, and sector of emissions of BC on human health in the US.

Calculation of the health impact function (including checkpointing) and its gradients takes approximately 3.9 times the computational cost of the health impact function alone (without checkpointing). The updated CMAQ adjoint model has been validated against both complex variable [Squire and Trapp, 1998] and finite difference sensitivities. The adjoint sensitivities are numerically accurate, as shown by the linear regression of adjoint sensitivities on finite difference sensitivities of BC concentrations with respect to BC emissions ($R^2 = 0.99$, $m = 1.01$) for simulations that include all processes except horizontal transport (see Supplemental Information). Tests including horizontal advection indicate that the adjoint sensitivities can be used at the grid scale to estimate changes in total national premature deaths to within one death (see Figure 2.11).

2.4 Results and Discussion

2.4.1 Forward Model Simulations

CMAQ was run from December 21, 2006, to December 31, 2007, to generate gridded annual average concentrations. The annual average BC concentrations were then used in the health impact function (Equation 2.1) to estimate the premature deaths attributed to exposure to BC in 2007. For computational expediency, CMAQ model configurations did not include gas-phase chemistry, which has a negligible effect on simulated BC concentrations.

We first evaluate simulated annual average BC concentrations via comparison to observations from the Interagency Monitoring of Protected Visual Environments [Malm et al., 2004] (IMPROVE) and Chemical Speciation Network [Flanagan et al., 2006] (CSN) monitoring networks (Figure 2.1). The IMPROVE and CSN monitoring networks use different protocols to measure aerosol carbon fraction, therefore we convert the CSN measurements to IMPROVE-equivalent values using the seasonal conversion factors from Hu et al. [2009] (this conversion is not necessary for recent years, due to the recent update to the CSN protocol). While a majority of locations show similar concentrations between model and observations, some points have substantial differences. Simulated annual average BC concentrations tend to overestimate the largest concentrations (simulated annual average concentrations > 1.5 $\mu g/m^3$) when compared to IMPROVE data (mean bias of 0.09 $\mu g/m^3$, see Table 2.1). However, at lower concentrations (simulated annual average concentrations < 1 $\mu g/m^3$) CMAQ tends to compare well with IMPROVE, as shown by the coefficient of determination of 0.65 and the root mean squared error (RMSE) of 0.14 $\mu g/m^3$ (mean absolute error of 0.13 $\mu g/m^3$). Comparisons to the adjusted CSN measurements, on the other hand, tend to be worse. While CMAQ and CSN concentrations are similar for smaller concentrations, there is a large amount of scatter in the higher CSN values not captured by the model, likely owing to sub-grid variability in concentrations near the urban CSN sites. However, as with the comparison to IMPROVE observations, the RMSE is small (0.45 $\mu g/m^3$, mean absolute er-

ror = 0.50 μg/m^3) for comparisons between CMAQ and CSN concentrations. Further, while the coefficient of determination is small when comparing to CSN observations ($R^2 = 0.19$), the simulated concentrations have a small normalized mean bias of -17% (mean bias of -0.22 μg/m^3).

By combining the forward model BC concentrations with gridded baseline mortality rates in the continental US using Equation 2.1, we estimate approximately 12,600 (8,700 - 16,500, see Supplemental Information for uncertainty calculation details) national premature deaths attributed to exposure to BC for 2007. This is consistent with previous studies, taking into account that about 5-10% of $PM_{2.5}$ mass is BC [US EPA, 2012a]. As one might expect, a majority of premature deaths attributed to exposure to BC occur around major cities (Figure 2.13).

2.4.2 Sensitivity of BC Health Effects to Anthropogenic Emissions

A comparison of yearly average BC concentrations to average BC concentrations calculated from 12 weeks (Figure 2.12) shows that results from these 12 weeks provide an accurate ($R^2 = 0.88$, RMSE = 0.07 μg/m^3) representation of the annual average. To reduce the computational cost of this analysis, adjoint simulations were run (in parallel) for 12 1-week periods from the 1st to the 7th of each month. For each 1-week adjoint simulation, we used a 4 day spin-up period. Semi-normalized sensitivities ($\frac{\partial J}{\partial E} \cdot E$, Figure 2.2a) with respect to emissions (E) were accumulated throughout the entire week of the adjoint run, and the resulting sensitivities were summed over the 12 individual simulations and scaled to represent a yearly value.

We refer to semi-normalized sensitivities as contributions, because they quantify the contribution of the BC emissions in each grid cell to the model estimate of total national premature deaths. For example, our analysis estimates that emissions in the grid cell that contains New York City result in 174 premature deaths associated with exposure to BC in the continental US. Therefore, emissions in this grid cell have a contribution of 174 premature

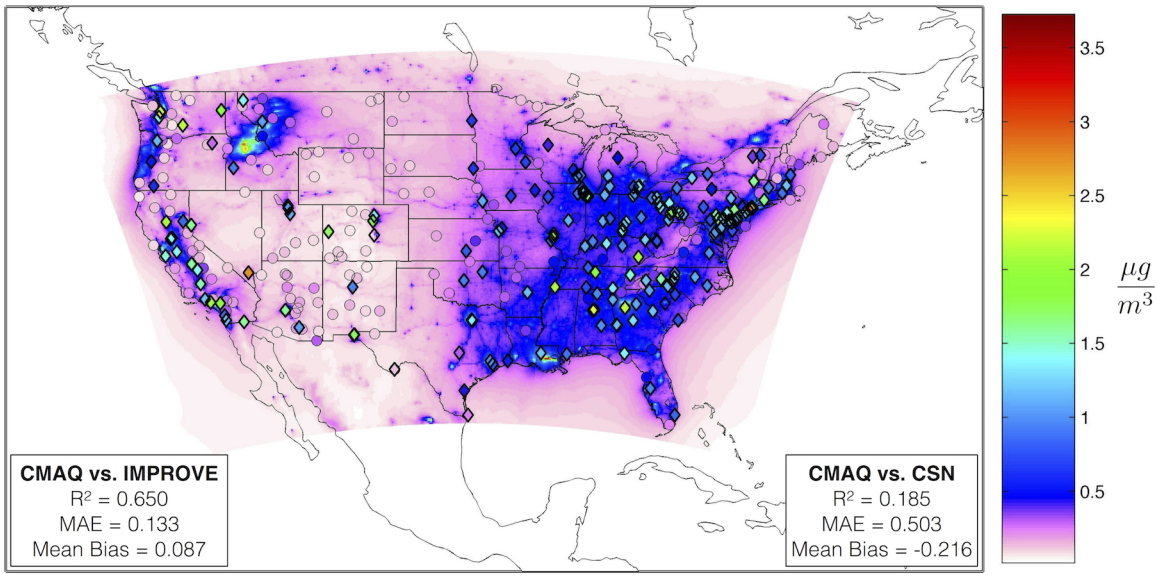

Figure 2.1: Comparison of simulated annual average BC concentrations (μg/m^3) to observations from the IMPROVE network (circles), and CSN network (diamonds). CSN observations were scaled per Hu et al. [2009]

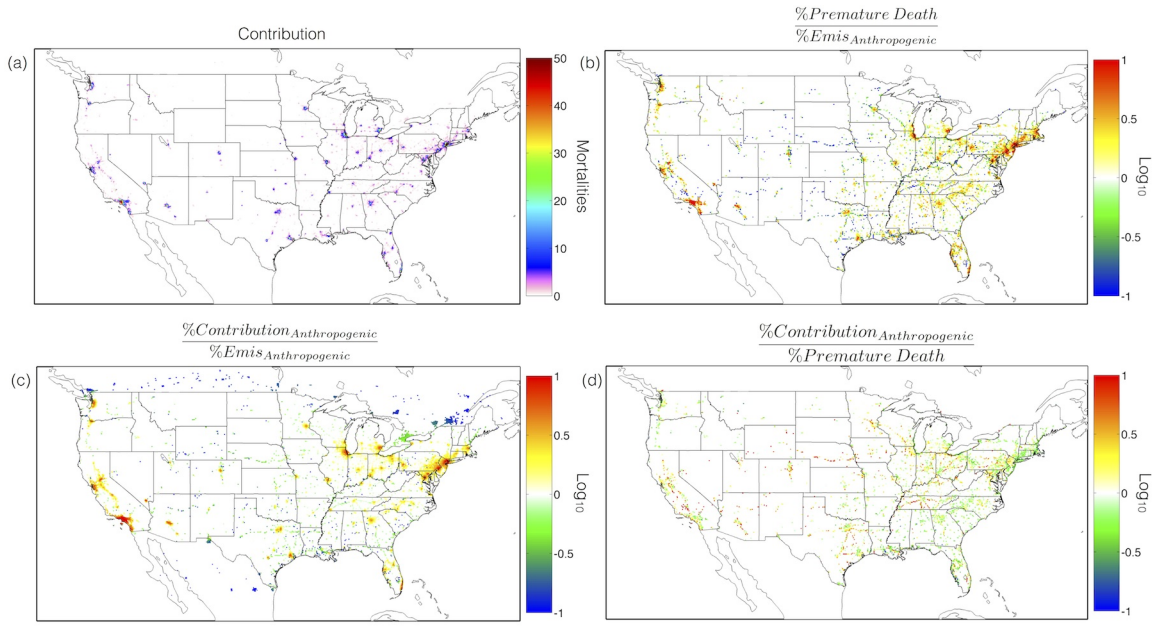

Figure 2.2: (a) Semi-normalized sensitivities ($\frac{\partial J}{\partial E} \cdot E$) showing the sensitivity of national premature death to emissions in each grid cell. A maximum of 174 premature deaths are attributed to BC emitted from New York, NY. (b) Ratio of gridded premature death percentage over gridded anthropogenic emission percentage, plotted on a log scale. (c) Ratio of gridded contribution percentage from anthropogenic emissions over gridded anthropogenic emission percentage, plotted on a log scale. (d) Ratio of gridded contribution percentage from anthropogenic emissions over gridded premature death percentage, plotted on a log scale. For larger versions of each panel, see Figures 2.17-2.20.

deaths to the national total. The contribution percentage is defined as the percent of the total continental US deaths owing to BC emissions from a single grid cell. For example, the contribution percentage of the grid cell that contains New York City is 174/12,200 x 100% = 1.4%. From our analysis, we estimate that anthropogenic emissions of BC account for 12,200 (8,400 - 16,000) premature deaths (approximately 95% of total premature deaths from exposure to BC). It has often been assumed that the damages (contribution per unit emission) of BC emissions are constant, or proportional to the magnitude of emissions across large domains [Muller et al., 2011]. However, our analysis shows that damages vary greatly by region (see Figure 2.14), with damage estimates ranging two orders of magnitude and being largest in urban centers.

We generated plots (Figures 2.2b-d) for various ratios on a log scale. When generating these ratio plots, only a fraction of the grid cells were included in order to emphasize the cells with larger values while also omitting cells that might have large ratios but small overall impacts. Of the ∼97,000 grid cells in the domain, data from only ∼10,000 grid cells were used. For each ratio plot, the largest values for the numerator and denominator (summing to approximately 95% for each) are displayed in the plot.

To analyze the spatial differences between the magnitude of emissions and the magnitude of exposure on a grid-cell by grid-cell basis, we have plotted the ratio of premature death percentage to anthropogenic emission percentages (Figure 2.2b). Warm (cool) colors indicate locations with a larger (smaller) premature death percentage than the corresponding anthropogenic emission percentage. Highly populated urban areas have larger premature death percentages than anthropogenic emission percentages. In contrast, grid cells along many interstates in rural areas have larger anthropogenic emission percentages than premature death percentages. This is expected, as transportation emissions account for a majority of anthropogenic US BC emissions (∼80% [US EPA, 2012a]), and one would not expect many premature deaths attributed to BC exposure to occur near interstate highways in rural areas. However, near highways passing through urban areas (e.g., Highway 99 in Modesto

and Fresno, CA) there are larger premature death percentages than anthropogenic emission percentages due to the proximity of populous areas to the highway.

Next, the ratio of contribution percentage to anthropogenic emission percentage (Figure 2.2c) demonstrates the variability in the difference between the magnitude of emissions and their marginal damages (the incremental change in damage resulting from an increase or decrease in emissions). Warm (cool) colors show locations with higher (lower) contribution percentages than anthropogenic emission percentages. Highly populated urban areas tend to have larger contribution percentages than anthropogenic emission percentages. However, in rural areas, such as eastern Texas and Tennessee, some major roadways have larger anthropogenic emission percentages than contribution percentages. The fact that rural roadways often have higher emission percentages than contribution percentages in many parts of the country suggests that additional restrictions on vehicle emissions would not be the most efficient means of reducing national premature deaths attributed to exposure to BC. However, Figure 2.2c does not provide sufficient information to weigh this against the impact of vehicle emissions near the urban areas. Further analysis of net sectoral impacts is provided in the Seasonal and Sectoral Trends section.

Given the short lifetime of BC, one might expect that contributions might be reduced most efficiently through reductions to emissions in highly populated areas. Adjoint sensitivity analysis quantitatively separates the influence of emission location and population distributions from atmospheric transport, which is shown by the ratio of gridded contribution percentage over gridded premature death percentage (Figure 2.2d). Warm (cool) colors show locations with higher (lower) contribution percentage than premature death percentage. Many of the major roadways have contribution percentages greater than premature death percentages. However, along some major roadways (such as Interstate-90 in NY), there are larger premature death percentages than contribution percentages. Areas downwind of major emission locations have more premature deaths than accounted for by emissions in the corresponding grid cells (e.g., Connecticut, Rhode Island, eastern Massachusetts are down-

wind of emissions from northern New Jersey, and show larger premature death percentages than contribution percentages). Additionally, many of the areas with higher contribution percentage than premature death percentage are upwind of highly populated areas (northern New Jersey, west-southwest of New York City). As with the northeastern US, the California region shows higher premature death percentages downwind of high emission areas.

We next compare premature death and contribution percentages to population and anthropogenic emission percentages across the nation to determine national-scale trends (Figures 2.3 and 2.15). Locations with the highest anthropogenic emissions do not necessarily correspond to the highest contributions for BC premature deaths (see Figure 2.3). In fact, the second largest anthropogenic emissions considered (0.18%) has a corresponding contribution percentage of only 0.02%. These values correspond to a grid cell that encompasses Gary, IN. As such, the emissions in this grid cell are in and near locations of high population, and the large discrepancy between emissions and contributions cannot be attributed to large emissions occurring in rural, low-populated areas. Additionally, 21 of the 50 largest emissions are in the lowest 50% of contributions. As one might expect, contribution is strongly correlated with population ($R^2 = 0.79$) and premature death ($R^2 = 0.88$). Premature deaths are also highly correlated with population, with a coefficient of determination of approximately 0.85. This is expected, as population is the most spatially variable factor in our definition of the impact function (Equation 2.1). It might be expected that anthropogenic emissions would be highly correlated with population; however, our analysis shows a coefficient of determination of only 0.41. When comparing anthropogenic emissions with contribution and premature death, we obtain R^2 values of 0.46 and 0.35, respectively. Regression of premature death on emission shows that 83 of the 200 largest premature deaths are in the lowest 50% of emissions. The grid-scale contributions calculated with the CMAQ adjoint identify locations where BC control strategies would have the greatest impact on national premature deaths. However, it is interesting to also consider the efficiency of strategies developed without such results. Our analysis shows that the best proxy for identifying lo-

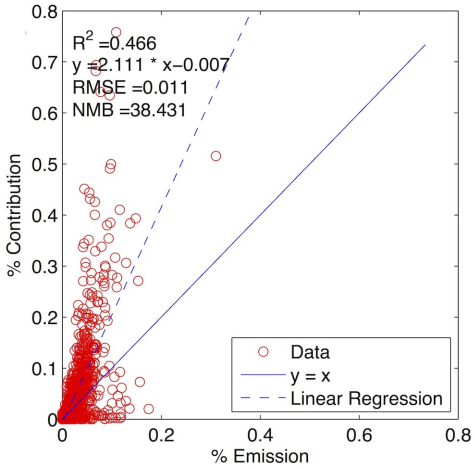

Figure 2.3: Comparison of contribution percentage from anthropogenic emissions to anthropogenic emission percentage.

cations where BC emissions have the highest contributions (i.e., the most effective locations to target for reducing health impacts) is areas with the largest premature deaths, rather than locations with the highest emissions or population. US National Ambient Air Quality Standards (NAAQS) focus on regions with concentration exceedences. Therefore, the most effective means of reducing health impacts is being addressed only where high concentrations coincide with high premature deaths.

2.4.3 Sensitivity of BC Health Effects to Anthropogenic Emissions, Summed by State

In this section, we aggregate our grid-level sensitivity results on a per-state basis, following Hakami et al. [2006]. While the results presented here generally emphasize the importance of transport of BC, this type of analysis, if repeated for health impact functions focusing on individual states, could be used to quantify interstate transport of BC. All grid cells were included for these plots, and we consider differences in state-level results (as opposed to the previous ratio analysis) since values in every state are of the same order of magnitude. Figure 2.16a shows the contribution percentage on a per-state basis. A majority

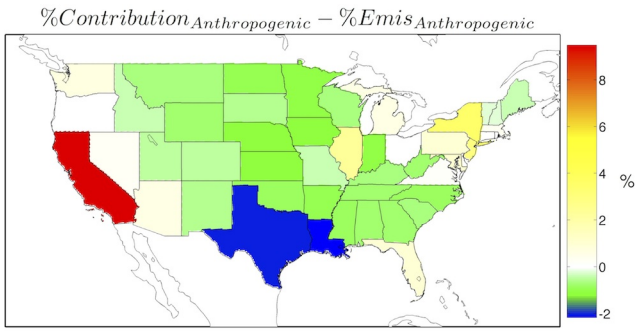

Figure 2.4: State based analysis of adjoint sensitivities. Contribution percentage from anthropogenic emissions minus anthropogenic emission percentage.

of contributions are attributed to emissions from California (with approximately 15.8%, or 2,000 premature deaths), followed by Illinois, New York, and Texas (each with approximately 6.7%, or 800 premature deaths).

We next consider which states are experiencing more than their share (when compared to emissions) of national premature deaths (see Figure 2.16b). There are many states that have higher anthropogenic emission percentages than premature death percentages, such as California (by 6.9%) and New York (by 6.3%). However, while the maximum positive difference is 6.9% (California), a majority of the states with larger anthropogenic emission percentages than premature death percentages have a negative difference smaller than -1%.

In addition, we compare contribution percentages to anthropogenic emission percentages (Figure 2.4). Figure 2.4 shows that emissions originating in California account for a smaller percent of national BC emissions than the percent of national premature deaths. While there are many states with a higher anthropogenic emission percentage than contribution percentage, such as Texas and Louisiana, a majority of these states have a difference below 1%.

To determine states that have emissions that contribute to more premature deaths than there are in that state, we analyze the differences between contribution and premature death percentages for each state (Figure 2.16c). This type of analysis allows us to estimate which states contribute disproportionately to the national health burden (red) and which

would benefit the most from national-scale uniform emissions reductions (blue). A majority of states in the southeastern US have higher premature death percentages than contribution percentages. Most states west of the Mississippi have higher contribution percentages than premature death percentages. Emissions originating in California contribute to more premature deaths than there are premature deaths in California (however, this analysis does not allow us to specify where the surplus premature deaths occur), while there are more premature deaths attributed to exposure to BC in New York than can be accounted for by BC emissions in New York. This suggests that, even for short-lived species, transport processes influence the distribution of damages from pollutant emissions at national scales. Still, despite these potentially interesting differences, overall differences across states are small, particularly compared to the order of magnitude variability in the grid-scale analysis. Therefore, there is more room for enhancing the effectiveness of BC control strategies within states or particular sectors (see next section) rather than developing state-specific caps to BC emissions.

2.4.4 Seasonal and Sectoral Trends

Here we perform an analysis of the seasonal and sectoral trends of emissions and the corresponding contributions (Figure 2.5). The sectors are sorted by contribution percentage, with the largest contributions being from onroad diesel emissions. Emissions from the fire sector have been halved for scale, while contributions from the fire sector are unaltered.

Seasonal trends in emissions do not necessarily correspond to similar seasonal trends in contributions for most sectors. For example, onroad diesel emissions are largest in the JJA months, followed by MAM, SON, and DJF, respectively. However, the contributions from these emissions are largest in the MAM season, followed closely by DJF. While onroad diesel emissions in the winter months account for the smallest percentage of annual onroad diesel emissions, their emissions in winter contribute nearly the most of any season to annual premature deaths. This is most likely attributed to the lower planetary boundary layer in

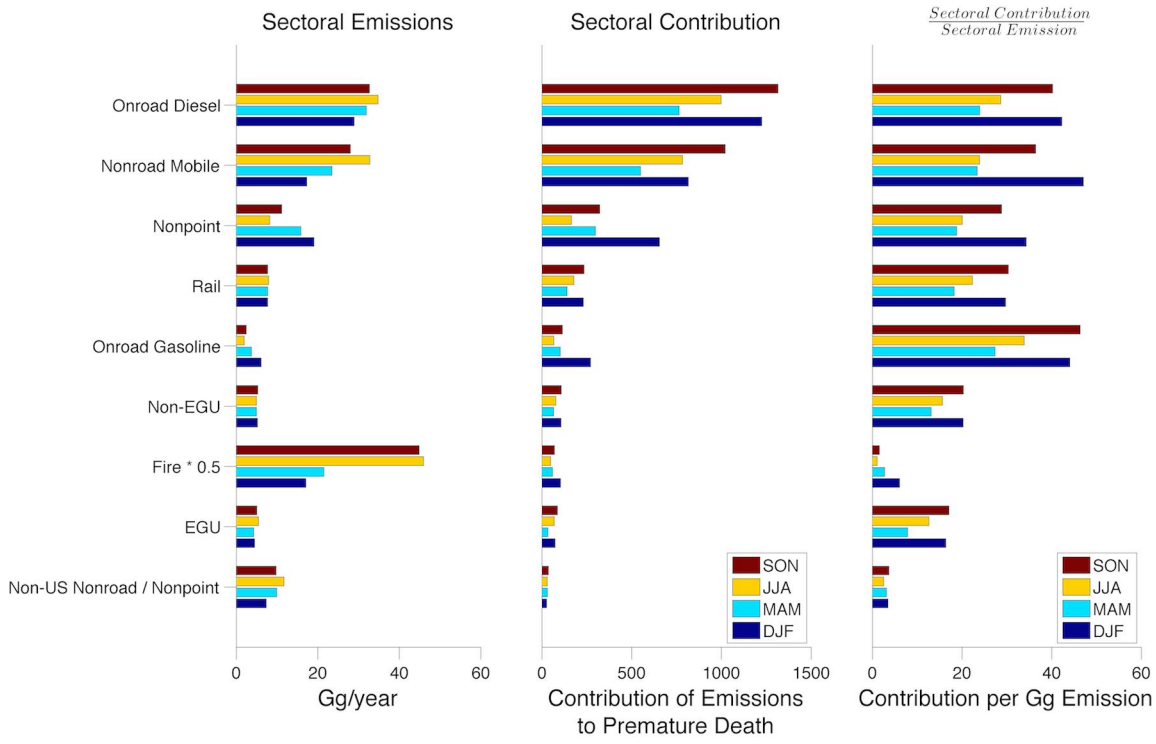

Figure 2.5: Seasonal and sectoral analysis of emissions (left), contributions (middle), and contribution per emission (right).

the winter, which results in larger ground-level concentrations per unit emitted.

In addition to seasonal variability in damages, Figure 2.5 shows that the magnitude of emissions from a sector is not necessarily an accurate predictor of the magnitude of contributions from those emissions. Fire emissions exemplify this behavior. The percent of BC emitted by fires is nearly 40% but only 3.2% of contributions come from fire emissions, which can largely be explained by the rural location of the majority of these emissions. Onroad gasoline emissions also support our finding that the magnitude of emissions are not always a good predictor of the magnitude of contributions. Onroad gasoline emissions account for approximately 2.1% of emissions, yet result in approximately 5% of premature deaths attributed to exposure to BC. Non-EGU ($\sim$3.1%) and EGU ($\sim$2.9%) sources both have larger emissions than onroad gasoline, yet the contributions from non-EGU ($\sim$3.3%) and EGU ($\sim$2.5%) sources are smaller than those from onroad gasoline emissions. However, this trend does not hold for the largest contributors. Onroad diesel and nonroad mobile sectors are the two largest contributors (with 38% and 28%, respectively), as well the two largest emitters (with 19% and 15%, respectively) excluding fire emissions. While the results presented in Figure 2.2c suggest that additional restrictions on vehicle emissions along some highways might not be the most efficient means of reducing national premature deaths attributed to exposure to BC, Figure 2.5 includes sectoral contribution information from the urban areas and suggests that the transportation sector is indeed an effective target for emissions controls.

Figure 2.5 also shows that the efficiency of BC emissions to result in premature deaths (right column) is consistently greater in the winter months. With the exception of fire emissions and non-US emissions, every sector shows significantly larger contributions per unit emission in the SON and DJF months than the JJA and MAM months. Additionally, while there are approximately 8 times more contributions from onroad diesel emissions than onroad gasoline emissions, onroad gasoline emissions of BC result in more premature deaths per unit emission than any other sector.

2.5 Conclusions

While previous source attribution studies of $PM_{2.5}$ health impacts have used simplified, reduced-form, or coarser models, we used an alternative approach (using the adjoint of CMAQ) that provides source-receptor relationships at highly-resolved sectoral, spatial, and temporal scales. Many previous studies that analyzed damages associated with air pollution assumed a single damage estimate across multiple locations and sources [Muller et al., 2011]; however, our analysis allows us to identify the damages of emissions for all locations, which are highly variable. Through adjoint-based analysis, we have shown that highly populated urban areas have larger premature death percentages than BC emission percentages. Additionally, we compared damage percentages (percent of premature deaths resulting from emissions in a specific location) to premature death, population, and emission percentages. We found that while damage percentages are highly correlated with premature death and population percentages, there is little correlation between damage percentages and emission percentages, suggesting that controls on the largest emitters would not be an efficient means of reducing damages associated with exposure to BC. In addition to the gridded analysis, we performed a state-level analysis of the results. However, the overall differences in emission, damage, and premature death percentage are small at these scales, suggesting that optimal control strategies for BC need to be developed at a state and sector level. While our analysis provides source-receptor relationships at high sectoral, spatial, and temporal scales, there are some drawbacks. Our analysis utilized a single chemical transport model, as opposed to other studies in the broader field of air quality modeling that have used an ensemble of simulations to minimize uncertainty owing to any single model [Mallet and Sportisse, 2006; Stevenson et al., 2006; van Noije et al., 2006; Koch et al., 2009]. There is also uncertainty associated with the health impact function. We chose to use a concentration response factor that corresponds to the relative risk of exposure to $PM_{2.5}$, as opposed to using a concentration response factor specific to exposure to BC. Additionally, our analysis exclusively considered prema-

ture deaths attributed to pollutant exposure for the entire adult population, as opposed to focusing on certain demographics that have been shown to be at a higher risk [Flachs et al., 2013; Wilhelm et al., 2009; Bell and Dominici, 2008; Neidell, 2004]. While our analysis uses emission profiles from 2007, mobile emissions have been declining in the US[Dallmann and Harley, 2010]. This decrease in mobile emissions would most likely result in fewer estimated health impacts. Also, our estimate of health impacts does not include premature deaths in Canada or Mexico, yet emissions of BC in the US can result in premature deaths in neighboring countries. Furthermore, previous studies have shown that premature death estimates from forward model studies can vary largely for different horizontal grid resolutions [Punger and West, 2013; Thompson and Selin, 2012; Li et al., 2015], with premature death estimates decreasing at coarser grid resolutions. Based on these studies, we estimate that our analysis (performed at the 12 km resolution) has a low bias relative to higher resolution simulations (4 km) of only a few percent. However, our estimate would likely present a lower bound for this bias as neither 12 km nor 4 km simulations are at a fine enough resolution to accurately resolve near-roadway gradients in BC concentrations. Finally, while this paper's focus is on premature deaths in the US associated with exposure to BC, this work could be extended to analyze the effects of BC emissions on premature death within a specified region, state, or socio-economic demographic. This work can also be extended to analyze sources contributing to premature death owing to exposure of total $PM_{2.5}$, similar to previous studies that used adjoints sensitivities from coarser models [Dedoussi and Barrett, 2014].

2.6 Acknowledgements

This research was supported by NASA Applied Sciences Program grant NNX09AN77G. This paper has been subjected to the United States Environmental Protection Agency's administrative review and approved for publication but solely reflects the views of the authors. Shannon L. Capps was supported by an appointment to the Research Participation Program at the Office of Research and Development, US EPA, administered by ORISE.

2.7 Supplemental Information

Table 2.1: Statistical analysis of CMAQ model performance for BC concentrations.

Observation Network	R^2	MAE	Mean Bias	RMSE	NMB
IMPROVE	0.65	0.13	0.09	0.14	33.6%
CSN	0.19	0.50	-0.22	0.45	-17.8%

2.7.1 CMAQ Adjoint Validation

An adjoint of the entire AERO5 module in CMAQ has been developed. In order to verify that the adjoint has been correctly derived, one needs to compare the calculated adjoint sensitivities to another form of sensitivity calculation. The validation performed for this project compares adjoint sensitivities to first-order finite difference sensitivities, with varying percentage perturbations. First-order finite difference (FD) sensitivities are calculated by

$$\frac{\partial f}{\partial x} = \frac{f(x+h) - f(x)}{h} \tag{2.2}$$

where $f(x)$ is the concentration output from the default inputs, h is the perturbation, and $f(x+h)$ is the concentration output from the perturbed inputs. One problem with the finite difference approximation is the dependence on the perturbation size. Choosing a perturbation that is too small can result in errors due to subtractive cancellation. However, perturbation sizes too large can result in errors due to the nonlinearity of the model.

For certain cases where finite difference calculations do not provide correct sensitivities, complex variable sensitivities were used in order to confirm that the adjoint is providing correct results. Complex variable sensitivities are calculated by

$$\frac{\partial f}{\partial x} \approx \frac{Im[f(x+ih)]}{h} \tag{2.3}$$

The complex variable estimate is not subject to subtractive cancellation, since it does not involve a difference operation. In order to compute complex variable sensitivities for

the CMAQ model, the entire model (or part of the model that is being validated) must be modified to perform all calculations with complex numbers, as opposed to real numbers. Simulations performed with complex arithmetic not only have longer runtimes, but also use approximately double the memory requirements.

When performing the adjoint validation simulations, gradient data were generated for the entire U.S. domain at a 36-km resolution. Simulations were run for varying durations (ranging from 1 timestep simulations to 1-day simulations) using inputs for April 03, 2008. In an effort provide a more physically-relevant initial condition profile, a spin-up simulation was performed, running from April 01, 2008 through April 02, 2008. However, for certain cases it was necessary to replace initial concentrations for some species with larger values. For example, after the two day spin-up simulation certain species still had concentrations of 1.0E-30 $\frac{\mu g}{m^3}$. Applying any percentage perturbation smaller than 100% to a value this small results in an incorrect sensitivity value of 0, due to the fact that the perturbation is outside the numerical precision of the computer.

2.7.1.1 Aerosol Module Validation

For Figures 2.6 and 2.7, sensitivities are calculated for the list of species given in Table 2.2.

When performing finite difference sensitivity calculations, we found it best to not include aerosol thermodynamics (ISORROPIA) in the aerosol module. ISORROPIA is a highly nonlinear, discontinuous aerosol thermodynamics model, which is subject to substantial cancellation errors when sensitivities are calculated with the finite difference method. ANISORROPIA (the adjoint of ISORROPIA), however, has been validated by comparing adjoint sensitivities to complex variable sensitivities [Capps et al., 2011]. Therefore, we can generate finite difference sensitivities of the aerosol adjoint without ISORROPIA and still be confident in the accuracy of the full aerosol adjoint.

Series of simulations were run with different forcings (adjoint) and perturbations (finite

NO2	Nitrogen Dioxide
N2O5	Dinitrogen Pentoxide
HNO3	Nitric Acid
HCL	Hydrochloric acid
ASO4J	Accumulation mode sulfate aerosol
ASO4I	Aitken mode sulfate aerosol
ANH4J	Accumulation mode ammonium aerosol
ANH4I	Aitken mode ammonium aerosol
ANO3J	Accumulation mode nitrate aerosol
ANO3I	Aitken mode nitrate aerosol
AECJ	Accumulation mode elemental carbon
AECI	Aitken mode elemental carbon
AH2OJ	Accumulation mode water aerosol
AH2OI	Aitken mode water aerosol
ANAJ	Accumulation mode sodium aerosol
ACLJ	Accuulation mode chlorine aerosol
ACLI	Aitken mode chlorine aerosol
NH3	Ammonia

Table 2.2: List of species used in Jacobian sensitivity calculations

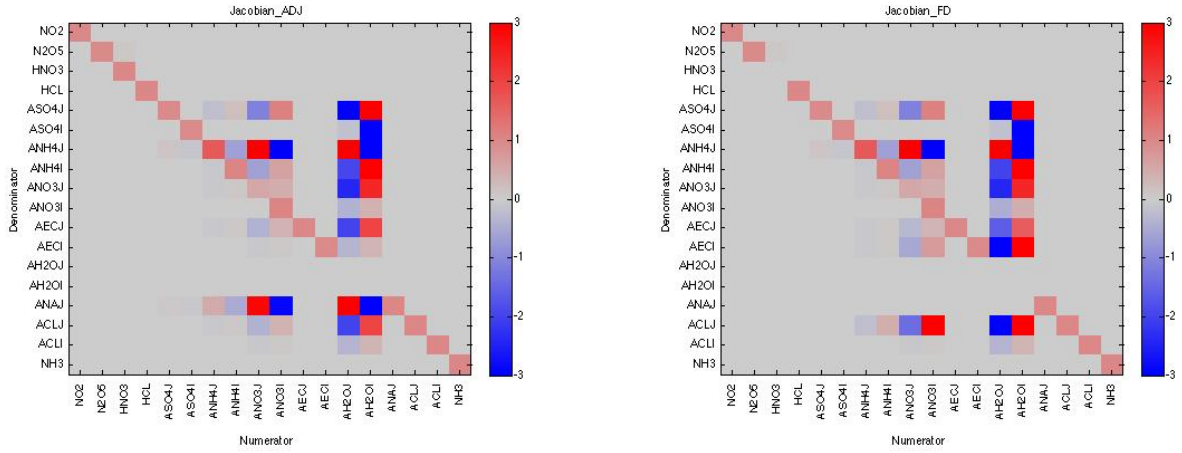

(a) (b)

Figure 2.6: Partial Jacobian plots of (a) adjoint sensitivities and (b) FD sensitivities for aerosol-only simulations without aerosol thermodynamics. Simulations were run for two timesteps.

difference) in order to generate partial Jacobian data for aerosol-only simulations without ISORROPIA. When comparing the adjoint Jacobian (Figure 2.6(a)) to the FD Jacobian (Figure 2.6(b)) for two timesteps, it is evident that while the sensitivities are comparable for many relationships, there are some relationships for which the adjoint and FD do not match. Specifically, instances with accumulation mode sodium (ANAJ) in the denominator show sensitivities of zero for FD, while the adjoint provides non-zero values. Additionally, the sensitivity of nitric acid (HNO_3) with respect to nitric acid shows a sensitivity of zero in the FD test, yet shows a value of approximately one in the adjoint.

The differences between adjoint and finite-difference sensitivities are most likely attributable to failure of the finite-difference simulations to accurately calculate the sensitivities. In order to confirm this, similar tests were performed comparing adjoint sensitivities (Figure 2.7(a)) to complex variable method (CVM) sensitivities (Figure 2.7(b)), however for a single timestep. Simulations to generate the CVM partial Jacobian were performed by Shunliu Zhao at Carleton University.

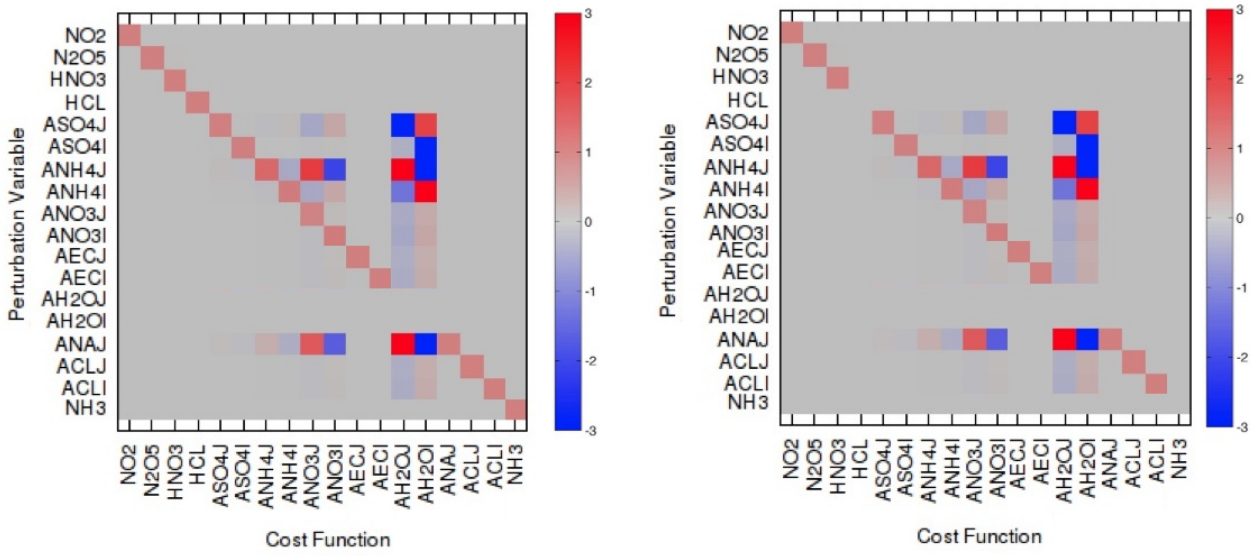

(a) (b)

Figure 2.7: Partial Jacobian plots of (a) adjoint sensitivities and (b) CVM sensitivities for aerosol-only simulations that exclude aerosol thermodynamics. Simulation was run for one timestep.

From Figure 2.7 it is apparent that the zero sensitivity values with ANAJ in the denominator in the previous figure (Figure 2.6) are attributed to a failure in the FD calculations. Additionally, for this specific configuration of the aerosol module, it can be determined that the aerosol module is behaving properly. However, there are still a few instances where the adjoint and CVM sensitivities do not match; specifically, sensitivities of NH_3 with respect to NH_3, and sensitivities of HCL with respect to HCL, where the adjoint provides sensitivities of one, and the CVM provides sensitivities of zero. However, the finite difference calculations provide values of one for these relationships. One would expect the sensitivity of a species to itself to be one for a single timestep, hence the disagreement between adjoint and CVM sensitivities for these cases is likely owing to an error in the CVM calculation.

2.7.1.2 Emission Sensitivity Validation

By default, the CMAQ adjoint calculates the sensitivity of a given cost function with respect to concentrations. While sensitivities with respect to concentrations provide vital information for many studies, there are a large number of applications that require sensitivities with respect to emissions. As with the development of the aerosol adjoint, the inclusion of emission sensitivity calculation requires its own validation tests.

As opposed to the validation of the aerosol module, the validation of the emission sensitivity calculation cannot simply treat the domain as an array of box models. Within the CMAQ model, the injection of emissions into the model occurs in the vertical diffusion (VDIFF) module. The VDIFF module transports concentrations vertically between layers. Because of the transport between layers, validation of the vertical diffusion (VDIFF) and vertical advection (ZADV) was performed for simulations where the domain was treated as an array of column models.

For the first-order finite difference sensitivity calculations of BC with respect to BC emissions, a 0.01% perturbation was applied to concentrations in entire columns. After allowing the simulations to run for four hours, scaled sensitivity values were calculated by

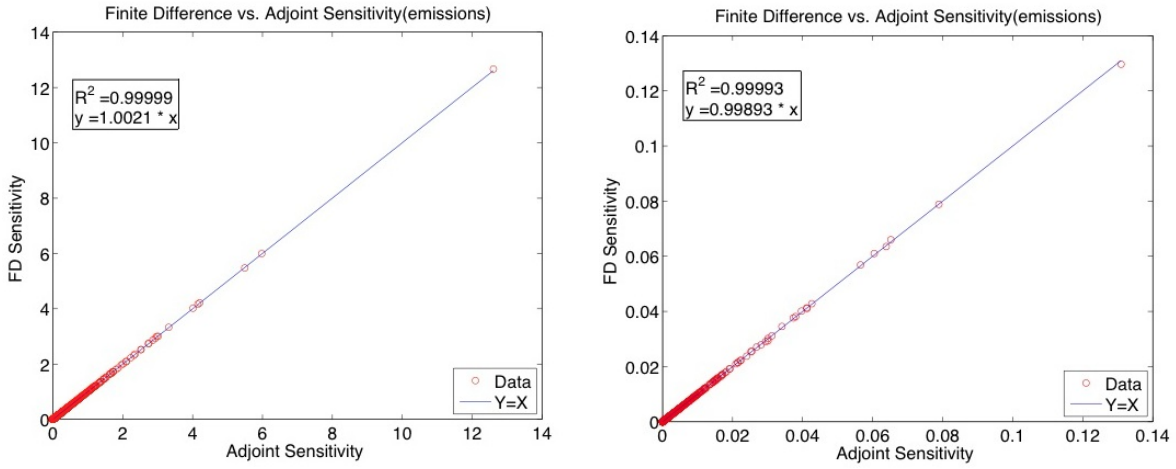

(a) (b)

Figure 2.8: Finite Difference $\frac{\Delta Conc}{SF_{emis}}$ vs. Adjoint emission sensitivity ($\frac{\partial J_{layer}}{\partial emis} * emis$) for (a) layer 1, and (b) layer 12. Model configuration included only VDIFF and ZADV.

dividing the change in output concentrations in a single layer by the emissions scaling factor, or perturbation ($\frac{\Delta Conc}{SF_{emis}}$). On the other hand, semi-normalized adjoint sensitivities were calculated by applying a forcing in a single layer (the same layer for which concentrations were analyzed in the finite difference calculations) at the end of the four hour simulation and then looking at output sensitivity values summed over the entire column, scaled by the emissions ($\frac{\partial J_{layer}}{\partial emis} * emis$). Since every layer between layer two and TOA are handled the same within the vertical transport code, it is only necessary to validate one of these layers in order to confirm the accuracy of the adjoint code.

Initial emission sensitivity validation was performed for a configuration that included only vertical diffusion (VDIFF) and vertical advection (ZADV). Since the vertical layer closest to the surface (layer one) is handled separately from the rest of the vertical layers, validation tests were performed for two different layers, layer one (Figure 2.8(a)) and layer twelve (Figure 2.8(b)).

One can see from Figure 2.8 that the adjoint gradients match the finite difference gradients for both layer one and layer twelve nearly perfectly. For the validation of both

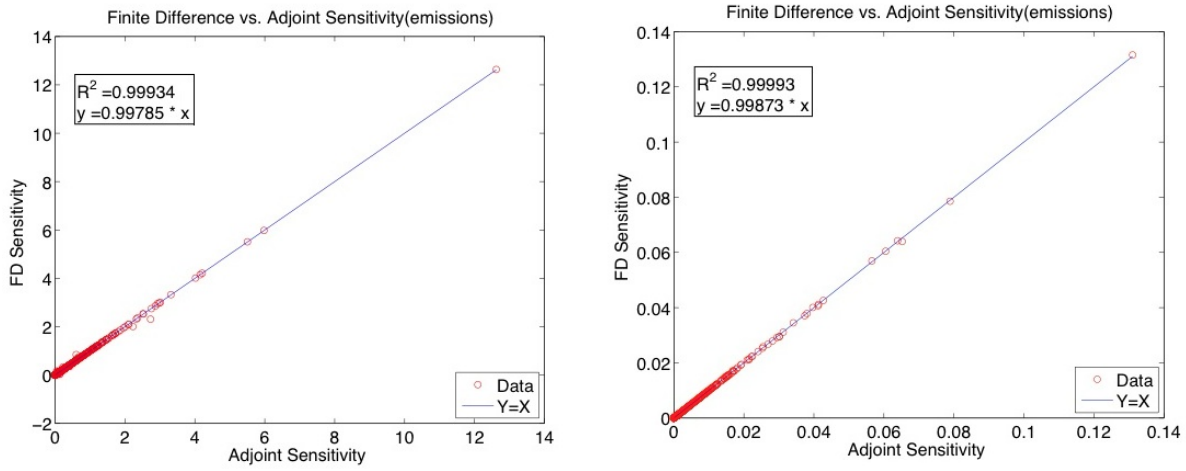

(a) (b)

Figure 2.9: Finite Difference $\frac{\partial Conc}{SF_{emis}}$ vs. Adjoint emission sensitivity ($\frac{\partial J_{layer}}{\partial emis} * emis$) for (a) layer 1, and (b) layer 12. Model configuration included VDIFF, ZADV, and AERO5.

layers, we have an R^2 value that is nearly one. Additionally, the scatter plots show that all points lie essentially on the one-to-one line. Because of this, we can conclude that the calculation of sensitivities with respect to emissions has been properly implemented.

In addition to the above validation tests that were performed with a model configuration that included only VDIFF and ZADV, validation of sensitivity with respect to emissions were also performed for a configuration that included the aerosol module (AERO5, VDIFF, ZADV). As in the validation above, validation tests for this configuration were performed for both layer one (Figure 2.9(a)) and layer twelve (Figure 2.9(b)).

Again, it can be seen from Figure 2.9 that the adjoint gradients match the finite difference gradients nearly perfectly for both layers. For the configuration that includes the AERO5 module the agreement between adjoint and FD sensitivities for layer one is slightly worse, with a few points falling off of the one-to-one line. However, the R^2 value is still nearly one and the points not on the one-to-one line are very close to lying on the line. Based on these emission sensitivity comparisons with the inclusion of the AERO5 module, it can be determined that the emissions sensitivity calculation has been implemented correctly. It can

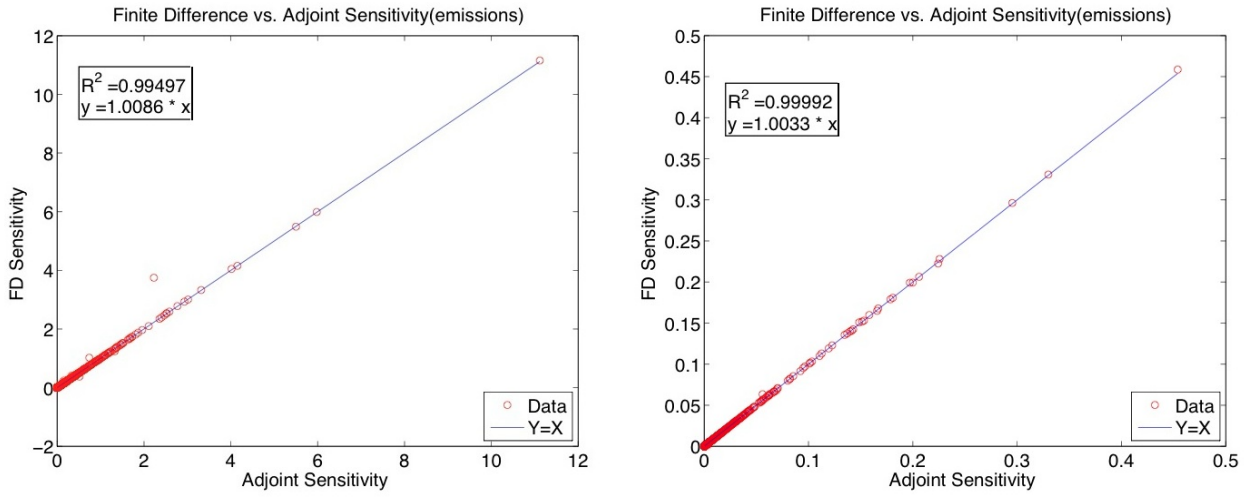

(a) (b)

Figure 2.10: Finite Difference $\frac{\partial Conc}{SF_{emis}}$ vs. Adjoint emission sensitivity ($\frac{\partial J_{layer}}{\partial emis} * emis$) for (a) layer 1, and (b) layer 8. Model configuration included VDIFF, ZADV, AERO, and CLOUDS.

also be determined that the aerosol module is correctly coded for sensitivities of BC with respect to BC.

Working towards a full model validation, another validation test was performed for a model configuration that included CLOUDS into the previous configuration. For this configuration validation was again performed for two separate layers. However, validation tests were performed for layer one (Figure 2.10(a)) and layer eight (Figure 2.10(b)), as opposed to layer twelve.

It can be determined from Figure 2.10 that, in addition to emissions sensitivity calculations being properly implemented, the cloud adjoint module is also correctly written for BC processes. The adjoint and finite difference sensitivities again match nearly perfectly for both layers, however the first layer scatterplot now contains a few points that are off the one-to-one line, one of which has a FD sensitivity value that is approximately 165% that of the adjoint sensitivity (FD $\approx$ 3.8, ADJ $\approx$ 2.3). This is most likely caused by nonlinearities in the model causing the finite difference calculation to result in an incorrect sensitivity value.

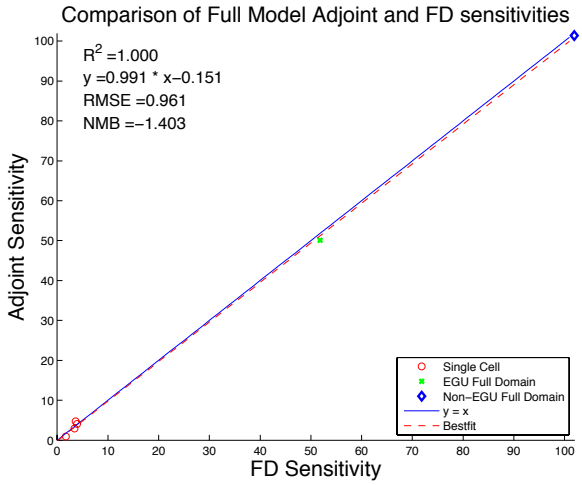

Figure 2.11: Comparison of adjoint and finite difference estimations of the premature deaths attributed to exposure to BC in the US from both single grid cell emissions, and single sector emissions.

2.7.1.3 Full Model Validation

We have performed a validation test for a model configuration that included all processes except gas-phase chemistry and aqueous chemistry. For this validation, we compare finite difference and adjoint estimations of premature deaths attributed to exposure to BC in the US. Validations were performed comparing both single grid cell estimates (for all sources), as well as single source estimates (for all grid cells). The resultant semi-normalized sensitivities give an estimate of the number of premature deaths attributed to emissions from any grid cell or source. Figure 2.11 presents the comparison between FD sensitivities and adjoint sensitivities, and shows that our results are accurate to within approximately ± 1 premature death.

2.7.2 Uncertainty Calculation

Calculation of the uncertainty in the estimate of premature deaths associated with exposure to BC was performed through propagation of errors (Equation 2.4)

$$\sigma_T = \frac{\sqrt{\sum_{i=1}^{N} \left(\frac{\partial J}{\partial \beta}\right)_i^2 \sigma_\beta^2 + \left(\frac{\partial J}{\partial C_{av,i}}\right)_i^2 \sigma_C^2}}{N} \tag{2.4}$$

where J is the cost function, i is the grid cell index, N is the total number of grid cells for which the cost function is calculated, β is the concentration response factor, $C_{av,i}$ is the annual average concentration for grid cell i, σ_C is the uncertainty in the simulated concentrations, and σ_β is the uncertainty in the concentration response factor. For σ_C, we use the mean absolute error when comparing the simulated annual average to the observed annual average from CSN sites ($\sigma_C = 0.503$). While the mean absolute error for comparing simulated to observed concentrations for IMPROVE sites is much lower, we chose to use the mean absolute error from the comparison to CSN sites since a majority of premature deaths occur in urban areas, and the CSN network has more observation sites in urban areas. We used a value for σ_β of 0.32, which was calculated from the range of relative risks provided in Krewski et al. [2009].

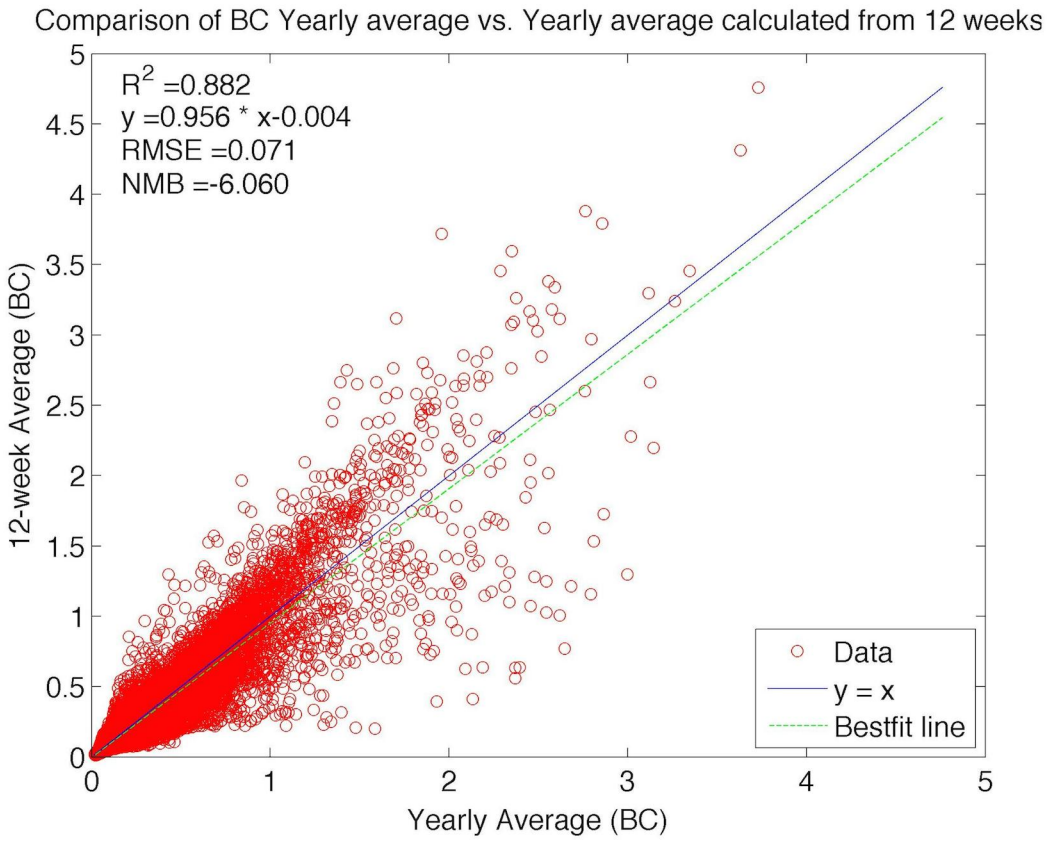

Figure 2.12: Comparison of yearly average BC concentrations to 12 week average BC concentrations.

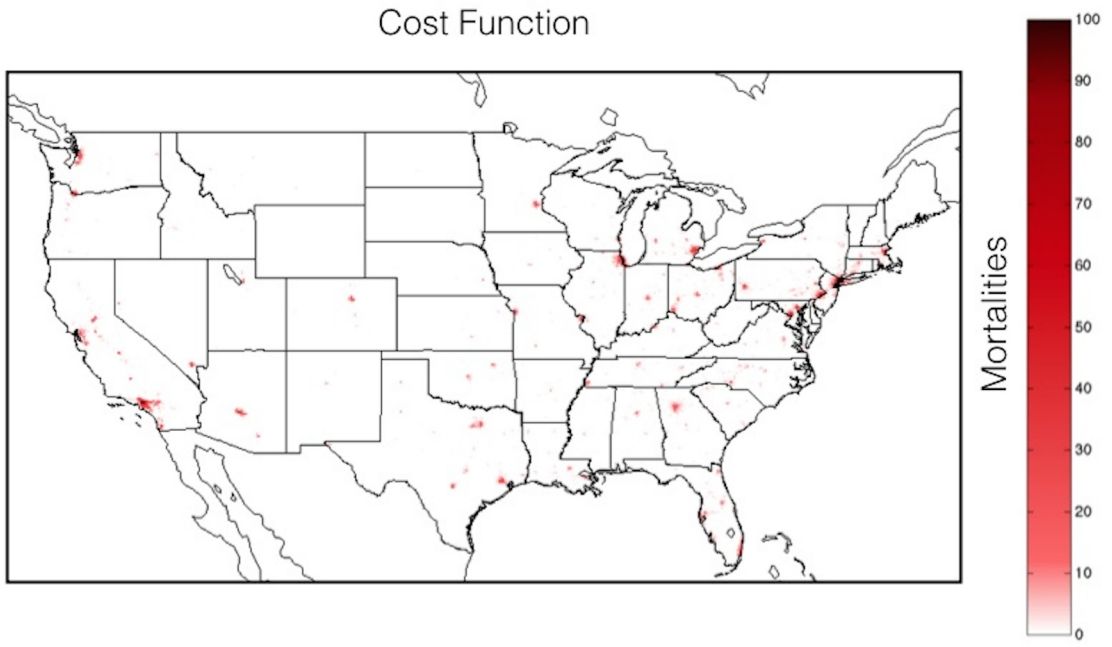

Figure 2.13: Gridded annual premature deaths associated with exposure to BC concentrations.

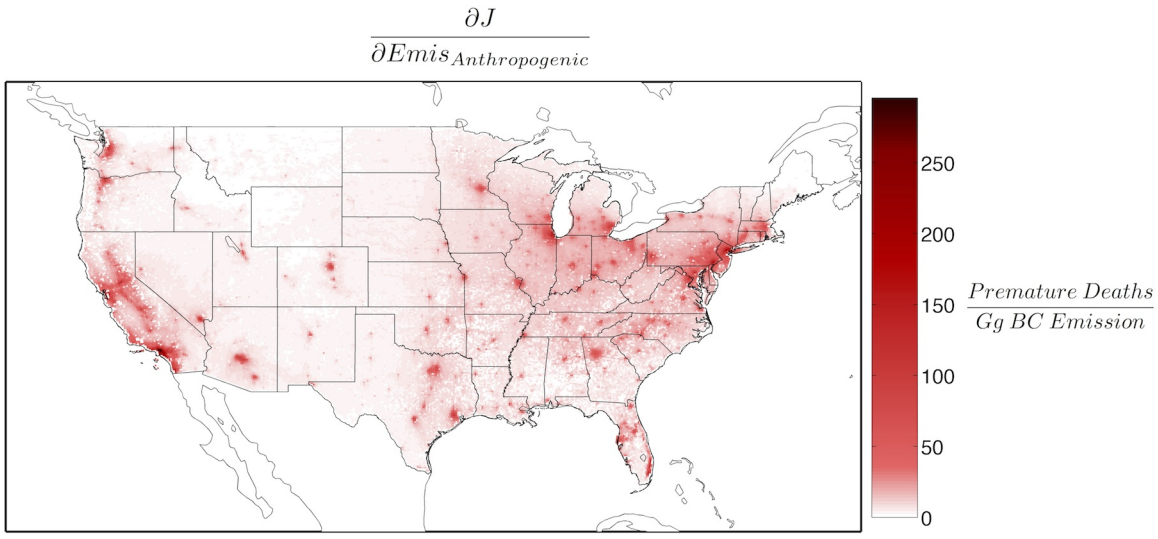

Figure 2.14: Gridded damage estimates ($\frac{\partial J}{\partial E}$) from BC emissions.

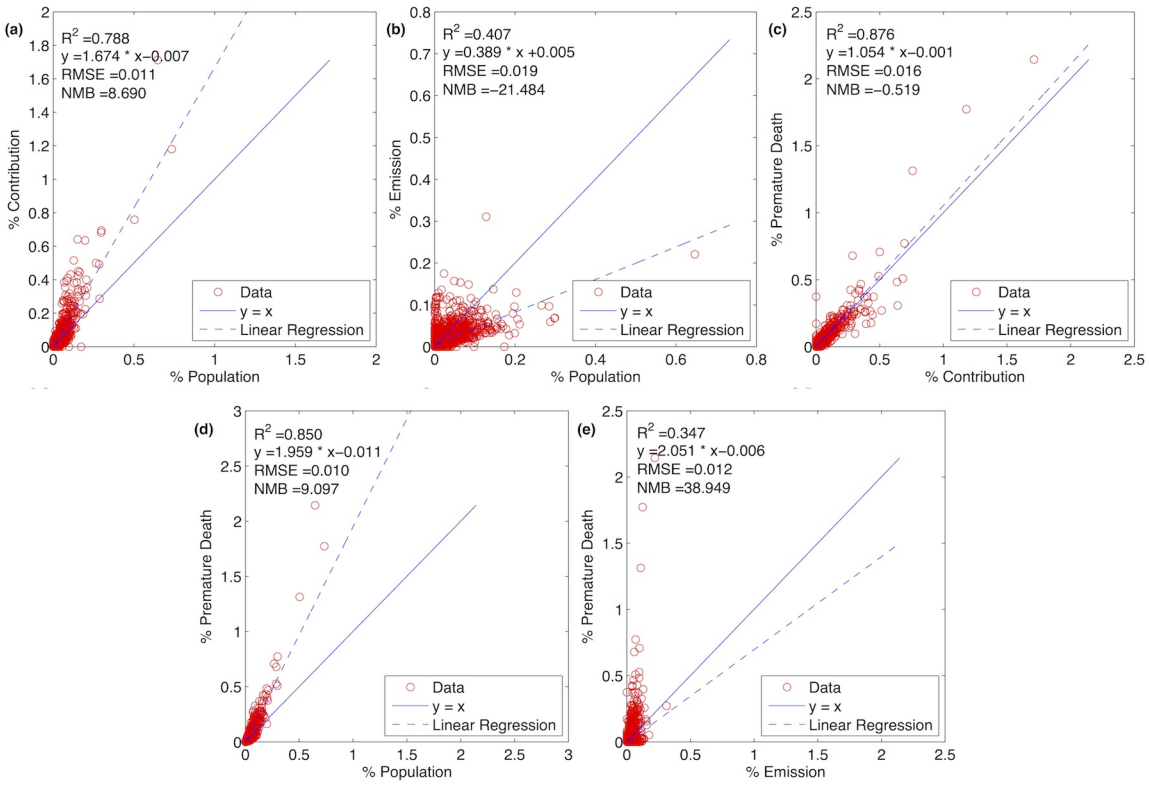

Figure 2.15: Comparison of (a) contribution percentage from anthropogenic emissions to population percentage, (b) anthropogenic emission percentage to population percentage, (c) premature death percentage to contribution percentage from anthropogenic emissions, (d) premature death percentage to population percentage, and (e) premature death percentage to anthropogenic emission percentage.

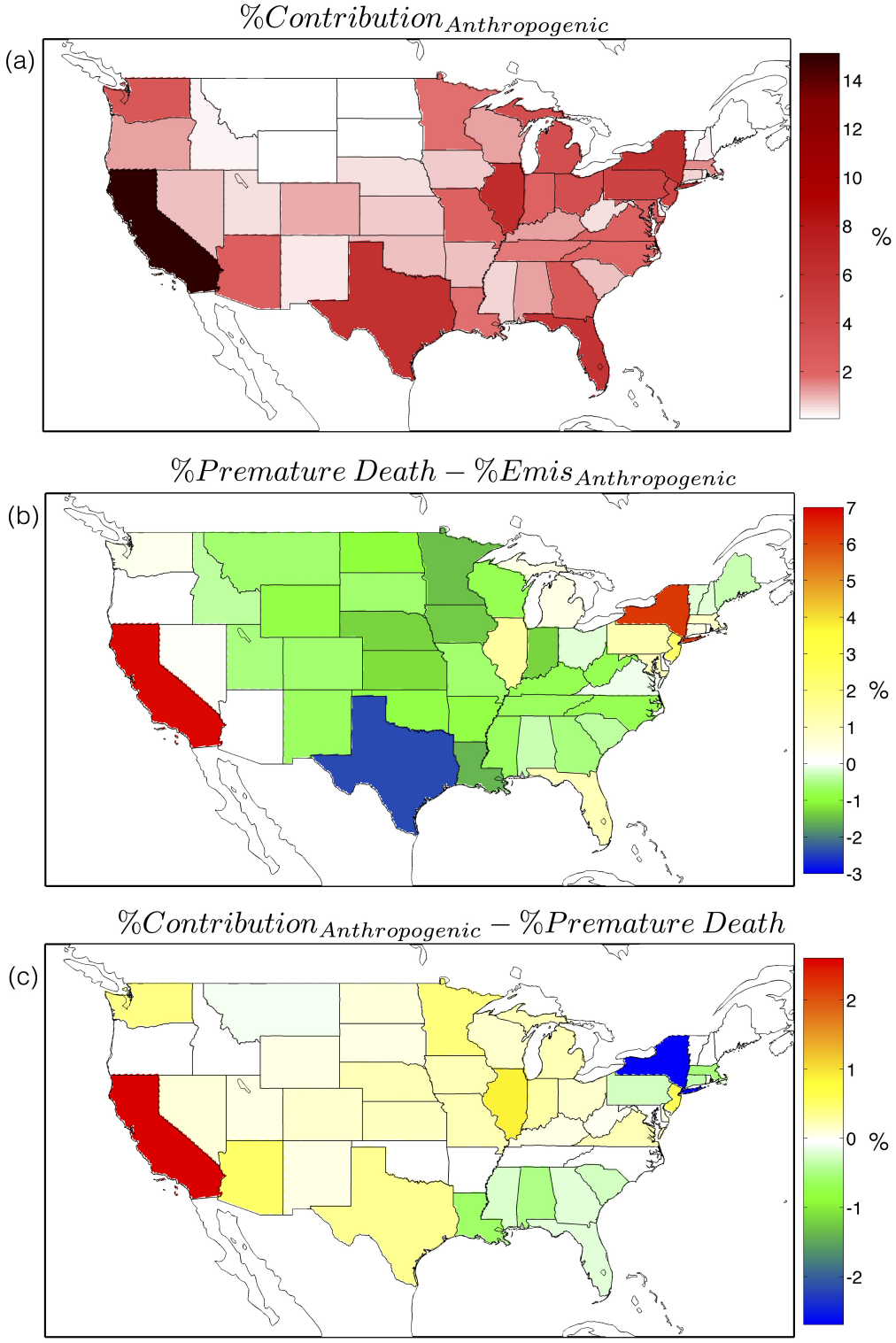

Figure 2.16: State based analysis of adjoint sensitivities. (a) Contribution percentage from anthropogenic emissions, (b) premature death percentages minus anthropogenic emission percentage, (c) contribution percentage from anthropogenic emissions minus premature death percentage.

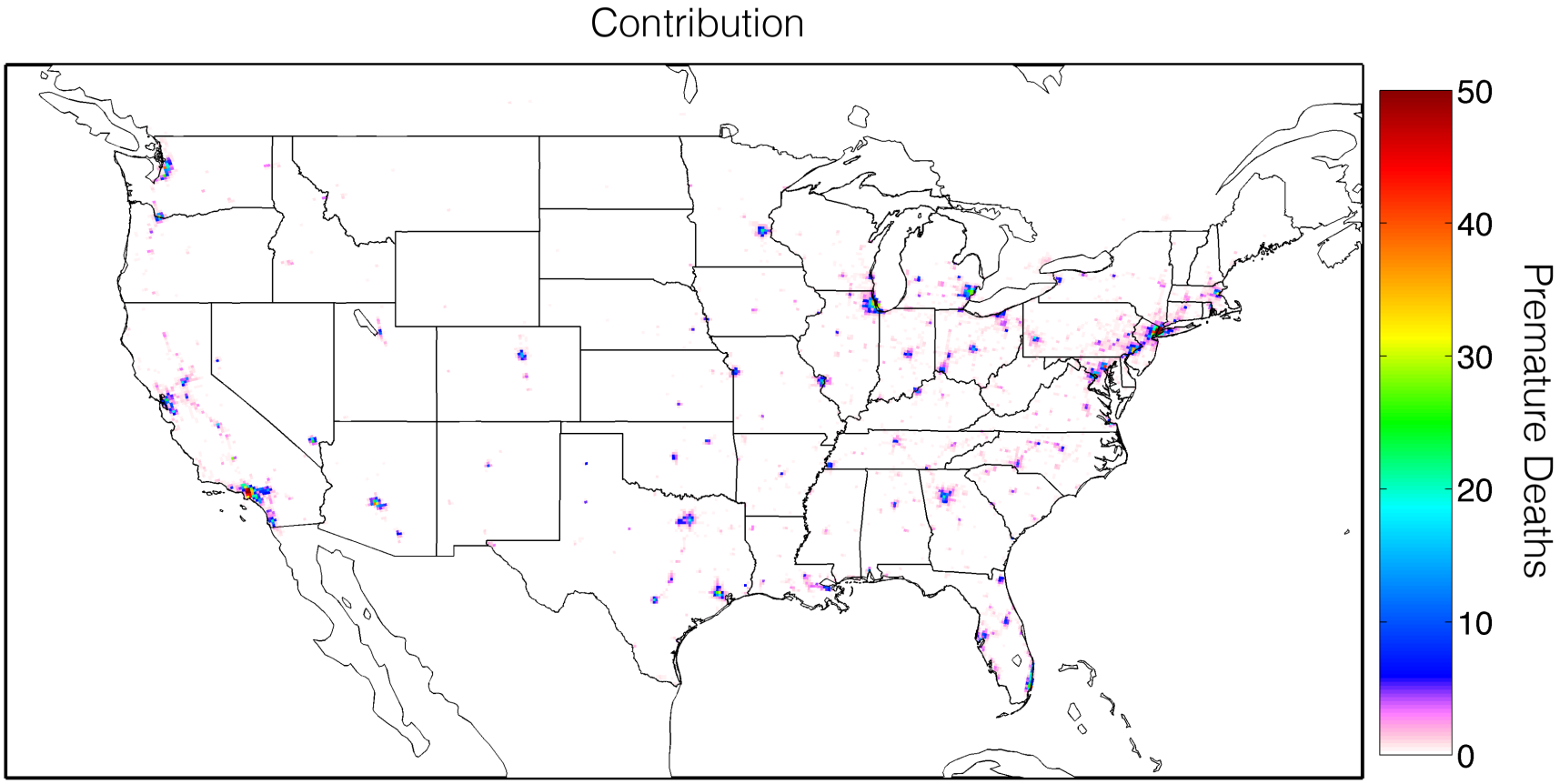

Figure 2.17: Semi-normalized sensitivities ($\frac{\partial J}{\partial Emis} \cdot Emis$) showing the sensitivity of national premature death to emissions in each grid cell. A maximum of 174 premature deaths are attributed to BC emitted from New York, NY.

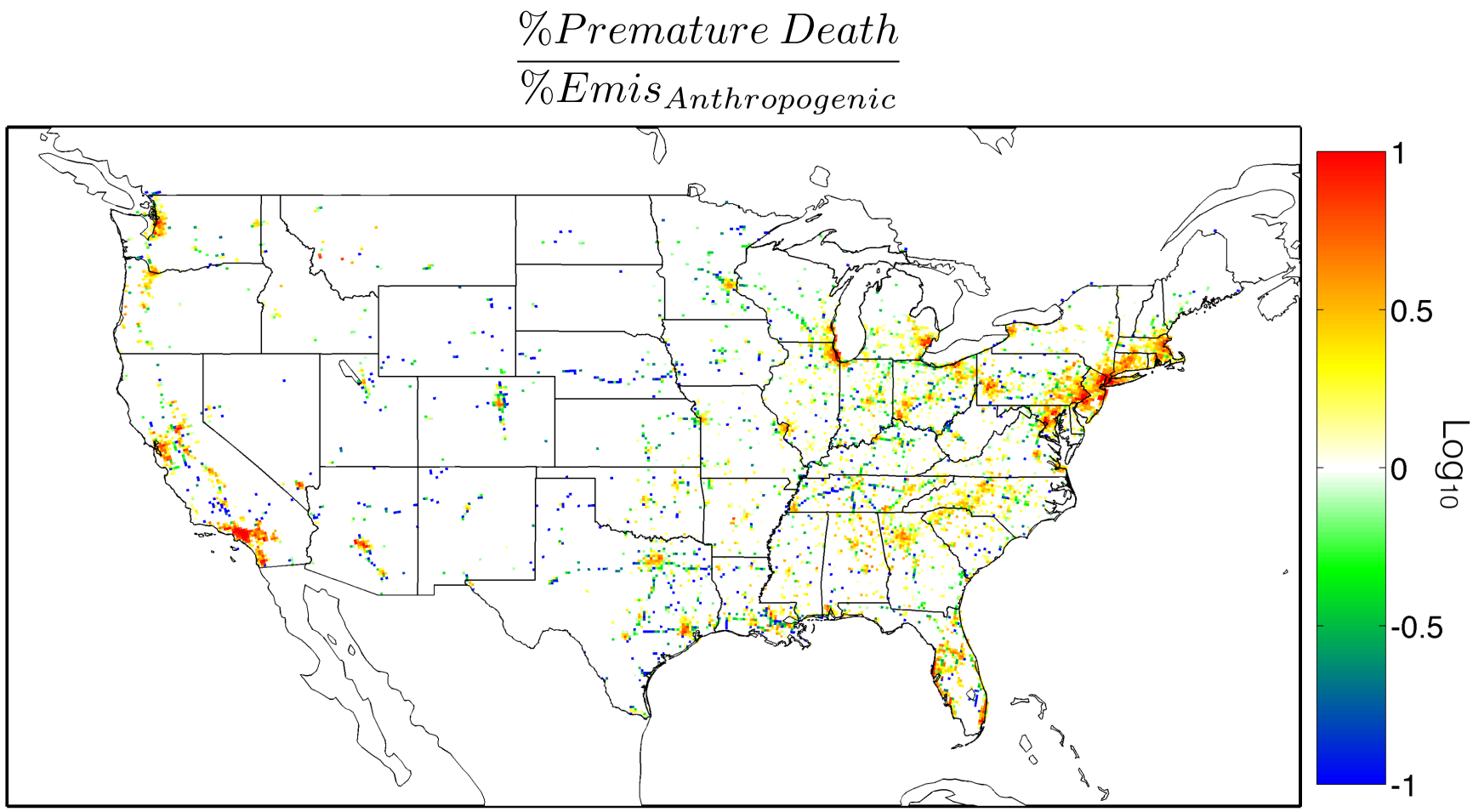

Figure 2.18: Ratio of gridded premature death percentage over gridded anthropogenic emission percentage, plotted on a log scale.

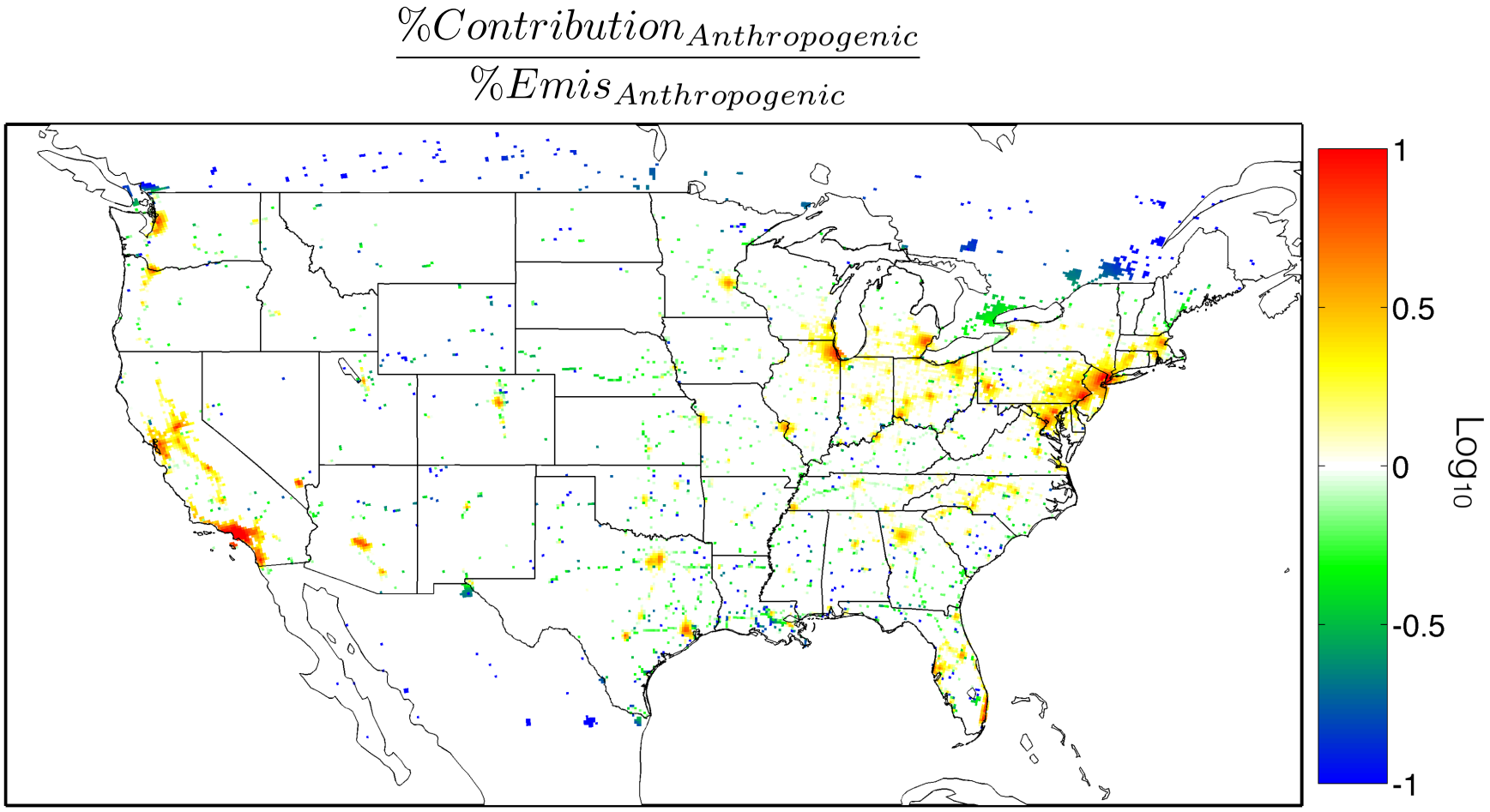

Figure 2.19: Ratio of gridded contribution percentage from anthropogenic emissions over gridded anthropogenic emission percentage, plotted on a log scale.

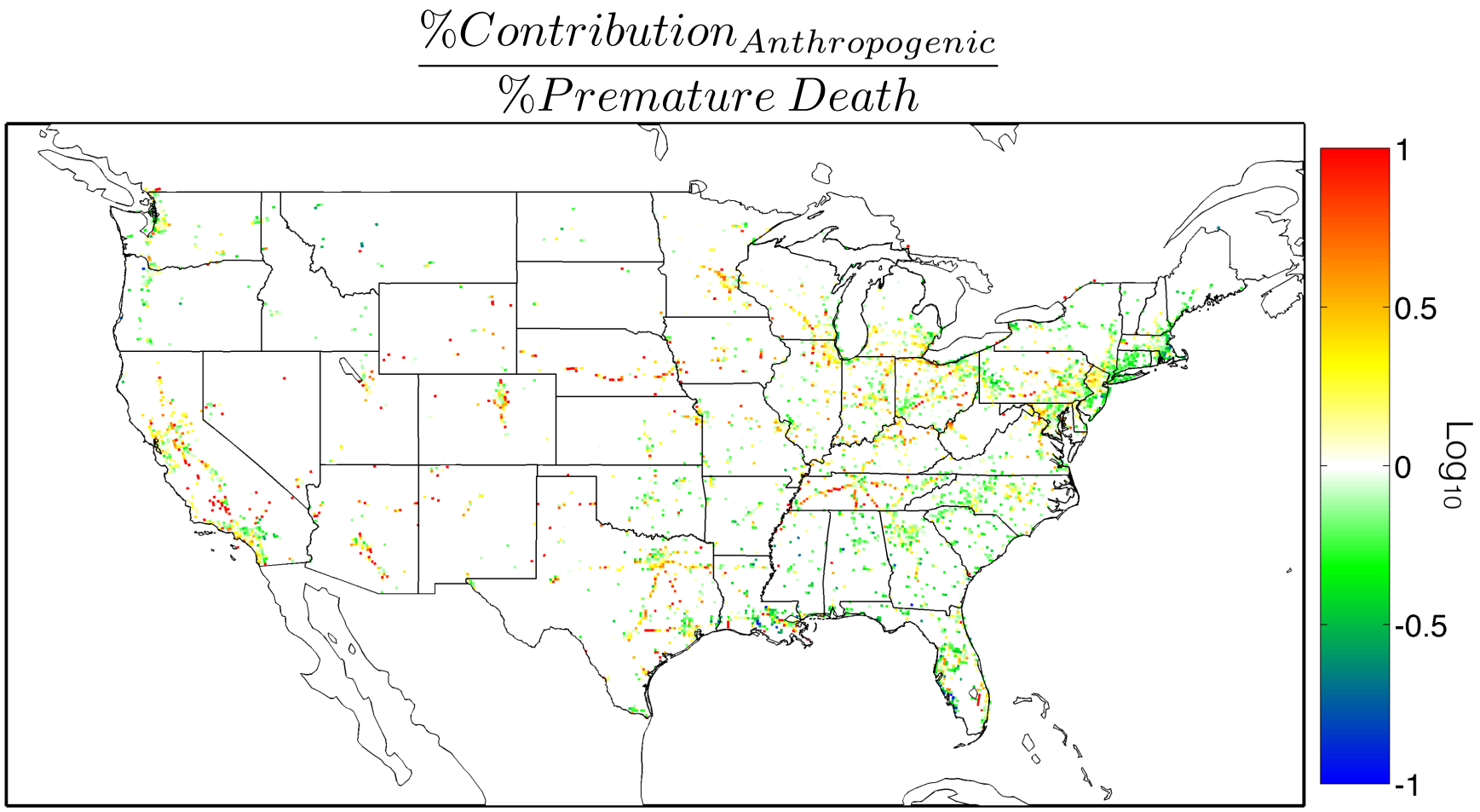

Figure 2.20: Ratio of gridded contribution percentage from anthropogenic emissions over gridded premature death percentage, plotted on a log scale.

2.8 References

Environmental Benefits and Mapping Program (BenMAP, Version 4.0.67). Abt Associates, Inc., 2013. Bethesda, MD.

SD Adar, DR Gold, BA Coull, J Schwartz, PH Stone, and H Suh. Focused exposures to airborne traffic particles and heart rate variability in the elderly. Epidemiology, 18(1): 95–103, January 2007.

SC Anenberg, K Talgo, S Arunachalam, P Dolwick, C Jang, and JJ West. Impacts of global, regional, and sectoral black carbon emission reductions on surface air quality and human mortality. Atmos. Chem. Phys., 11(14):7253–7267, 2011.

SC Anenberg, J Schwartz, D Shindell, M Amann, G Faluvegi, Z Klimont, G Janssens-Maenhout, L Pozzoli, R Van Dingenen, E Vignati, L Emberson, NZ Muller, JJ West, M Williams, V Demkine, WK Hicks, J Kuylenstierna, F Raes, and V Ramanathan. Global air quality and health co-benefits of mitigating near-term climate change through methane and black carbon emission controls. Environ. Health Perspect., 120(6):831–839, June 2012.

SE Bauer and S Menon. Aerosol direct, indirect, semidirect, and surface albedo effects from sector contributions based on the IPCC AR5 emissions for preindustrial and present-day conditions. J. Geophys. Res.: Atmos., 117:D01206, 2012.

ML Bell and F Dominici. Effect modification by community characteristics on the short-term effects of ozone exposure and mortality in 98 us communities. Am. J. Epidemiol., 167(8): 986–997, 2008.

ML Bell, K Ebisu, RD Peng, JM Samet, and F Dominici. Hospital admissions and chemical composition of fine particle air pollution. Am. J. Respir. Crit. Care Med., 179(12):1115–1120, June 2009.

TC Bond. Can warming particles enter global climate discussions? Environ. Res. Letters, 2 (4), 2007.

TC Bond, SJ Doherty, DW Fahey, PM Forster, T Berntsen, BJ DeAngelo, MG Flanner, S Ghan, B Kärcher, and D Koch. Bounding the role of black carbon in the climate system: A scientific assessment. J. Geophys. Res.: Atmos., 118(11):5380–5552, 2013.

D Byun and KL Schere. Review of the governing equations, computational algorithms, and other components of the Models-3 Community Multiscale Air Quality (CMAQ) modeling system. Appl. Mech. Rev., 59(1/6):51, 2006.

SL Capps, DK Henze, A Hakami, AG Russell, and A Nenes. Anisorropia: the adjoint of the aerosol thermodynamic model isorropia. Atmos. Chem. Phys., 11(8):23469–23511, 2011.

CJ Coats and MR Houyoux. Fast emissions modeling with the sparse matrix operator kernel emissions modeling system. In The Emissions Inventory: Key to Planning, Permits, Compliance, and Reporting, New Orleans, LA, 1996.

AJ Cohen, HR Anderson, B Ostro, KD Pandey, M Krzyzanowski, N Kuenzli, K Gutschmidt, CA Pope, I Romieu, JM Samet, and KR Smith. Mortality impacts of urban air pollution. In Majid Ezzati, AD Lopez, A Rodgers, and C Murray, editors, Comparative Quantification of Health Risks: Global and Regional Burden of Disease Due to Selected Major Risk Factors, Vol. 2. World Health Organization, Geneva, 2004.

TR Dallmann and RA Harley. Evaluation of mobile source emission trends in the united states. J. Geophys. Res.: Atmos., 115, 2010.

IC Dedoussi and SRH Barrett. Air pollution and early deaths in the united states. part ii: Attribution of pm2.5 exposure to emissions species, time, location and sector. Atmos. Environ., 99(C):610–617, December 2014.

O Dubovik, T Lapyonok, YJ Kaufman, M Chin, P Ginoux, RA Kahn, and A Sinyuk. Retrieving global aerosol sources from satellites using inverse modeling. Atmos. Chem. Phys., 8(2):209–250, 2008.

H Elbern, H Schmidt, O Talagrand, and A Ebel. 4d-variational data assimilation with an adjoint air quality model for emission analysis. Environ. Modell. Softw., 15(6-7):539–548, 2000.

J Ewer, ER Galea, M Patel, S Taylor, B Knight, and M Petridis. Smartfire: an intelligent cfd based fire model. J. Fire Protect. Eng., 10(1):13–27, 1999.

N Fann, CM Fulcher, and BJ Hubbell. The influence of location, source, and emission type in estimates of the human health benefits of reducing a ton of air pollution. Air Qual., Atmos. Health, 2(3):169–176, 2009. doi: 10.1007/s11869-009-0044-0.

N Fann, KR Baker, and CM Fulcher. Characterizing the pm2.5-related health benefits of emission reductions for 17 industrial, area and mobile emission sectors across the u.s. Environ. Int., 49(C):141–151, November 2012a.

N Fann, AD Lamson, SC Anenberg, K Wesson, D Risley, and BJ Hubbell. Estimating the national public health burden associated with exposure to ambient pm2.5 and ozone. Risk Analysis, 32(1):81–95, January 2012b.

M M Finkelstein, M Jerrett, and M R Sears. Traffic air pollution and mortality rate advancement periods. Am. J. Epidemiol., 160(2):173–177, July 2004.

MM Finkelstein. Environmental inequality and circulatory disease mortality gradients. J. Epidemiol. Commun. H., 59(6):481–487, June 2005.

EM Flachs, J Sørensen, J Bønløkke, and H Brønnum-Hansen. Population dynamics and air pollution: the impact of demographics on health impact assessment of air pollution. J. Environ. Public Health., 2013(6):1–12, 2013.

JB Flanagan, RKM Jayanty, EE Rickman, and MR Peterson. Pm2.5 speciation trends network: Evaluation of whole-system uncertainties using data from sites with collocated samplers. J. Air Waste Manage., 56(4):492–499, April 2006.

WJ Gauderman, F Gilliland, H Vora, E Avol, and D Stram. Association between air pollution and lung function growth in southern California children: Results from a second cohort. Am. J. Respir. Crit. Care Med., 166:76–84, June 2002.

U Gehring, J Heinrich, U Krmer, V Grote, M Hochadel, D Sugiri, M Kraft, K Rauchfuss, GH Eberwein, and HE Wichmann. Long-term exposure to ambient air pollution and cardiopulmonary mortality in women. Epidemiology, 17(5):545–551, September 2006.

TJ Grahame, R Klemm, and RB Schlesinger. Public health and components of particulate matter: The changing assessment of black carbon. J. Air Waste Manage., 64(6):620–660, May 2014.

A Hakami, DK Henze, JH Seinfeld, T Chai, Y Tang, GR Carmichael, and A Sandu. Adjoint inverse modeling of black carbon during the asian pacific regional aerosol characterization experiment. J. Geophys. Res.: Atmos., 110(D14301), 2005.

A Hakami, JH Seinfeld, T Chai, Y Tang, GR Carmichael, and A Sandu. Adjoint sensitivity analysis of ozone nonattainment over the continental united states. Environ. Sci. Technol., 40(12):3855–3864, June 2006.

A Hakami, DK Henze, JH Seinfeld, K Singh, A Sandu, S Kim, D Byun, and Q Li. The adjoint of CMAQ. Environ. Sci. Technol., 41(22):7807–7817, 2007.

DK Henze, JH Seinfeld, W Liao, A Sandu, and GR Carmichael. Inverse modeling of aerosol dynamics: Condensational growth. J. Geophys. Res.: Atmos., 109(D14), 2004.

DK Henze, A Hakami, and JH Seinfeld. Development of the adjoint of geos-chem. Atmos. Chem. Phys., 7(9):2413–2433, 2007.

Y Hu, MT Odman, and AG Russell. Top-down analysis of the elemental carbon emissions inventory in the United States by inverse modeling using Community Multiscale Air Quality model with decoupled direct method (CMAQ-DDM). J. Geophys. Res.: Atmos., 114 (D24), December 2009.

N Huneeus, O Boucher, and F Chevallier. Simplified aerosol modeling for variational data assimilation. Geosci. Model Dev., 2(2):213–229, 2009.

MZ Jacobson. Short-term effects of controlling fossil-fuel soot, biofuel soot and gases, and methane on climate, Arctic ice, and air pollution health. J. Geophys. Res.: Atmos., 115, 2010.

NAH Janssen, G Hoek, M Simic-Lawson, P Fischer, L van Bree, H ten Brink, M Keuken, RW Atkinson, HR Anderson, B Brunekreef, and FR Cassee. Black carbon as an additional indicator of the adverse health effects of airborne particles compared with PM10 and PM2. 5. Environ. Health Perspect., 119(12):1691–1699, August 2011.

K Katanoda, T Sobue, H Satoh, K Tajima, T Suzuki, H Nakatsuka, T Takezaki, T Nakayama, H Nitta, K Tanabe, and S Tominaga. An association between long-term exposure to ambient air pollution and mortality from lung cancer and respiratory diseases in japan. J. Epidemiol., 21(2):132–143, 2011.

I Kazuhiko, R Mathes, Z Ross, A Nádas, G Thurston, and T Matte. Fine particulate matter constituents associated with cardiovascular hospitalizations and mortality in New York City. Environ. Health Perspect., 119(4):467, April 2011.

D Koch, M Schulz, S Kinne, C McNaughton, JR Spackman, Y Balkanski, S Bauer, T Berntsen, TC Bond, O Boucher, M Chin, A Clarke, N De Luca, F Dentener, T Diehl, O Dubovik, R Easter, D W Fahey, J Feichter, D Fillmore, S Freitag, S Ghan, P Ginoux, S Gong, L Horowitz, T Iversen, A Kirkevag, Z Klimont, Y Kondo, M Krol, X Liu, R Miller, V Montanaro, N Moteki, G Myhre, JE Penner, J Perlwitz, G Pitari, S Reddy, L Sahu, H Sakamoto, G Schuster, JP Schwarz, O Seland, P Stier, N Takegawa, T Takemura, C Textor, JA van Aardenne, and Y Zhao. Evaluation of black carbon estimations in global aerosol models. Atmos. Chem. Phys., 9(22):9001–9026, 2009.

J Koo, Q Wang, DK Henze, IA Waitz, and SRH Barrett. Spatial sensitivities of human health risk to intercontinental and high-altitude pollution. Atmos. Environ., 71:140–147, June 2013.

D Krewski, M Jerrett, RT Burnett, R Ma, E Hughes, Y Shi, MC Turner, CA Pope, G Thurston, EE Calle, MJ Thun, B Beckerman, P DeLuca, N Finkelstein, K Ito, DK Moore, KB Newbold, T Ramsay, Z Ross, H Shin, and B Tempalski. Extended follow-up and spatial analysis of the American Cancer Society study linking particulate air pollution and mortality. Technical Report HEI Research Report 140, Health Effects Institute, Boston, Mass., USA, 2009. URL `http://ephtracking.cdc.gov/docs/RR140-Krewski.pdf`.

K Lapina, DK Henze, JB Milford, M Huang, M Lin, AM Fiore, GR Carmichael, GG Pfister, and K Bowman. Assessment of source contributions to seasonal vegetative exposure to ozone in the US. J. Geophys. Res.: Atmos., 119(1):324–340, 2014.

J Lepeule, F Laden, D Dockery, and J Schwartz. Chronic exposure to fine particles and mortality: an extended follow-up of the harvard six cities study from 1974 to 2009. Environ. Health Perspect., 120(7):965–970, July 2012.

JI Levy, LK Baxter, and J Schwartz. Uncertainty and variability in health-related damages from coal-fired power plants in the united states. Risk Analysis, 29(7):1000–1014, 2009.

Y Li, DK Henze, D Jack, and PL Kinney. The influence of air quality model resolution on health impact assessment for fine particulate matter and its components. Air Qual., Atmos. Health, 2015.

V Mallet and B Sportisse. Uncertainty in a chemistry-transport model due to physical parameterizations and numerical approximations: An ensemble approach applied to ozone modeling. J. Geophys. Res.: Atmos., 11(1), 2006.

WC Malm, BA Schichtel, ML Pitchford, LL Ashbaugh, and RA Eldred. Spatial and monthly trends in speciated fine particle concentration in the united states. J. Geophys. Res.: Atmos., 109(D3), 2004.

PT Martien and RA Harley. Adjoint sensitivity analysis for a three-dimensional photochemical model: Implementation and method comparison. Environ. Sci. Technol., 40(8): 2663–2670, 2006.

SM Mesbah, A Hakami, and S Schott. Optimal ozone reduction policy design using adjoint-based nox marginal damage information. Environ. Sci. Technol., 47(23):13528–13535, 2013.

NZ Muller and R Mendelsohn. Efficient pollution regulation: getting the prices right. Am. Econ. Rev., pages 1714–1739, 2009.

NZ Muller, R Mendelsohn, and W Nordhaus. Environmental accounting for pollution in the United States economy. Am. Econ. Rev., 101(5):1649–1675, August 2011.

MJ Neidell. Air pollution, health, and socio-economic status: the effect of outdoor air quality on childhood asthma. J. Health Econ., 23(6):1209–1236, 2004.

AJ Pappin and A Hakami. Attainment vs exposure: Ozone metric responses to source-specific nox controls using adjoint sensitivity analysis. Environ. Sci. Technol., 47(23): 13519–13527, December 2013a.

AJ Pappin and A Hakami. Source attribution of health benefits from air pollution abatement in Canada and the United States: an adjoint sensitivity analysis. Environ. Health Perspect., 121(5):572–579, May 2013b.

RD Peng, ML Bell, AS Geyh, A McDermott, SL Zeger, JM Samet, and F Dominici. Emergency admissions for cardiovascular and respiratory diseases and the chemical composition of fine particle air pollution. Environ. Health Perspect., 117(6):957–963, February 2009.

TE Pierce and T Waldruff. PC-BEIS: A personal computer version of the biogenic emissions inventory system. J. Air Waste Manage., 41(7):937–941, 1991.

CA Pope, RT Burnett, MJ Thun, EE Calle, D Krewski, K Ito, and GD Thurston. Lung cancer, cardiopulmonary mortality, and long-term exposure to fine particulate air pollution. J. Am. Med. Assoc., 287(9):1132–1141, 2002.

MC Power, MG Weisskopf, and SE Alexeeff. Traffic-related air pollution and cognitive function in a cohort of older men. Environ. Health Perspect., 119(5):682–687, 2011.

RC Puett, JE Hart, JD Yanosky, C Paciorek, J Schwartz, H Suh, FE Speizer, and F Laden. Chronic fine and coarse particulate exposure, mortality, and coronary heart disease in the Nurses' Health Study. Environ. Health Perspect., 117(11):1697–1701, June 2009.

EM Punger and JJ West. The effect of grid resolution on estimates of the burden of ozone and fine particulate matter on premature mortality in the USA. Air Qual., Atmos. Health, 6(3):563–573, May 2013.

A Sandu, DN Daescu, GR Carmichael, and T Chai. Adjoint sensitivity analysis of regional air quality models. J. Comput. Phys., 204(1):222–252, 2005a.

A Sandu, W Liao, GR Carmichael, DK Henze, and JH Seinfeld. Inverse modeling of aerosol dynamics using adjoints: Theoretical and numerical considerations. Aerosol Sci. Technol., 39(8):677–694, 2005b.

D Shindell, JCI Kuylenstierna, E Vignati, R Van Dingenen, M Amann, Z Klimont, SC Anenberg, NZ Muller, G Janssens-Maenhout, F Raes, J Schwartz, G Faluvegi, L Pozzoli, K Kupiainen, L Hoeglund-Isaksson, L Emberson, D Streets, V. Ramanathan, K Hicks, NTK Oanh, G Milly, M Williams, V Demkine, and D Fowler. Simultaneously mitigating near-term climate change and improving human health and food security. Science, 335(6065): 183–189, 2012.

WC Skamarock, JB Klemp, J Dudhia, DO Gill, DM Barker, W Wang, and JG Powers. A description of the advanced research wrf version 2. Technical report, National Center for Atmospheric Research (NCAR), Boulder, CO, USA, 2005. URL `http://www2.mmm.ucar.edu/wrf/users/docs/arw_v2_070111.pdf`.

W Squire and G Trapp. Using complex variables to estimate derivatives of real functions. Siam Review, 40(1):110–112, March 1998.

S Stevenson, FJ Dentener, and MG Schultz. Multimodel ensemble simulations of present-day and near-future tropospheric ozone. J. Geophys. Res.: Atmos., 111(D08301), 2006.

HH Suh and A Zanobetti. Exposure error masks the relationship between traffic-related air pollution and heart rate variability. J. Occup. Environ. Med., 52(7):685–692, July 2010.

M Tainio, JT Tuomisto, J Pekkanen, N Karvosenoja, K Kupiainen, P Porvari, M Sofiev, A Karppinen, L Kangas, and J Kukkonen. Uncertainty in health risks due to anthropogenic primary fine particulate matter from different source types in Finland. Atmos. Environ., 44(17):2125–2132, June 2010.

TM Thompson and NE Selin. Influence of air quality model resolution on uncertainty associated with health impacts. Atmos. Chem. Phys., 12(20):9753–9762, 2012.

US EPA. Meteorological model performance for annual 2007 simulations. Technical report, U.S. Environmental Protection Agency: Office of Air Quality Planning and Standards, Research Triangle Park, NC, USA, 2011. URL `http://epa.gov/ttn/scram/reports/EPA-454_R-11-007.pdf`.

US EPA. Report to Congress on Black Carbon. Technical report, U.S. Environmental Protection Agency, Washington, DC, March 2012a. URL `http://www.epa.gov/blackcarbon/2012report/fullreport.pdf`.

US EPA. Air quality modeling technical support document for the regulatory impact analysis for the revisions to the national ambient air quality standards for particulate matter. Technical report, U.S. Environmental Protection Agency: Office of Air Quality Planning and Standards, Research Triangle Park, NC, USA, December 2012b. URL http://www.epa.gov/ttn/naaqs/standards/pm/data/201212aqm.pdf.

US EPA. Technical Support Document (TSD): Preparation of Emissions Inventories for the Version 5.0, 2007 Emissions Modeling Platform. Technical report, U.S. Environmental Protection Agency: Office of Air and Radiation, Research Triangle Park, NC, USA, September 2013. URL http://epa.gov/ttn/chief/emch/2007v5/2007v5_2020base_EmisMod_TSD_13dec2012.pdf.

TPC van Noije, HJ Eskes, FJ Dentener, DS Stevenson, K Ellingsen, MG Schultz, O Wild, M Amann, CS Atherton, DJ Bergmann, I Bey, KF Boersma, T Butler, J Cofala, J Drevet, AM Fiore, M Gauss, DA Hauglustaine, LW Horowitz, ISA Isaksen, MC Krol, JF Lamarque, MG Lawrence, RV Martin, V Montanaro, JF Muller, G Pitari, MJ Prather, JA Pyle, A Richter, JM Rodriguez, NH Savage, SE Strahan, K Sudo, S Szopa, and M van Roozendael. Multi-model ensemble simulations of tropospheric no_2 compared with gome retrievals for the year 2000. Atmos. Chem. Phys., 6(10):2943–2979, 2006.

WHO. Health risks of particulate matter from long-range transboundary air pollution. Technical report, World Health Organization Regional Office of Europe, Copenhagen, 2006. URL http://www.euro.who.int/__data/assets/pdf_file/0006/78657/E88189.pdf.

WHO. Health effects of black carbon. Technical report, World Health Organization, European Centre for Environment and Health, Bonn Office, April 2012. URL http://www.euro.who.int/__data/assets/pdf_file/0004/162535/e96541.pdf.

M Wilhelm, L Qian, and B Ritz. Outdoor air pollution, family and neighborhood environment, and asthma in la fans children. Health Place, 15(1):25–36, March 2009.

EH Wilker, MA Mittleman, BA Coull, A Gryparis, ML Bots, J Schwartz, and D Sparrow. Long-term exposure to black carbon and carotid intima-media thickness: the Normative Aging Study. Environ. Health Perspect., 121(9):1061–1067, September 2013a.

EH Wilker, E Mostofsky, SH Lue, D Gold, J Schwartz, GA Wellenius, and MA Mittleman. Residential proximity to high-traffic roadways and poststroke mortality. J. Stroke. Cerebrovasc. Dis., 22(8):e366–e372, November 2013b.

S Zhao, AJ Pappin, SM Mesbah, JYJ Zhang, NL MacDonald, and A Hakami. Adjoint estimation of ozone climate penalties. Geophys. Res. Lett., 40(20):5559–5563, 2013.

Chapter 3

Sector-Specific Health Impacts of BC Emissions in six Urban US Regions

Matthew D. Turner[1], Daven K. Henze[1], Shannon L. Capps[1], Amir Hakami[2], Shunliu Zhao[2], Jaroslav Resler[3], Gregory R. Carmichael[4], Charles O. Stanier[4], Jaemeen Baek[4], Adrian Sandu[5], Armistead G. Russell[6a], Athanasios Nenes[6b], Rob W. Pinder[7], Sergey L. Napelenok[7], Jesse O. Bash[7], Peter B. Percell[8], and Tianfeng Chai[9]

[1]Mechanical Engineering Department, University of Colorado, Boulder, Colorado 80309, United States

[2]Department of Civil and Environmental Engineering, Carleton University, Ottawa, Ontario K1S 5B6, Canada

[3]Nonlinear Modeling, Institute of Computer Science, Prague 182 07, Czech Republic

[4]Department of Chemical and Biochemical Engineering, University of Iowa, Iowa City, Iowa 52242, United States

[5]Computer Science, Virginia Tech, Blacksburg, Virginia 24061, United States

[6a]School of Civil and Environmental Engineering, and [6b]School of Earth and Atmospheric Sciences, Georgia Tech, Atlanta, Georgia 30331, United States

[7]Atmospheric Modeling and Analysis Division, U.S. EPA, Research Triangle Park, North Carolina 27711, United States

[8]Department of Geosciences, University of Houston, Houston, Texas 77004, United States

[9]College of Computer, Mathematical, and Natural Sciences, University of Maryland, College Park, Maryland 20742, United States

3.1 Abstract

Recent studies have shown that exposure to particulate black carbon (BC) has significant adverse health effects, and may be more detrimental to human health than exposure to $PM_{2.5}$ as a whole. BC emission controls have successfully decreased BC emissions from mobile sources to less than half of what they were 30 years ago, with most mobile source emission controls applying to diesel emissions. However, additional analysis is required to quantify the benefits of previous and future emission controls. In this study we use the adjoint of the Community Multiscale Air Quality (CMAQ) model to estimate highly-resolved spatial distributions of benefits related to emission reductions for six urban regions within the continental US. Emissions from outside each of the six chosen regions account for between 7% and 27% of the premature deaths attributed to exposure to BC within the region. While we estimate that nonroad mobile and onroad diesel emissions account for the largest number of premature deaths attributable to exposure to BC, onroad gasoline is shown to have more than double the benefit per unit emission than that of nonroad mobile and onroad diesel. Within the region encompassing New York City and Philadelphia, reductions in emissions from large industrial combustion sources that are not classified as EGUs (i.e., non-EGU) are estimated to have up to triple the benefits per unit emission than reductions to onroad diesel sectors, and provide similar benefits per unit emission to that of onroad gasoline emissions in the region. In the San Joaquin Valley, we note that the dis-benefits per unit of additional emissions are highest along the CA-99 route, which will be subject to increased nonroad mobile emissions in the near-term owing to construction of new rail systems, potentially balanced in the long term by reductions in vehicle emissions. While onroad mobile emissions have been decreasing in the past 30 years and a majority of vehicle emission controls that regulate PM focus on diesel emissions, our analysis shows the most efficient target for stricter controls is actually onroad gasoline emissions.

3.2 Introduction

Epidemiological studies have identified significant relationships between exposure to ambient fine particulate matter ($PM_{2.5}$) and an array of adverse health effects, including premature death [Krewski et al., 2009; WHO, 2006; Pope et al., 2002; Katanoda et al., 2011; Lepeule et al., 2012; Kazuhiko et al., 2011; Puett et al., 2009; Gauderman et al., 2002; Cohen et al., 2004b; Beelen et al., 2007; Laden et al., 2006]. Relative risk values from this literature have been applied to quantify the health burden of exposure to $PM_{2.5}$ both in the US and globally [Fann et al., 2013, 2012; Silva et al., 2013; Brauer et al., 2012; Anenberg et al., 2010; Cohen et al., 2004a]. Recent studies have found a stronger link between adverse health effects and exposure to black carbon (BC) than exposure to $PM_{2.5}$ as a whole [Suh and Zanobetti, 2010; Adar et al., 2007; Peng et al., 2009; WHO, 2012; Power et al., 2011; Wilker et al., 2013; Qiao et al., 2014]. Janssen et al. [2011] found that reducing a unit of BC increases life expectancy by four to nine times that of reducing a unit of $PM_{2.5}$. Grahame et al. [2014] performed a review of epidemiological and toxicological literature regarding BC and suggested that exposure to BC is causally linked to premature death.

Fortunately, onroad mobile source emissions of BC have decreased by approximately 66% in the past 30 years [McDonald et al., 2015]; however, a majority of the vehicle emission controls that regulate PM emissions focus on diesel emissions [US EPA, 2012, 2001]. To understand the benefits of these controls, there have been numerous investigations of the human health impacts of BC emission reductions, including the role of varying geographical locations and emission sources. Fann et al. [2009] used a reduced-form air quality model to estimate the benefits-per-ton of total carbonaceous aerosol emission reductions for several US urban regions. They found that benefits-per-ton vary not only by emission source but also by geographical location, with estimates ranging from $65,000 for EGU and non-EGU (large industrial combustion sources that are not classified as EGUs) sources of carbonaceous aerosol in Salt Lake City to $2,500,000 for area sources of carbonaceous aerosol in Phoenix.

Anenberg et al. [2011] used a global chemical transport model to evaluate the effects of sectoral BC emission reductions on premature deaths. They found that global emission reductions in the transportation sector resulted in the highest number of avoided premature deaths in North America (2,000 - 3,000 avoided deaths), while reductions of global BC emissions in the residential sector resulted in up to 1000 avoided deaths. Caiazzo et al. [2013] used the CMAQ model to investigate the health impacts of major emission sectors in the US and found that onroad vehicles accounted for the largest population-weighted concentration of BC.

While these studies have shown that the human health benefits of emission reductions have orders of magnitude variability across different geographical regions and sectors, they relied on coarser approaches that limited the number or specificity of emissions reductions for which benefits could be estimated. Other studies have used the adjoint modeling approach, which can more specifically estimate the benefits of reductions to emissions from numerous times and locations at less computational cost than forward sensitivity analysis. Dedoussi and Barrett [2014] used the GEOS-Chem adjoint to attribute premature deaths from exposure to $PM_{2.5}$ to emission sectors and locations. Their analysis found that a maximum number of premature deaths (approximately 8,000) are attributed to road emissions in California, while road emissions in Georgia result in approximately 1,500 premature deaths. In Turner et al. [2015], we used the CMAQ adjoint to estimate the BC emission sources that contribute the most to total premature deaths annually throughout the US. We found that onroad diesel and nonroad vehicle emissions account for a majority of the premature deaths in the US associated with exposure to BC. We also analyzed the benefits-per-ton of BC emission reductions and found that reductions to emissions in the cold seasons resulted in an average of approximately 15 more premature deaths per sector (per unit emission) than emissions in the warm seasons. The adjoint approach has also been used to estimate ozone health impacts [Pappin and Hakami, 2013b,a; Mesbah et al., 2013; Zhao et al., 2013].

While the work of Dedoussi and Barrett [2014], Lee et al. [2015], and Turner et al. [2015]

utilized adjoint models to perform source attribution studies at high spatial, temporal, and sectoral resolutions, each study focused on health impacts across a large domain, such as the entire globe or the entire US. The extent to which emissions from individual locations and sources cause adverse health effects in specific urban areas has thus yet to be addressed. Such information is required for determining the extent to which local versus distant sources impact individual metropolitan regions. For this purpose, here we use the adjoint of the CMAQ model to quantify the importance of transport of BC from distant emission sources on premature deaths in six major US urban regions. Additionally, we estimate the spatial distribution of benefits-per-ton of emission reductions for each of the six areas. The analysis in this work allows for the determination of sources and locations of BC emissions whose reduction could most effectively mitigate human health impacts attributed to exposure to BC, with specific attention paid to comparisons between onroad diesel and onroad gasoline emissions. Finally, the analysis in this work also estimates the adverse health impacts of potential future emissions.

3.3 Materials and Methods

Annual average BC concentrations for 2007 were simulated using the CMAQ model v4.7.1 [Byun and Schere, 2006]. The resultant concentrations are used to estimate premature deaths attributed to exposure to BC in six urban regions. Simulated annual average BC concentrations are evaluated through comparison to measurements from the Interagency Monitoring of Protected Visual Environments [Malm et al., 2004] (IMPROVE) and Chemical Speciation Network [Flanagan et al., 2006] (CSN) and are found to be similar to observed concentrations for both IMPROVE (mean bias = 0.09 μg/m^3) and CSN (mean bias = -0.22 μg/m^3), with lower accuracy at the largest concentrations. For discussion of the meteorology inputs, emissions inputs, and further details regarding model performance, see Supporting Information and Turner et al. [2015]

Estimates of premature deaths attributed to exposure to BC for six regions (Denver, Dallas, Houston, Phoenix, San Joaquin Valley, and a region that encompasses New York City and Philadelphia (referred to as NY/PHI), see Figure 3.4) are calculated using the following health impact function:

$$J = \sum_{i=1}^{N} M_i \cdot (1 - e^{-\beta \cdot C_{av,i}}) \tag{3.1}$$

where M_i is the gridded annual non-accidental premature deaths in the region of interest for people age 30 or older, $C_{av,i}$ is the gridded annual average BC concentration, i is the grid cell index, N is the number of grid cells, and β is the concentration response factor. While previous studies [Krewski et al., 2009; Laden et al., 2006] have shown that β values differ across different regions, we use a constant β across each region to allow for our results to be consistent with the value currently used by the US EPA for policy development [US EPA, 2009]. Further details of the forward model simulations, as well as the calculation of the health impact function can be found in Turner et al. [2015]. When estimating benefits per unit emission, we used a value of statistical life (VSL) of $6.2 million, consistent with the

value from Fann et al. [2009].

We use the CMAQ adjoint to obtain the sensitivities of regional premature deaths attributed to exposure to BC with respect to emissions for each region. See Turner et al. [2015] for full details of the development and validation of the CMAQ adjoint model. In order to reduce the computational cost of this analysis, adjoint simulations were run for the first week of each month. The resulting 12 week average has been shown to be an accurate representation of the year as a whole [Turner et al., 2015]. Semi-normalized sensitivities ($\frac{\partial J}{\partial E_{i,k,m}} \cdot E_{i,k,m}$) represent the contributions of BC emissions in grid cell i, sector k, and month m, to the number of estimated premature deaths attributed to exposure to BC. The ratio of these contributions to the emissions $E_{i,k,m}$ represents the number of premature deaths per unit emission, which we refer to as efficiency.

3.4 Results and Discussion

3.4.1 Sectoral Analysis

In this section, we perform an analysis of the contributions of different emission sectors to BC health impacts in each of the six regions. Figure 3.1 shows the sectoral contributions (left) and sectoral efficiencies (right) for each region. For the efficiency plot in Figure 3.1, emissions and contributions were summed over all grid cells within each region. The sectors are sorted by the magnitudes of contributions from each sector for NY/PHI. The contributions for NY/PHI are divided by four, for scale; the efficiency values for NY/PHI are unaltered.

Several interesting similarities and differences in sector-specific health impacts are evident across these regions. Nonroad mobile emissions are the largest contributor across all regions (followed closely by onroad diesel), however onroad diesel and nonroad mobile contributions are nearly identical for Denver. For most regions, onroad gasoline emissions are the third largest contributor by a significant margin (contributions from onroad gasoline in Phoenix are approximately three times larger than the next largest sector). However, Denver onroad gasoline contributions are nearly equal to nonpoint emissions. Additionally, EGU emissions contribute to over 7% of premature deaths due to BC exposure in NY/PHI yet EGU emissions contribute to a significantly smaller fraction of the premature deaths in the other regions. Also, contributions from nonroad mobile and onroad diesel sources in Phoenix are larger than contributions from the same sectors in Houston. However, contributions from onroad gasoline emissions are nearly twice as large in Houston than in Phoenix. Finally, while contributions from nonroad mobile sources are larger in the San Joaquin Valley than in Denver, contributions from onroad diesel sources are larger in Denver than in the San Joaquin Valley. This difference becomes even more pronounced when considering contributions as a percentage, since the San Joaquin Valley has approximately 30% more premature deaths attributed to exposure to BC than Denver.

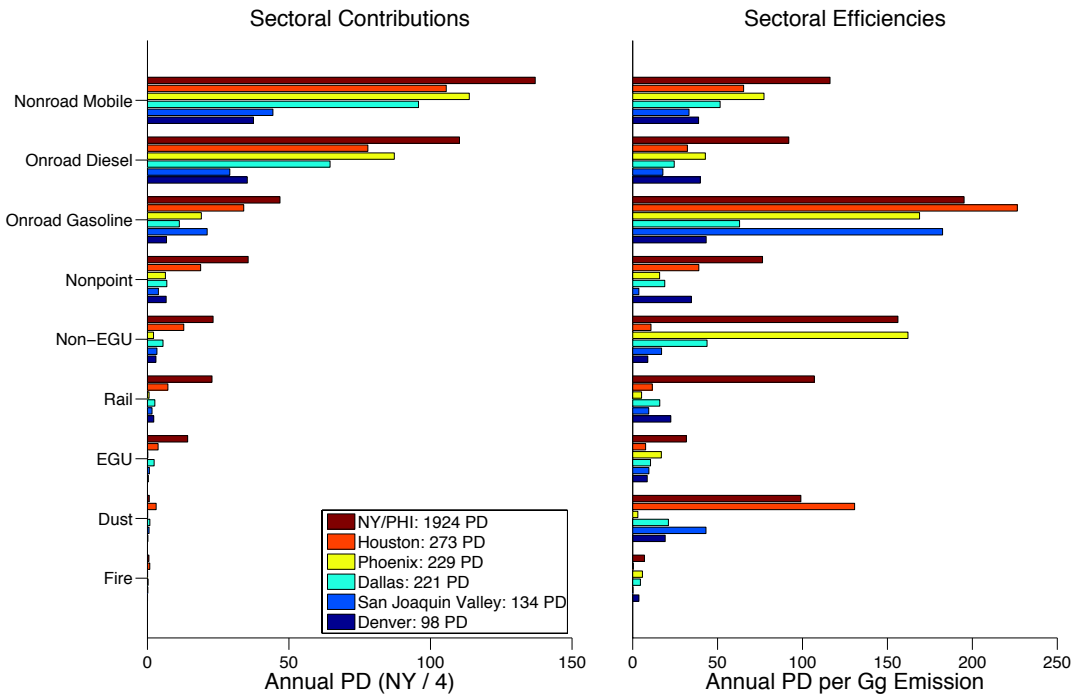

Figure 3.1: Sectoral comparison of contribution (left) and efficiency of emissions to result in premature deaths (right) for the NY/PHI, Dallas, Denver, Houston, Phoenix, and San Joaquin Valley regions. Contributions for NY/PHI region (left) are divided by four for scale, while contributions are unaltered for efficiency figure (right). PD = Premature Deaths.

In addition to the total number of premature deaths resulting from emissions in each sector, it is of interest to compare health effects on a per-unit-emission basis. As shown in Figure 3.1 (right), the efficiency of emissions to result in premature deaths can vary by up to two orders of magnitude across sectors in a single region. Nonroad mobile and onroad diesel sources are the two largest contributors in every region, with both sectors having two to three times as many contributions than onroad gasoline sources. However, onroad gasoline sources have larger efficiencies than both nonroad mobile and onroad diesel sources in every region, with Houston onroad gasoline sources having an efficiency nearly three times larger than nonroad mobile sources. Onroad gasoline sourses in Denver contribute to approximately 4 times less premature deaths than onroad diesel and nonroad mobile sources in Denver, yet the efficiency of onroad gasoline emissions is nearly equal to both nonroad mobile and onroad diesel (with the efficiency from onroad gasoline being slightly larger). While onroad gasoline emissions account for very few premature deaths when compared to onroad diesel and nonroad mobile emissions for each region, onroad gasoline emissions in NY/PHI, Houston, Phoenix, and San Joaquin Valley result in the largest number of premature deaths per unit emission (up to 10 times larger than efficiencies of onroad diesel emissions). This is attributed to the difference in driving patterns for onroad diesel and onroad gasoline vehicles. While many onroad diesel vehicles are used for long-range transport of goods along interstates, onroad gasoline vehicles are used mainly for personal transportation in populated areas. In contrast, dust emissions of BC are shown to result in a negligible number of premature deaths for every region. Still, the efficiency of fugitive dust to result in premature deaths in NY/PHI and Houston is larger than the efficiencies from EGU and nonpoint BC emissions. This is attributed to, in these two regions, the largest dust emissions occuring within the most populous grid cells. The proximity of the dust emissions to high populations greatly increases the exposure, resulting in a larger efficiency. In the other regions, the dust emissions are more distributed throughout the region and result in lower efficiencies.

Another potentially important result obtained from Figure 3.1 (right) relates to the

efficiency of non-EGU emissions. In most regions, the efficiency of non-EGU emissions to result in premature deaths is rather low when compared to the other sectors, with non-EGU contributions in Houston being approximately 25% that of nonroad mobile contributions. However, for NY/PHI and Phoenix, the non-EGU emission efficiency is larger than both the nonroad mobile and onroad diesel sectors, and is nearly equal to the efficiency of onroad gasoline emissions. Additionally, the efficiency of commercial railroad emissions to result in premature deaths is substantial in NY/PHI. This is attributed to the proximity of commercial railways within the region to the major population centers. Finally, while non-EGU, rail, and fugitive dust contributions show little variation across regions, these sources have efficiencies that range between approximately 10 premature deaths per Gg of emission to approximately 160 premature deaths per Gg of emission. Analysis of the spatial distribution of efficiencies is presented in the Supporting Information. From a spatial analysis of the efficiencies in the San Joaquin Valley (Figure 3.2), a majority of the significant efficiencies coincidentally occurring along CA-99. This suggests that, when considering the health impacts of vehicle emissions, it is preferable for onroad vehicles to travel on I-5 than CA-99. This is significant, as emissions from the construction and operation of the new California rail system [AECOM et al., 2013] will be occurring within the locations of highest efficiency. This suggests that, in the short term, there will be significantly more premature deaths from nonroad mobile emissions in the region while the rail system is being constructed. However, in the long term, the reduction in onroad mobile contributions along CA-99 will likely be greater than the increase in rail contributions from the new rail system.

3.4.2 Spatial Distribution of Contributions

Figure 3.3 shows contour plots of the contributions for each of the six regions summed across all sectors k and months m. In each of these plots, the contours show the regions in which emissions of BC in the fewest number of grid cells account for a given percentage of contributions in the region. For example, the 50% contour in each plot shows the locations

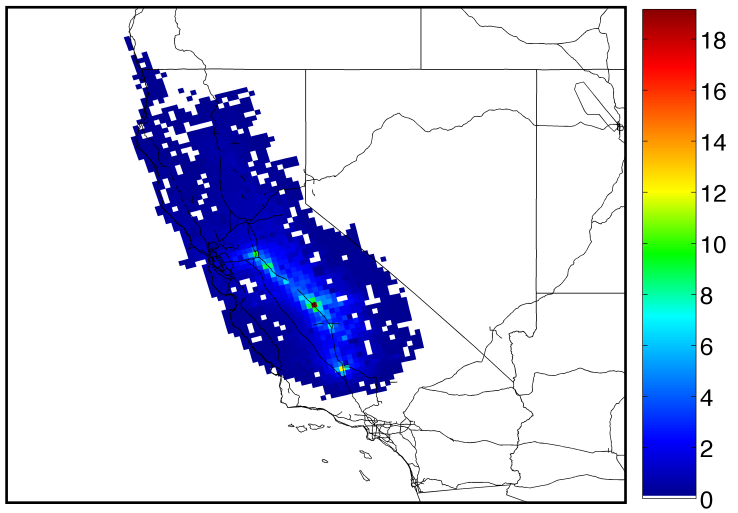

Figure 3.2: Plot of the efficiency of emissions to result in premature deaths $\left(\frac{Contribution}{Emission}\right)$ from exposure to BC in the San Joaquin Valley region. Data presented as premature deaths per Gg of BC emitted.

in which emissions account for 50% of the premature deaths attributed to exposure to BC in the region.

Figure 3.3a shows the contribution contours for premature deaths in NY/PHI. We estimate that 1,290 (95% CI: 860 - 1720, for details of uncertainty calculation see Supporting Information) premature deaths were attributed to exposure to BC in the region in 2007, and 78% of these premature deaths are attributed to emissions within the region (see Table 3.1). The largest contributors (the 30% contour) are New York City and northeastern New Jersey. These are followed closely by Philadelphia and the suburbs surrounding New York City, making up the 40% contour. The next largest contributors (the 50% and 60% contours) include other suburbs around the urban centers, as well as the major roadways within the region. This reinforces the conclusion from Figure 3.1 that mobile sources account for a majority of the premature deaths in the region attributed to exposure to BC. Additionally, in order to account for 80% of the premature deaths in the region, emissions from as far away as Detroit, MI must be included in the analysis. Finally, the background (sensitivities that create the 90-100% contours, Figure 3.5) includes emissions from as far away as the I-5

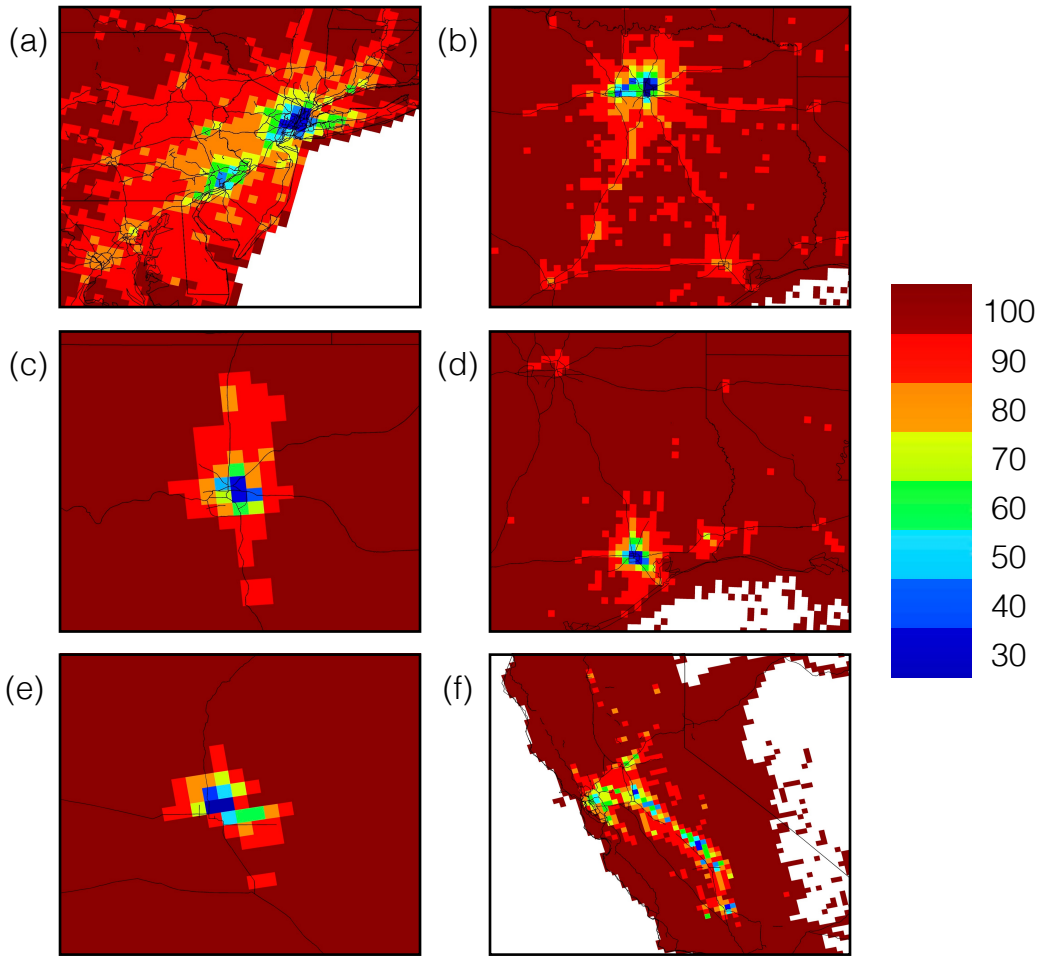

Figure 3.3: Contour plots of contributions for (a) the NY/PHI region, (b) the Dallas region, (c) the Denver region, (d) the Houston region, (e) the Phoenix region, and (f) the San Joaquin Valley region.

Table 3.1: Analysis of annual premature death percentage attributed to exposure to BC from emission sources inside and outside of each region.

	PD (95% CI)	% Inside	PD Inside	PD Outside
NY/PHI	1,290 (860 - 1720)	78%	1013 (678 - 1347)	277 (186 - 368)
Dallas	220 (145 - 295)	83%	185 (124 - 246)	35 (23 - 46)
Denver	100 (65 - 135)	88%	87 (58 - 116)	13 (9 - 17)
Houston	270 (180 - 360)	88%	238 (159 - 317)	32 (21 - 43)
Phoenix	230 (145 - 315)	93%	214 (143 - 285)	16 (11 - 21)
San Joaquin	130 (85 - 175)	73%	95 (64 - 126)	35 (23 - 47)

corridor in northern California, Oregon, and Washington. While the sum of the emissions from Chicago, IL and Minneapolis, MN are required to reach the 90% contour, contributions from individual cities themselves are relatively small. For example, emissions from the greater Chicago area account for only 3 premature deaths (0.23%), and emissions from the greater Minneapolis area account for only 1 premature death (0.08%) in the NY/PHI region.

For Dallas (Figure 3.3b), we estimate a much smaller number of premature deaths attributed to exposure to BC (220 premature deaths) than in the NY/PHI region. Of these 220 (95% CI: 145 - 295) premature deaths, 83% come from emissions within the Dallas region. The largest contributions once again come from the urban centers within the region. As with NY/PHI, the 40-60% contours include the suburbs around the urban center, as well as major roadways in the area. However, the contours show that emissions from Houston, Austin, and San Antonio must be included to account for 80% of the premature deaths in Dallas. Many of the larger contributions that are not within the region of interest occur along the major roadways connecting nearby cities.

Figure 3.3c shows the contribution contours for premature deaths in the Denver region. We estimate 100 (95% CI: 65 - 135) premature deaths were attributed to exposure to BC in the region, 88% of which result from BC emissions within the region. The largest contributions are from Denver and the suburbs within Denver county, with other less-substantial contributions coming from Fort Collins and Colorado Springs. In fact, even though Col-

orado Springs is in close proximity Denver, emissions from Colorado Springs result in few premature deaths and only show up in the background. As opposed to Figures 3.3a and 3.3b, transport of BC from distant sources does not become important until considering the background (Figure 3.7). This is a result of the regions in Figures 3.3a and 3.3b having significant emission sources near to and upwind of the region. However, for Denver there are no significant nearby or upwind emissions sources.

While the above-background contours for Dallas (Figure 3.3b) clearly showed the contributions from mobile sources (as shown by the 80-90% contours forming a triangle of highways that connect other major cities), Figure 3.3d shows that a majority of the above-background contributions for Houston fall within the greater Houston area. Additionally, the largest contributions are from emissions within the city limits, with smaller contribution contours encompassing the suburbs surrounding Houston. While we estimate 220 premature deaths in the Dallas region, we estimate 270 (95% CI: 180 - 360) premature deaths in the Houston region (88% of which come from emissions in the region). The background in the contour plot for the Houston region (Figure 3.8) is similar to that of the Dallas region (Figure 3.6), since Houston and Dallas are in close proximity to each other.

Similarly to Denver, the Phoenix contour plot (Figure 3.3e) shows that all of the above-background contributions occur within the region of interest. The largest contributions again occur within the city limits, followed closely by the suburbs surrounding the city. Additionally, transport of BC from distant sources is not important until considering the background (Figure 3.9). We estimate that 230 (95% CI: 145 - 315) premature deaths are attributed to exposure to BC in Phoenix, with 93% of the premature deaths being attributed to BC emissions within the Phoenix region.

Lastly, Figure 3.3f shows the contour plots for the San Joaquin Valley. We estimate that 130 (95% CI: 85 - 175) premature deaths are attributed to exposure to BC in the San Joaquin Valley, 73% of which are attributed to BC emissions within the region. As with NY/PHI and Dallas, the San Joaquin Valley analysis suggests that onroad vehicle emissions account for

Table 3.2: Sectoral benefits-per-ton estimates of emission reductions in each of the six regions. Results in this table only include information from within the regions.

	Area Sources	Mobile Sources	EGU and Non-EGU Sources
NY/PHI	$880,000	$2,360,000	$1,150,000
Dallas	$260,000	$770,000	$190,000
Denver	$270,000	$780,000	$110,000
Houston	$440,000	$1,380,000	$85,000
Phoenix	$330,000	$1,110,000	$1,340,000
San Joaquin Valley	$180,000	$660,000	$110,000

a significant percentage of the contributions in the region. The largest contributions within this region occur near cities along CA-99 (Bakersfield, Fresno, Modesto), supporting the conclusion in Figure 3.1 that mobile sources are the largest contributors to premature death in the region associated with exposure to BC. Additionally, a majority of the locations within the 40-70% contours occur along the highways in the San Joaquin Valley, with additional contributions from the San Francisco Bay area. While only 73% of the premature deaths are attributed to emissions in the region, transport of BC from distant sources is only important when considering the background.

3.4.3 Comparison to Previously-Reported Values

Here we compare the estimates obtained in our analysis to the estimates obtained with a Response Surface Model by Fann et al.[Fann et al., 2009], and a global chemical transport model by Anenberg et al.[Anenberg et al., 2011] While there are many differences between the approach taken in this paper to estimate the benefits-per-ton of BC emission reductions and these previous studies, a comparison of the estimates is still informative. Our results are similar to Fann et al. [2009] for mobile sources in Dallas and the San Joaquin Valley, as well as area sources in Denver. In contrast, other source and region relationships

provide significantly different estimates (e.g., Fann et al. [2009] estimated a benefit-per-ton value of $2,500,000 for area sources in Phoenix, while we estimate a benefit-per-ton value of $330,000 for the same region and sector). However, the results are not directly comparable for many reasons. First, Fann et al. [2009] used 2001 National Emission Inventory (NEI) emission profiles and the relative risk estimate from Laden et al. [2006]. In this work, we use 2007 emission profiles based on the 2008 NEI, and we use the relative risk estimate from Krewski et al. [2009]. Second, the analysis in Fann et al. [2009] estimated the health effects (both morbidity and premature death) for all carbonaceous aerosol (BC and organic carbon), whereas out analysis only estimated premature deaths from BC.

Estimates of premature deaths per Gg of emission in this paper are much larger than those reported in the Anenberg paper. Anenberg et al. [2011] estimated approximately 10 avoided premature deaths per Gg emission in North America from halving anthropogenic BC emissions in the region, whereas here (Figure 3.1) we have shown sectoral efficiencies of up to 240 premature deaths per Gg emission. While we estimate sectoral efficiencies upward of 240 premature deaths per Gg emission, analysis of the efficiency for total BC emissions yields results that more closely match the results presented in Anenberg et al. [2011], with values ranging from approximately 15 to 98 premature deaths per Gg emission. Anenberg et al. [2011] used a global chemical transport model ($1.9^\circ \times 1.9^\circ$ resolution), while our analysis uses the adjoint of a regional chemical transport model at 12 km resolution. Coarser grid resolutions have been shown to provide lower premature death estimates attributed to exposure to BC (15% lower at $2^\circ \times 2.5^\circ$ than $0.5^\circ \times 0.66^\circ$ in Li et al. [2015], and 30% lower at 200km resolution than at 12 km relation in Punger and West [2013]). Additionally, Anenberg et al. [2011] analyzed North America as a whole while our analysis focused on urban regions where larger efficiencies would be observed because of the greater number of people in close proximity to the emission sources.

Finally, our estimate of benefits-per-ton for EGUs are larger than those presented in the NAS report [NAS, 2010], which estimated that directly emitted $PM_{2.5}$ reductions would

result in $32,000 per ton emission reduction. However, our analysis estimates benefits-per-ton ranging between $47,000 for Houston to $196,000 for NY/PHI. The differences in benefits-per-ton estimates can partially be explained by the different concentration response functions used. The NAS study used the relative risk estimates from Pope et al. [2002], while we use the relative risk estimate from Krewski et al. [2009]. Another major difference is that NAS [NAS, 2010] used emissions from the 2005 NEI, whereas our simulations were performed using 2007 emission profiles based on the 2008 NEI. Finally, the NAS study estimated health impact emission reduction benefits for $PM_{2.5}$ as a whole, while our analysis focuses specifically on BC emissions.

3.5 Conclusions

In this study we estimate the extent to which emissions from individual locations and sources throughout the US result in adverse health effects in six urban areas. While onroad gasoline emissions account for approximately half of the premature deaths of nonroad mobile and onroad diesel emissions, reductions to onroad gasoline emissions of BC result in the greatest benefit per unit emission. Some emission sources, such as fugitive dust emissions, result in a negligible amount of premature deaths, yet have significant estimates of premature deaths per unit emission (higher efficiencies than EGU and nonpoint for some regions). The large dust efficiency in some regions is attributed to the largest dust emissions in those regions occurring in the same location as the largest populations, whereas other regions have dust emissions that are more evenly distributed throughout the region. Additionally, in the NY/PHI and Phoenix regions non-EGU emissions have efficiencies close to that of onroad gasoline emissions, yet result in a fraction of the premature deaths of onroad gasoline emissions (approximately 10% for Phoenix, approximately 50% for NY/PHI). As expected for a short-lived primary pollutant, we find that the largest contributions occur within the urban centers in the regions of interest. However, contributions from emissions outside of the region account for between 7% and 27% of the premature deaths within each of the six regions. Finally, the largest efficiencies in the San Joaquin Valley coincidentally occur along CA-99, which is also the location along which the new California rail system is to be built. This suggests that, in the short term, there will be significantly more premature deaths from nonroad mobile emissions in the region while the rail system is being constructed. However, in the long term, the reduction in onroad mobile contributions along CA-99 will likely be greater than the increase in rail contributions from the new rail system.

Recent studies have shown that onroad mobile source emissions of BC have decreased by approximately 66% in the past 30 years and off road mobile engines are estimated to account for 37% of mobile emissions of BC in 2010 [McDonald et al., 2015]. Also, a majority of the

vehicle emission controls that regulate PM emissions focus on diesel emissions [US EPA, 2012, 2001]. However, the greatest benefit per unit emission for reductions of BC emissions occurs for onroad gasoline sources, suggesting that BC emissions from gasoline sources would be the ideal target for stricter controls. That being said, several caveats about the present analysis warrant consideration. First, our approach utilized a single chemical transport model, while other air quality modeling studies have used an ensemble of simulations to minimize uncertainty [Mallet and Sportisse, 2006; Stevenson et al., 2006; van Noije et al., 2006; Koch et al., 2009]. Additionally, our simulations were performed with emission profiles from 2007, which do not reflect further recent declines in the US [McDonald et al., 2015; Dallmann and Harley, 2010]. Second, our analysis used a single concentration response factor that corresponds to the relative risk of exposure to $PM_{2.5}$ for every region, while BC might have pronounced toxicity [Bell et al., 2009; Peng et al., 2009; WHO, 2012; Power et al., 2011; Wilker et al., 2013] and relative risks associated with exposure to pollution may vary by region [Krewski et al., 2009; Laden et al., 2006]. Third, our analysis only considers premature deaths attributed to BC exposure for the entire adult population, while certain demographic groups may be at a higher risk [Flachs et al., 2013; Wilhelm et al., 2009; Bell and Dominici, 2008; Neidell, 2004; Finkelstein et al., 2003; Su et al., 2009; Mensah et al., 2005]. Finally, studies have shown that estimates of premature deaths attributed to pollutant exposure have large variability depending on the horizontal model resolution [Punger and West, 2013; Thompson and Selin, 2012; Li et al., 2015], with estimates of premature deaths being greatest at finer resolution. Using the information presented in these studies, we estimate that our 12 km simulations have a low bias of a few percent, relative to higher resolution (4 km) simulations. However, neither 12 nor 4 km simulations are sufficient to accurately resolve near-roadway gradients in BC concentrations.

Overall, this paper shows the utility of the CMAQ adjoint model for analysis of air quality concerns within a specific city or state. The results not only allow for the determination of the fraction of premature deaths that are a result of emissions within the city or

state's jurisdiction, but also provide information about the emission sectors that offer the greatest potential benefits for additional emission controls. Additionally, this type of analysis can be extended to other metrics based on pollutant concentrations including analysis of the climate and health co-benefits of emission reductions.

3.6 Supplemental Information

3.6.1 Uncertainty Calculation

For each region, a separate uncertainty calculation was performed through propagation of errors (Equation 3.2), following Turner et al. [2015]

$$\sigma_T = \frac{\sqrt{\sum_{i=1}^{N} \left(\frac{\partial J}{\partial \beta}\right)_i^2 \sigma_\beta^2 + \left(\frac{\partial J}{\partial C_{av,i}}\right)_i^2 \sigma_C^2}}{N} \tag{3.2}$$

where β is the concentration response factor (calculated from the relative risk value in Krewski et al. [2009]), $C_{av,i}$ is the annual average BC concentration for grid cell i, N is the total number of grid cells in the region, J is the health impact function (Equation 3.1), σ_C is the uncertainty in the simulated annual average BC concentrations, and σ_β is the uncertainty in the concentration response factor. The uncertainty in the relative risk value was assumed to be constant across the regions considered, while the uncertainty in the model estimate was calculated separately for each region. For each region, contour plots were generated that show the regions in which emissions of BC in the fewest number of grid cells account for a given percentage of contributions in the region. Model uncertainty for each region was estimated by comparing observations within the 100% contour (see Figures 3.5-3.10 for full contour maps) obtained through the adjoint analysis to corresponding model estimates of yearly average concentration. We chose to use the 100% contour for the uncertainty estimate, as opposed to a smaller contour (or the observations within the defined region), due to the limited number of observations within certain regions. For example, while the 100% contour for the Phoenix region encompasses 50 observation locations, the 90% contour encompasses only a single CSN observation location. Additionally, the source attribution results presented in this study depend on model accuracy throughout the 100% contour region, as opposed to just the region for which the health impact function is calculated. For σ_C, we use the mean absolute error when comparing the simulated annual average to the observed annual average

from CSN sites within each region's 100% contour. We used a value for σ_β of 0.32, which was calculated from the range of relative risks provided in Krewski et al. [2009].

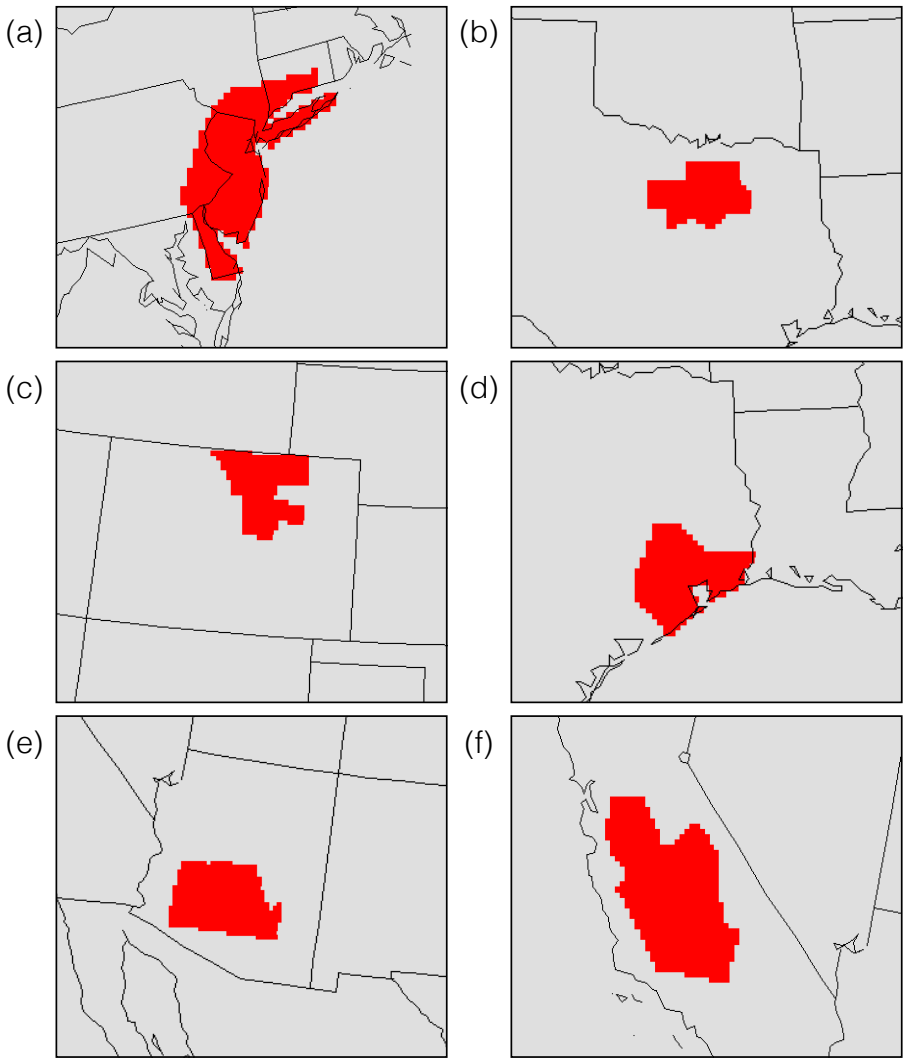

Figure 3.4: Definition of the cost function regions. (a) NY/PHI, (b) Dallas, (c) Denver, (d) Houston, (e) Phoenix, (f) San Joaquin Valley.

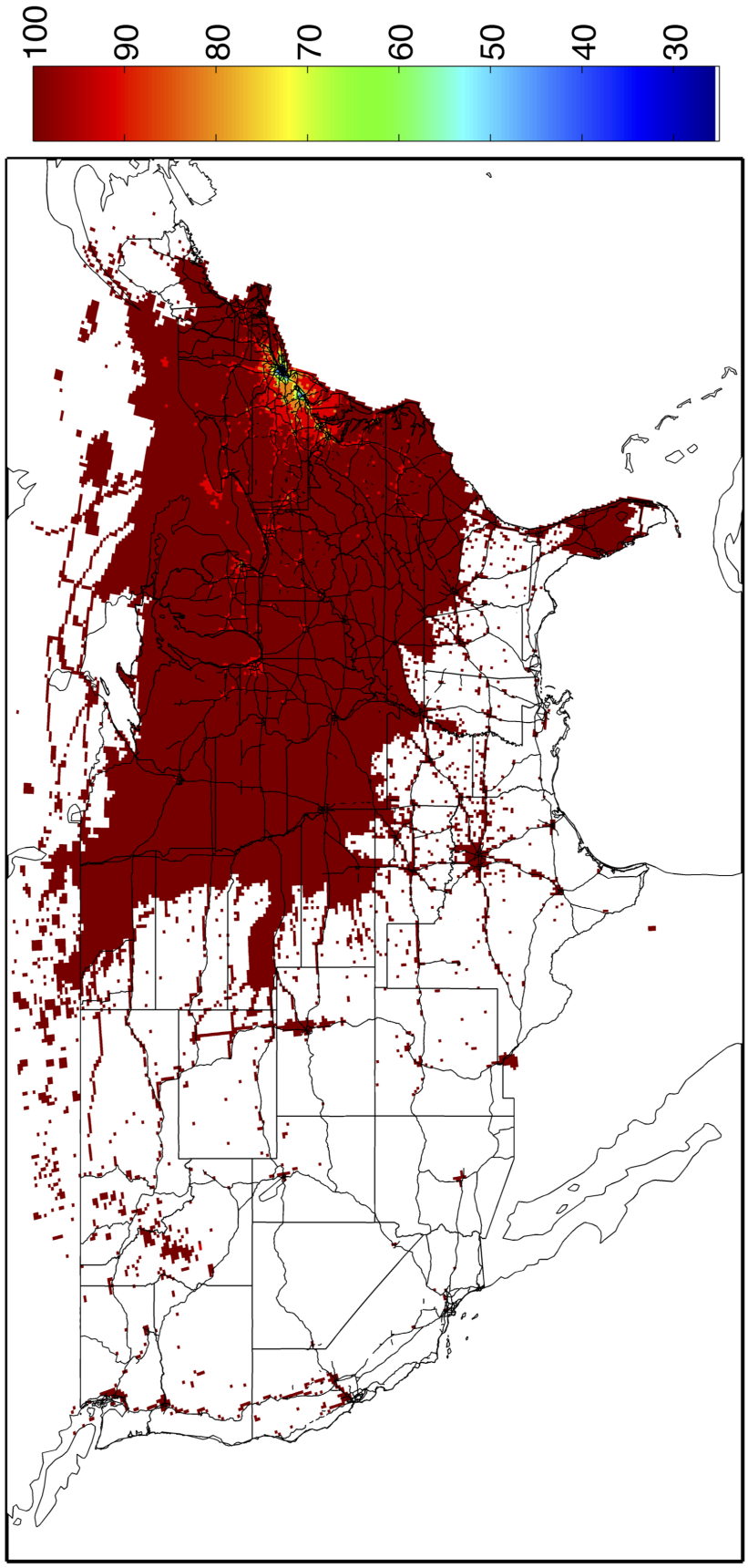

Figure 3.5: Contribution contour for the NY region.

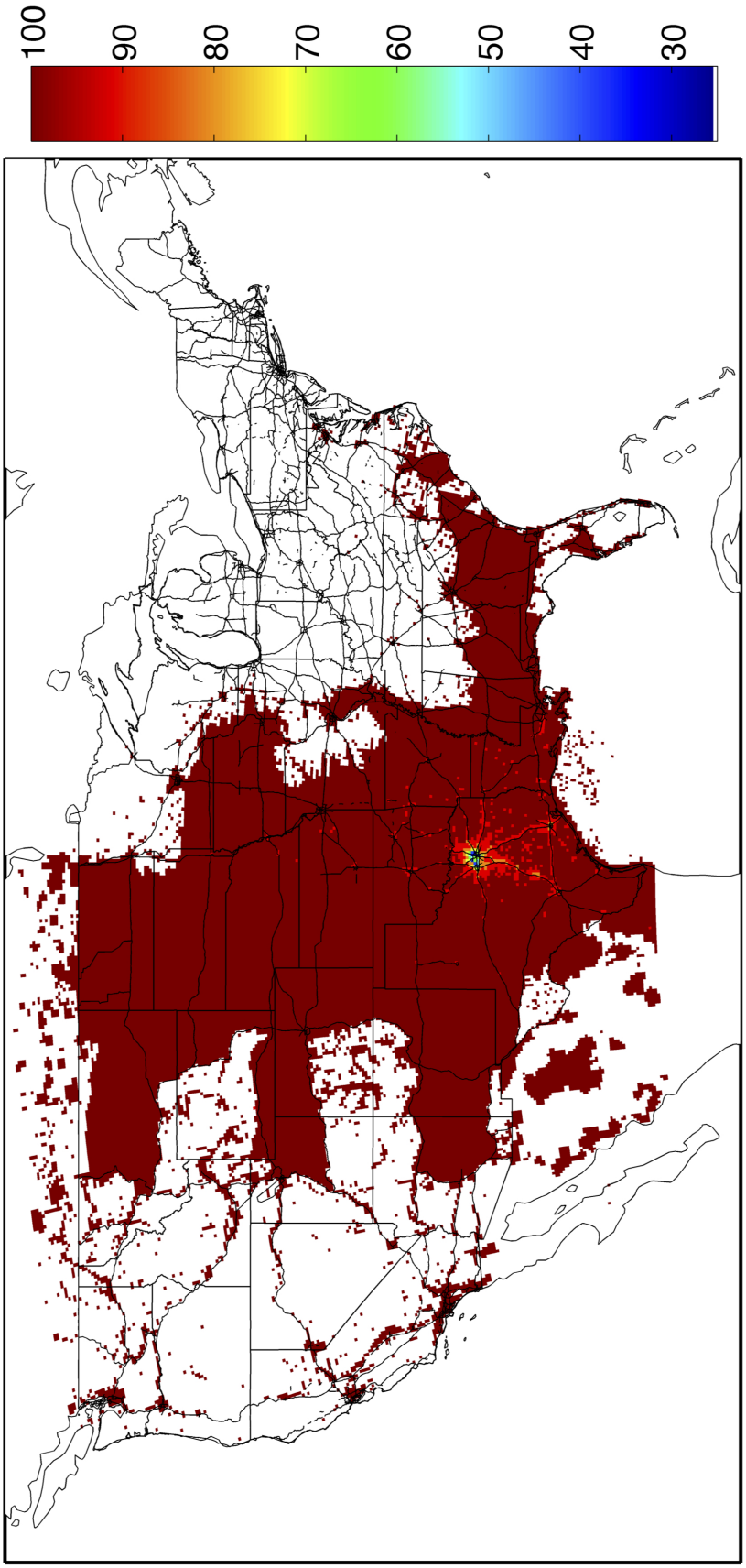

Figure 3.6: Contribution contour for the Dallas region.

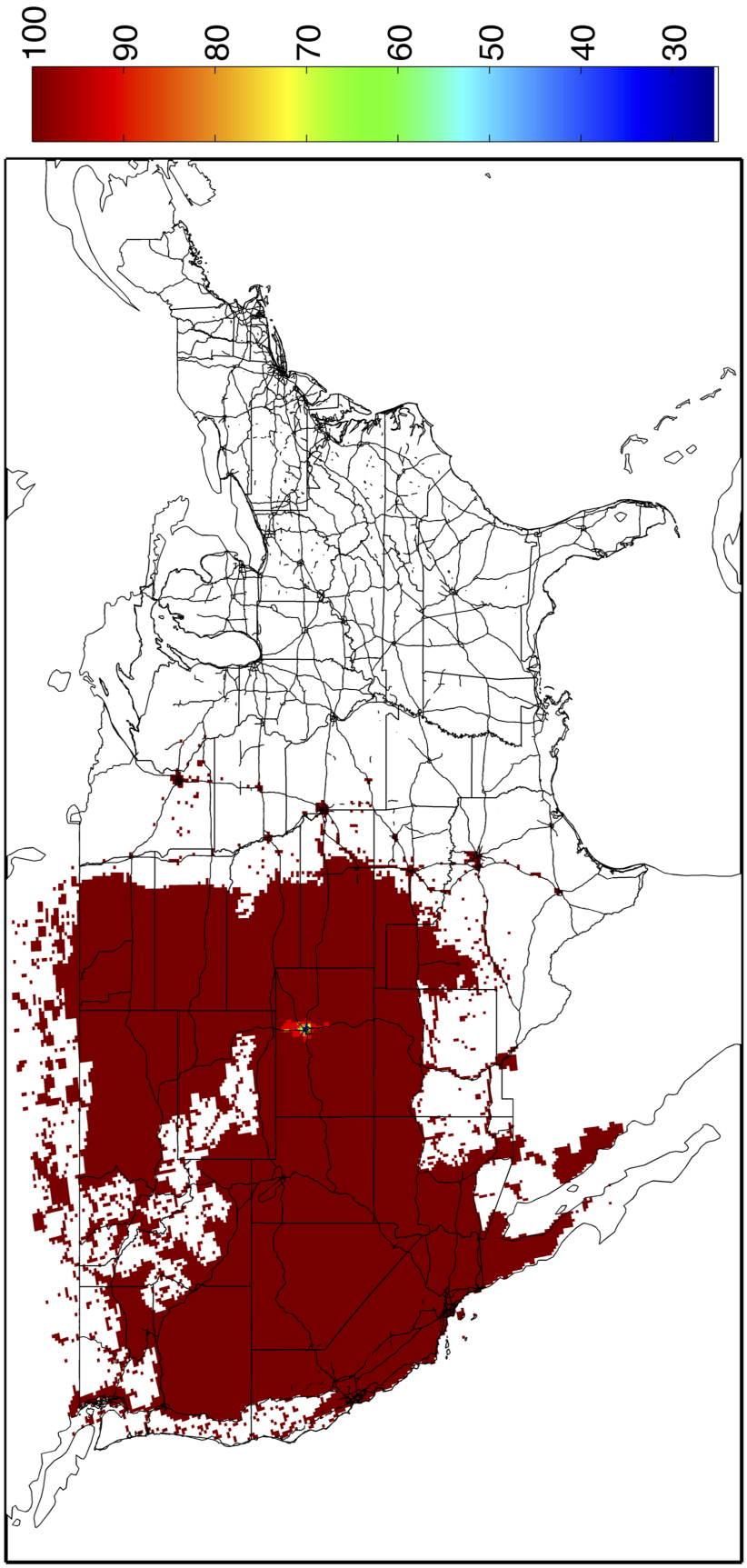

Figure 3.7: Contribution contour for the Denver region.

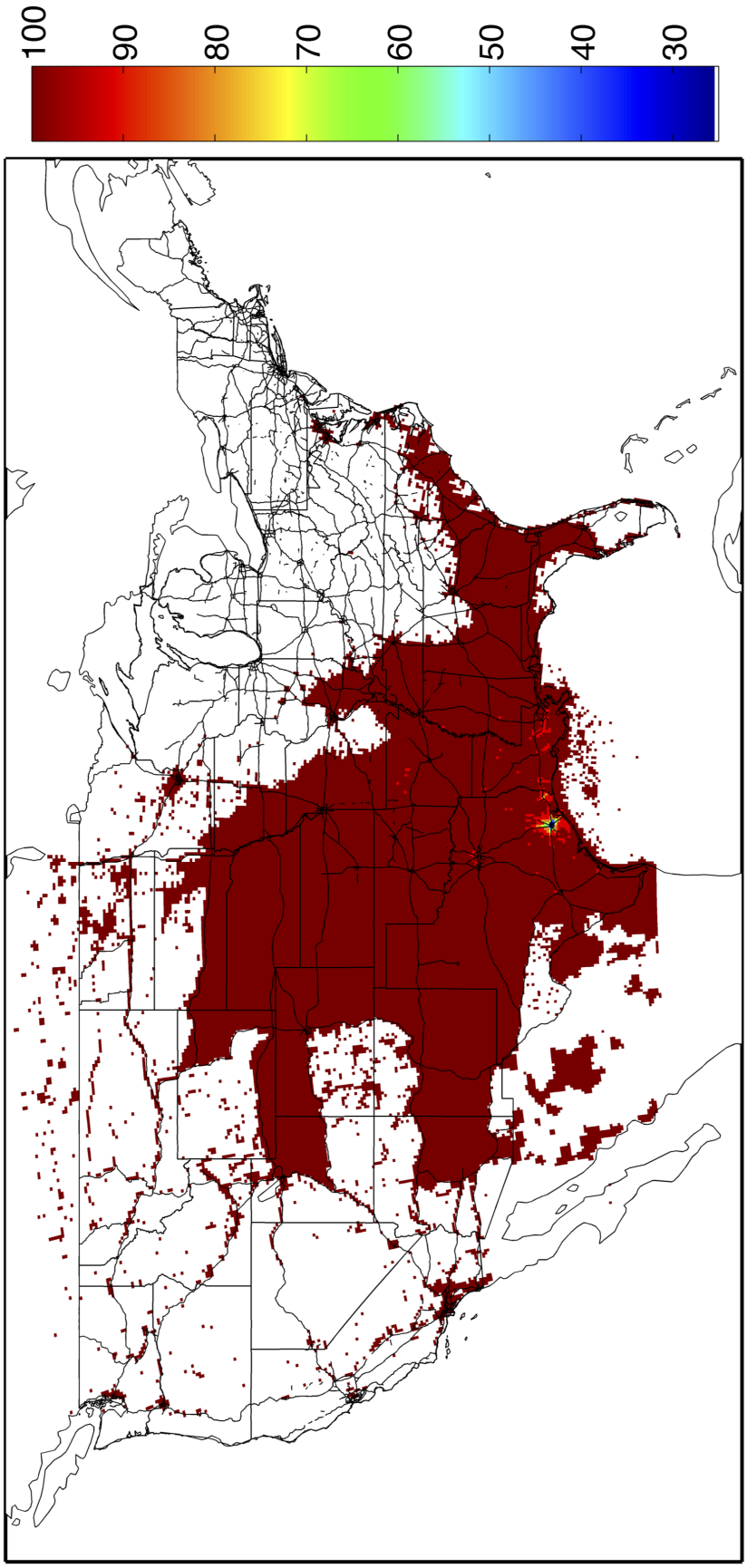

Figure 3.8: Contribution contour for the Houston region.

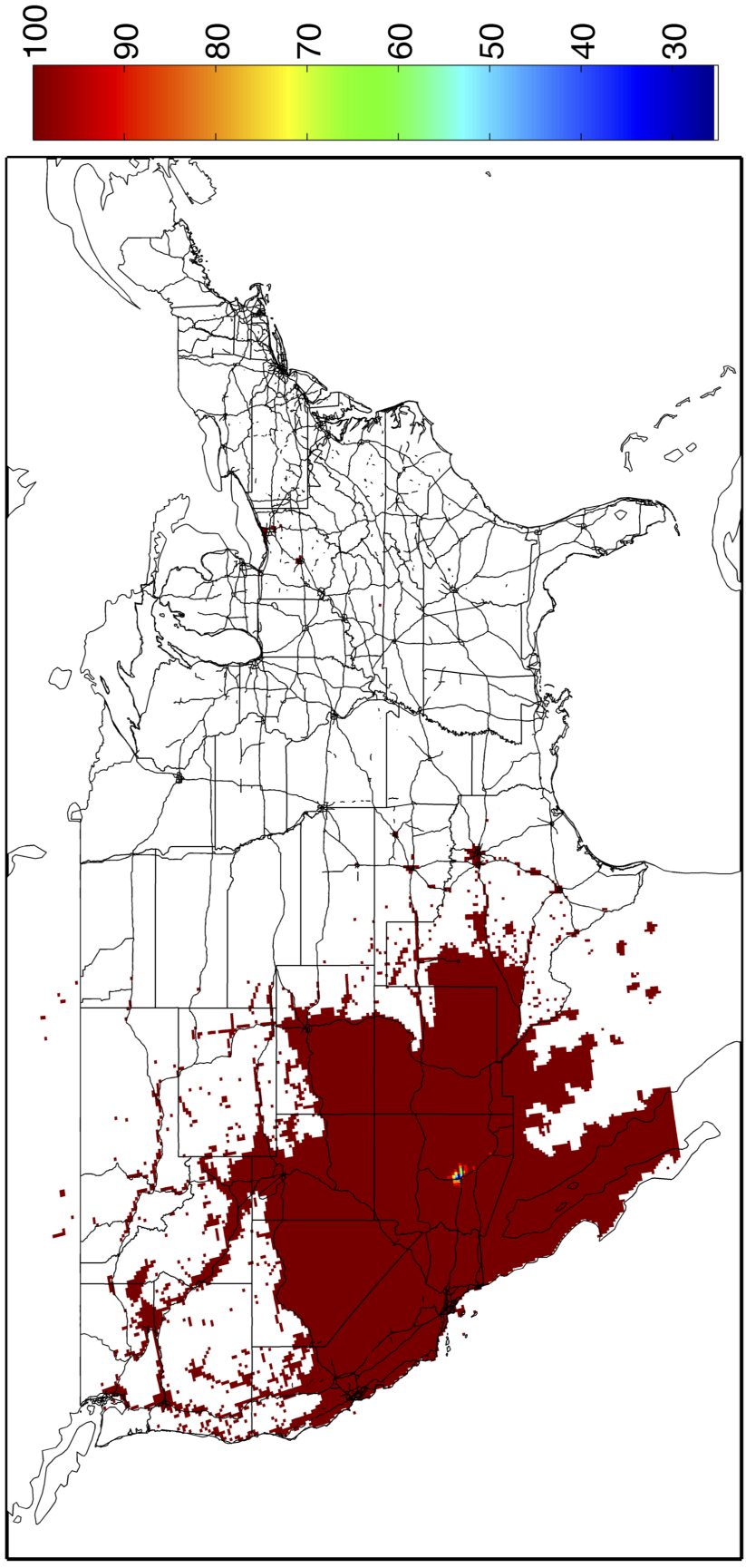

Figure 3.9: Contribution contour for the Phoenix region.

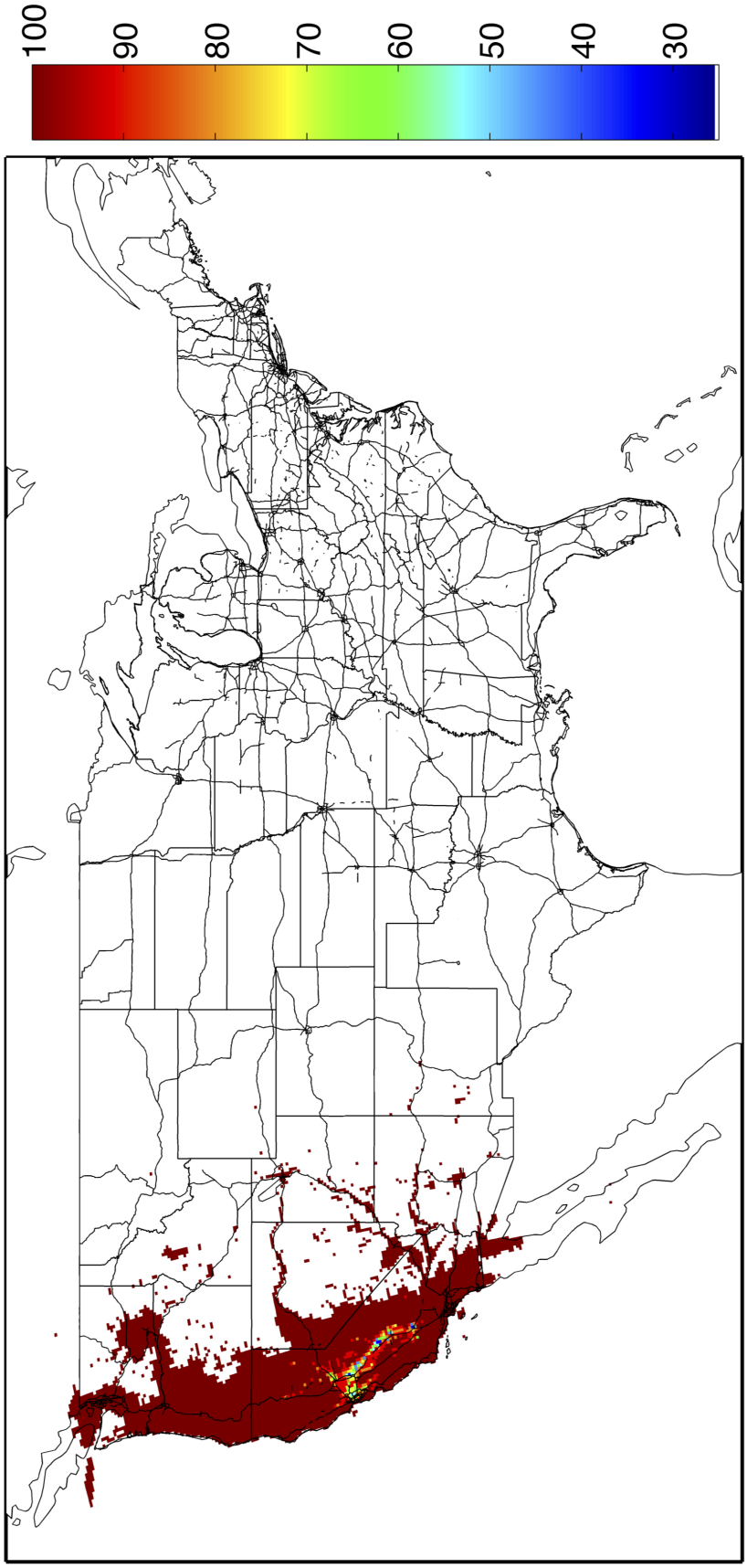

Figure 3.10: Contribution contour for the San Joaquin Valley region.

3.6.2 Efficiency of Emissions to Cause Premature Deaths

Analysis of the efficiency of emissions to cause premature deaths is important for determining the impact that the addition of new emissions in each location have on premature deaths, as well as providing insights toward the most cost-effective locations and sectors for which to develop stricter controls. A larger value means that more premature deaths occur on a per-unit-emission basis from emissions of BC. In contrast to contributions (Figure 2), efficiency estimates are independent of the magnitude of the BC emissions themselves, and thus show the role of transport and population density. Figure 3.11a shows the efficiency of BC emissions to result in premature deaths in the NY/PHI region. As expected, emissions in the urban centers have the highest efficiency values, with emissions in New York City resulting in over 45 premature deaths per Gg of BC emitted. While Figure 3.5 showed that emissions from as far west as the I-5 corridor must be considered in order to account for all of the premature deaths in the region, Figure 3.11a shows that (with a few exceptions) emissions within the region are the only ones with significant efficiencies. In fact, for every region emissions within the region are the only ones with significant efficiencies.

While Figure 3.11b also shows that emissions in the urban centers within the region have the highest efficiency, the highest efficiency for the Dallas region is just over 12 premature deaths per Gg of BC emitted. Also, while Figure 3.11b shows non-zero efficiencies west of the region, a majority of the non-zero efficiencies for the Dallas region are confined to an area north and south of the Dallas region. Figure 3.11c, on the other hand, has non-zero efficiencies radially outward of the Denver region, as well as west in to Utah. However, again we see that the largest efficiency values occur in the urban centers within the region, with a maximum efficiency of approximately 15 premature deaths per Gg of BC emitted.

While Figure 2b and Figure 2d showed very similar contour regions, Figure 3.11d shows that the spatial coverage of efficiencies of emissions to result in premature deaths in the Houston region differs significantly from the Dallas region. Figure 3.11b shows that the

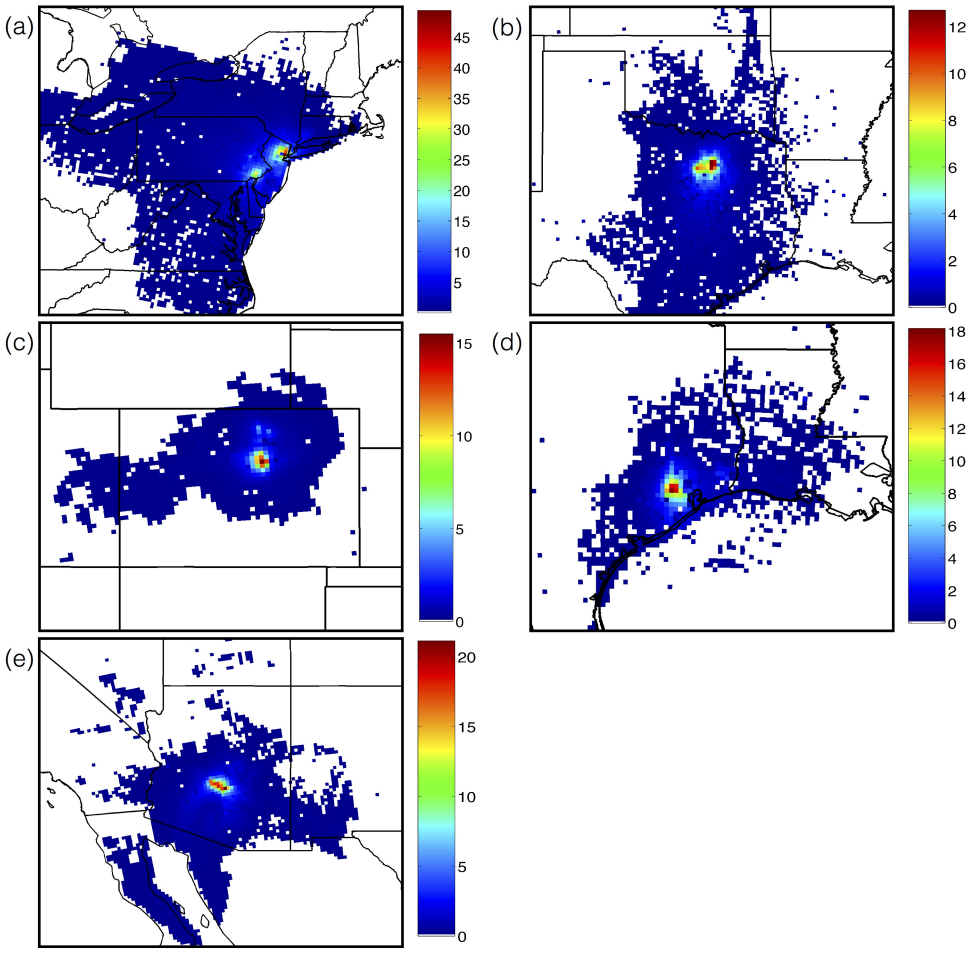

Figure 3.11: Plots of the efficiency of emissions to result in premature deaths ($\frac{Contribution}{Emission}$) from exposure to BC in the (a) NY/PHI region, (b) Dallas region, (c) Denver region, (d) Houston region, and (e) Phoenix region. Data in all figures presented as premature deaths per Gg of BC emitted.

efficiency for the Dallas region is confined to an area north and south of the region, with very little non-zero efficiencies east and west of the region. For the Houston region, however, a majority of the non-zero efficiency values come from the east and west of the region, with very little non-zero efficiencies showing up north and south of the region. Additionally, the Houston region has a larger maximum efficiency (18 premature deaths per Gg of BC emitted) than that of Dallas (12 premature deaths per Gg of BC emitted). The Phoenix region (Figure 3.11e) has a maximum efficiency of 20 premature deaths per Gg of BC emitted, and the San Joaquin Valley region has a maximum efficiency of 18 premature deaths per Gg of BC emitted.

3.7 References

SD Adar, DR Gold, BA Coull, J Schwartz, PH Stone, and H Suh. Focused exposures to airborne traffic particles and heart rate variability in the elderly. Epidemiology, 18(1): 95–103, January 2007.

AECOM, Cambridge Systematics, and Arellano Associates. 2013 California State Rail Plan. AECOM, Oakland, CA, 2013. URL `http://californiastaterailplan.dot.ca.gov/docs/Final_Copy_2013_CSRP.pdf`.

SC Anenberg, LW Horowitz, DQ Tong, and JJ West. An estimate of the global burden of anthropogenic ozone and fine particulate matter on premature human mortality using atmospheric modeling. Environ. Health Perspect., 118(9):1189–1195, April 2010.

SC Anenberg, K Talgo, S Arunachalam, P Dolwick, C Jang, and JJ West. Impacts of global, regional, and sectoral black carbon emission reductions on surface air quality and human mortality. Atmos. Chem. Phys., 11(14):7253–7267, 2011.

R Beelen, G Hoek, PA van den Brandt, RA Goldbohm, P Fischer, LJ Schouten, M Jerrett, E Hughes, B Armstrong, and B Brunekreef. Long-term effects of traffic-related air pollution on mortality in a Dutch cohort (NLCS-AIR study). Environ. Health Perspect., 116 (2):196–202, November 2007.

ML Bell and F Dominici. Effect modification by community characteristics on the short-term effects of ozone exposure and mortality in 98 US communities. Am. J. Epidemiol., 167(8): 986–997, 2008.

ML Bell, K Ebisu, RD Peng, JM Samet, and F Dominici. Hospital admissions and chemical composition of fine particle air pollution. Am. J. Respir. Crit. Care Med., 179(12):1115–1120, June 2009.

M Brauer, M Amann, RT Burnett, A Cohen, F Dentener, M Ezzati, SB Henderson, M Krzyzanowski, RV Martin, R Van Dingenen, A van Donkelaar, and GD Thurston. Exposure assessment for estimation of the global burden of disease attributable to outdoor air pollution. Environ. Sci. Technol., 46(2):652–660, January 2012.

D Byun and KL Schere. Review of the governing equations, computational algorithms, and other components of the Models-3 Community Multiscale Air Quality (CMAQ) modeling system. Appl. Mech. Rev., 59(1/6):51, 2006.

F Caiazzo, A Ashok, IA Waitz, SHL Yim, and SRH Barrett. Air pollution and early deaths in the United States. Part I: Quantifying the impact of major sectors in 2005. Atmos. Environ., 79(198-208), 2013.

AJ Cohen, HR Anderson, B Ostro, KD Pandey, M Krzyzanowski, N Kuenzli, K Gutschmidt, CA Pope, I Romieu, JM Samet, and KR Smith. Comparative Quantification of Health

Risks, volume 2, chapter 17, pages 1353–1433. World Health Organization, European Centre for Environment and Health, Bonn Office, 2004a. URL http://www.who.int/publications/cra/chapters/volume2/1353-1434.pdf?ua=1.

AJ Cohen, HR Anderson, B Ostro, KD Pandey, M Krzyzanowski, N Kuenzli, K Gutschmidt, CA Pope, I Romieu, JM Samet, and KR Smith. Mortality impacts of urban air pollution. In Majid Ezzati, AD Lopez, A Rodgers, and C Murray, editors, Comparative Quantification of Health Risks: Global and Regional Burden of Disease Due to Selected Major Risk Factors, Vol. 2. World Health Organization, Geneva, 2004b.

TR Dallmann and RA Harley. Evaluation of mobile source emission trends in the United States. J. Geophys. Res.: Atmos., 115, 2010.

IC Dedoussi and SRH Barrett. Air pollution and early deaths in the United States. Part II: Attribution of PM2.5 exposure to emissions species, time, location and sector. Atmos. Environ., 99(C):610–617, December 2014.

N Fann, CM Fulcher, and BJ Hubbell. The influence of location, source, and emission type in estimates of the human health benefits of reducing a ton of air pollution. Air Qual., Atmos. Health, 2(3):169–176, 2009. doi: 10.1007/s11869-009-0044-0.

N Fann, AD Lamson, SC Anenberg, K Wesson, D Risley, and BJ Hubbell. Estimating the national public health burden associated with exposure to ambient PM2.5 and ozone. Risk Analysis, 32(1):81–95, January 2012.

N Fann, CM Fulcher, and K Baker. The recent and future health burden of air aollution apportioned across U.S. sectors. Environ. Sci. Technol., 47(8):3580–3589, April 2013.

MM Finkelstein, M Jerrett, P DeLuca, N Finkelstein, DK Verma, K Chapman, and MR Sears. Relation between income, air pollution and mortality: a cohort study. Can. Med. Assoc. J., 169(5):397–402, 2003.

EM Flachs, J Sørensen, J Bønløkke, and H Brønnum-Hansen. Population dynamics and air pollution: the impact of demographics on health impact assessment of air pollution. J. Environ. Public Health., 2013(6):1–12, 2013.

JB Flanagan, RKM Jayanty, EE Rickman, and MR Peterson. PM2.5 speciation trends network: Evaluation of whole-system uncertainties using data from sites with collocated samplers. J. Air Waste Manage., 56(4):492–499, April 2006.

WJ Gauderman, F Gilliland, H Vora, E Avol, and D Stram. Association between air pollution and lung function growth in southern California children: Results from a second cohort. Am. J. Respir. Crit. Care Med., 166:76–84, June 2002.

TJ Grahame, R Klemm, and RB Schlesinger. Public health and components of particulate matter: The changing assessment of black carbon. J. Air Waste Manage., 64(6):620–660, May 2014.

NAH Janssen, G Hoek, M Simic-Lawson, P Fischer, L van Bree, H ten Brink, M Keuken, RW Atkinson, HR Anderson, B Brunekreef, and FR Cassee. Black carbon as an additional indicator of the adverse health effects of airborne particles compared with PM10 and PM2. 5. Environ. Health Perspect., 119(12):1691–1699, August 2011.

K Katanoda, T Sobue, H Satoh, K Tajima, T Suzuki, H Nakatsuka, T Takezaki, T Nakayama, H Nitta, K Tanabe, and S Tominaga. An association between long-term exposure to ambient air pollution and mortality from lung cancer and respiratory diseases in japan. J. Epidemiol., 21(2):132–143, 2011.

I Kazuhiko, R Mathes, Z Ross, A Nádas, G Thurston, and T Matte. Fine particulate matter constituents associated with cardiovascular hospitalizations and mortality in New York City. Environ. Health Perspect., 119(4):467, April 2011.

D Koch, M Schulz, S Kinne, C McNaughton, JR Spackman, Y Balkanski, S Bauer, T Berntsen, TC Bond, O Boucher, M Chin, A Clarke, N De Luca, F Dentener, T Diehl, O Dubovik, R Easter, D W Fahey, J Feichter, D Fillmore, S Freitag, S Ghan, P Ginoux, S Gong, L Horowitz, T Iversen, A Kirkevag, Z Klimont, Y Kondo, M Krol, X Liu, R Miller, V Montanaro, N Moteki, G Myhre, JE Penner, J Perlwitz, G Pitari, S Reddy, L Sahu, H Sakamoto, G Schuster, JP Schwarz, O Seland, P Stier, N Takegawa, T Takemura, C Textor, JA van Aardenne, and Y Zhao. Evaluation of black carbon estimations in global aerosol models. Atmos. Chem. Phys., 9(22):9001–9026, 2009.

D Krewski, M Jerrett, RT Burnett, R Ma, E Hughes, Y Shi, MC Turner, CA Pope, G Thurston, EE Calle, MJ Thun, B Beckerman, P DeLuca, N Finkelstein, K Ito, DK Moore, KB Newbold, T Ramsay, Z Ross, H Shin, and B Tempalski. Extended follow-up and spatial analysis of the American Cancer Society study linking particulate air pollution and mortality. Technical Report HEI Research Report 140, Health Effects Institute, Boston, Mass., USA, 2009. URL `http://ephtracking.cdc.gov/docs/RR140-Krewski.pdf`.

F Laden, J Schwartz, F E Speizer, and D W Dockery. Reduction in fine particulate air pollution and mortality - Extended follow-up of the Harvard six cities study. American Journal Of Respiratory And Critical Care Medicine, 173(6):667–672, 2006.

C Lee, R Martin, DK Henze, M Brauer, A Cohen, and A van Donkelaar. Response of global particulate-matter-related mortality to changes in local precursor emissions. Environ. Sci. Technol., 49(7):4335–4344, 2015. doi: 10.1021/acs.est.5b00873.

J Lepeule, F Laden, D Dockery, and J Schwartz. Chronic exposure to fine particles and mortality: an extended follow-up of the Harvard Six Cities study from 1974 to 2009. Environ. Health Perspect., 120(7):965–970, July 2012.

Y Li, DK Henze, D Jack, and PL Kinney. The influence of air quality model resolution on health impact assessment for fine particulate matter and its components. Air Qual., Atmos. Health, 2015.

V Mallet and B Sportisse. Uncertainty in a chemistry-transport model due to physical parameterizations and numerical approximations: An ensemble approach applied to ozone modeling. J. Geophys. Res.: Atmos., 11(1), 2006.

WC Malm, BA Schichtel, ML Pitchford, LL Ashbaugh, and RA Eldred. Spatial and monthly trends in speciated fine particle concentration in the United States. J. Geophys. Res.: Atmos., 109(D3), 2004.

BC McDonald, AH Goldstein, and RA Harley. Long-term trends in california mobile source emissions and ambient concentrations of black carbon and organic aerosol. Environ. Sci. Technol., 49(8):5178–5188, 2015.

GA Mensah, AH Mokdad, ES Ford, KJ Greenlund, and JB Croft. State of disparities in cardiovascular health in the United States. Circulation, 111(10):1233–1241, 2005.

SM Mesbah, A Hakami, and S Schott. Optimal ozone reduction policy design using adjoint-based NOx marginal damage information. Environ. Sci. Technol., 47(23):13528–13535, 2013.

NAS. Hidden costs of energy: Unpriced consequences of energy production and use. Technical report, National Research Council Committee on Health, Environmental, and Other External Costs and Benefits of Energy Production and Consumption, The National Academies Press, Washington, DC, 2010. URL `http://www.nap.edu/catalog/12794/hidden-costs-of-energy-unpriced-consequences-of-energy-production-and`.

MJ Neidell. Air pollution, health, and socio-economic status: the effect of outdoor air quality on childhood asthma. J. Health Econ., 23(6):1209–1236, 2004.

AJ Pappin and A Hakami. Attainment vs exposure: Ozone metric responses to source-specific nox controls using adjoint sensitivity analysis. Environ. Sci. Technol., 47(23): 13519–13527, December 2013a.

AJ Pappin and A Hakami. Source attribution of health benefits from air pollution abatement in Canada and the United States: an adjoint sensitivity analysis. Environ. Health Perspect., 121(5):572–579, May 2013b.

RD Peng, ML Bell, AS Geyh, A McDermott, SL Zeger, JM Samet, and F Dominici. Emergency admissions for cardiovascular and respiratory diseases and the chemical composition of fine particle air pollution. Environ. Health Perspect., 117(6):957–963, February 2009.

CA Pope, RT Burnett, MJ Thun, EE Calle, D Krewski, K Ito, and GD Thurston. Lung cancer, cardiopulmonary mortality, and long-term exposure to fine particulate air pollution. J. Am. Med. Assoc., 287(9):1132–1141, 2002.

MC Power, MG Weisskopf, and SE Alexeeff. Traffic-related air pollution and cognitive function in a cohort of older men. Environ. Health Perspect., 119(5):682–687, 2011.

RC Puett, JE Hart, JD Yanosky, C Paciorek, J Schwartz, H Suh, FE Speizer, and F Laden. Chronic fine and coarse particulate exposure, mortality, and coronary heart disease in the Nurses' Health Study. Environ. Health Perspect., 117(11):1697–1701, June 2009.

EM Punger and JJ West. The effect of grid resolution on estimates of the burden of ozone and fine particulate matter on premature mortality in the USA. Air Qual., Atmos. Health, 6(3):563–573, May 2013.

L Qiao, J Cai, H Wang, W Wang, M Zhou, S Lou, R Chen, H Dai, C Chen, and H Kan. PM2.5 constituents and hospital emergency-room visits in Shanghai, China. Environ. Sci. Technol., 48(17):10406–10414, 2014.

RA Silva, JJ West, Y Zhang, SC Anenberg, JF Lamarque, DT Shindell, WJ Collins, S Dalsoren, G Faluvegi, G Folberth, LW Horowitz, T Nagashima, V Naik, S Rumbold, R Skeie, K Sudo, T Takemura, D Bergmann, P Cameron-Smith, I Cionni, RM Doherty, V Eyring, B Josse, IA MacKenzie, D Plummer, M Righi, DS Stevenson, S Strode, S Szopa, and G Zeng. Global premature mortality due to anthropogenic outdoor air pollution and the contribution of past climate change. Environ. Res. Lett., 8(3), 2013.

S Stevenson, FJ Dentener, and MG Schultz. Multimodel ensemble simulations of present-day and near-future tropospheric ozone. J. Geophys. Res.: Atmos., 111(D08301), 2006.

JG Su, R Morello-Frosch, BM Jesdale, AD Kyle, B Shamasunder, and M Jerrett. An index for assessing demographic inequalities in cumulative environmental hazards with application to Los Angeles, California. Environ. Sci. Technol., 43(20):7626–7634, 2009.

HH Suh and A Zanobetti. Exposure error masks the relationship between traffic-related air pollution and heart rate variability. J. Occup. Environ. Med., 52(7):685–692, July 2010.

TM Thompson and NE Selin. Influence of air quality model resolution on uncertainty associated with health impacts. Atmos. Chem. Phys., 12(20):9753–9762, 2012.

MD Turner, DK Henze, A Hakami, S Zhao, J Resler, GR Carmichael, CO Stanier, J Baek, A Sandu, AG Russell, A Nenes, GR Jeong, SL Capps, PB Percell, RW Pinder, SL Napelenok, JO Bash, and T Chai. Differences between magnitudes and health impacts of BC emissions across the United States using 12 km scale seasonal source apportionment. Environ. Sci. Technol., 49(7):4362–4371, 2015. doi: 10.1021/es505968b.

US EPA. Control of air pollution from new motor vehicles: Heavy-duty engine and vehicle standards and highway diesel fuel sulfur control requirements. U.S. Environmental Protection Agency, Washington, DC, 2001. URL `http://www.gpo.gov/fdsys/pkg/FR-2001-01-18/pdf/01-2.pdf`.

US EPA. Integrated Science Assessment for Particulate Matter. Technical report, U.S. Environmental Protection Agency: National Center for Environmental Assessment, Washington, DC, December 2009. URL `http://www.epa.gov/ncea/pdfs/partmatt/Dec2009/PM_ISA_full.pdf`.

US EPA. Second report to congress: Highlights of the diesel emissions reduction program. U.S. Environmental Protection Agency, Washington, DC, 2012. URL http://www.epa.gov/cleandiesel/documents/420r12031.pdf.

TPC van Noije, HJ Eskes, FJ Dentener, DS Stevenson, K Ellingsen, MG Schultz, O Wild, M Amann, CS Atherton, DJ Bergmann, I Bey, KF Boersma, T Butler, J Cofala, J Drevet, AM Fiore, M Gauss, DA Hauglustaine, LW Horowitz, ISA Isaksen, MC Krol, JF Lamarque, MG Lawrence, RV Martin, V Montanaro, JF Muller, G Pitari, MJ Prather, JA Pyle, A Richter, JM Rodriguez, NH Savage, SE Strahan, K Sudo, S Szopa, and M van Roozendael. Multi-model ensemble simulations of tropospheric no_2 compared with gome retrievals for the year 2000. Atmos. Chem. Phys., 6(10):2943–2979, 2006.

WHO. Health risks of particulate matter from long-range transboundary air pollution. Technical report, World Health Organization Regional Office of Europe, Copenhagen, 2006. URL http://www.euro.who.int/__data/assets/pdf_file/0006/78657/E88189.pdf.

WHO. Health effects of black carbon. Technical report, World Health Organization, European Centre for Environment and Health, Bonn Office, April 2012. URL http://www.euro.who.int/__data/assets/pdf_file/0004/162535/e96541.pdf.

M Wilhelm, L Qian, and B Ritz. Outdoor air pollution, family and neighborhood environment, and asthma in LA FANS children. Health Place, 15(1):25–36, March 2009.

EH Wilker, MA Mittleman, BA Coull, A Gryparis, ML Bots, J Schwartz, and D Sparrow. Long-term exposure to black carbon and carotid intima-media thickness: the Normative Aging Study. Environ. Health Perspect., 121(9):1061–1067, September 2013.

S Zhao, AJ Pappin, SM Mesbah, JYJ Zhang, NL MacDonald, and A Hakami. Adjoint estimation of ozone climate penalties. Geophys. Res. Lett., 40(20):5559–5563, 2013.

Chapter 4

Comparison of Multiple Risk-Based Approaches to Air Pollution Management

Matthew D. Turner[1], Daven K. Henze[1], Shannon L. Capps[1], Amir Hakami[2], Shunliu Zhao[2], Jaroslav Resler[3], Gregory R. Carmichael[4], Charles O. Stanier[4], Jaemeen Baek[4], Adrian Sandu[5], Armistead G. Russell[6a], Athanasios Nenes[6b], Rob W. Pinder[7], Sergey L. Napelenok[7], Jesse O. Bash[7], Peter B. Percell[8], and Tianfeng Chai[9]

[1]Mechanical Engineering Department, University of Colorado, Boulder, Colorado 80309, United States

[2]Department of Civil and Environmental Engineering, Carleton University, Ottawa, Ontario K1S 5B6, Canada

[3]Nonlinear Modeling, Institute of Computer Science, Prague 182 07, Czech Republic

[4]Department of Chemical and Biochemical Engineering, University of Iowa, Iowa City, Iowa 52242, United States

[5]Computer Science, Virginia Tech, Blacksburg, Virginia 24061, United States

[6a]School of Civil and Environmental Engineering, and [6b]School of Earth and Atmospheric Sciences, Georgia Tech, Atlanta, Georgia 30331, United States

[7]Atmospheric Modeling and Analysis Division, U.S. EPA, Research Triangle Park, North Carolina 27711, United States

[8]Department of Geosciences, University of Houston, Houston, Texas 77004, United States

[9]College of Computer, Mathematical, and Natural Sciences, University of Maryland, College Park, Maryland 20742, United States

4.1 Abstract

Previous studies have shown that exposure to ambient particulate black carbon (BC) is associated with adverse health effects, including premature death. In this study we use the adjoint of the Community Multiscale Air Quality (CMAQ) model to estimate the impact of emissions in the US in 2007 on three different health-based metrics: premature deaths for specific demographic groups, premature death rates (average individual risk), and a metric independent of population and baseline mortality rates (risk modification factor). We find strong correlations between contribution percentage and population percentage for each demographic group, with correlation coefficients ranging between 0.77 for persons with above a high school education to 0.85 for persons below 50% of the poverty level. An inter-comparison of the contribution and population distributions between demographic groups shows that there is much less variability in the types of people harmed by BC emissions than there is in the variability of population demographics themselves. Additionally, we find that individual emission sectors have small variability (1-3%) in their contributions to premature deaths for the different demographic groups. Analysis of the effects of BC emissions on risk modification factor in the US shows that the largest risk modification factors result from emissions in drier climates, due to the increased atmospheric lifetime of particles being emitted in these climates. While average individual risk is independent of population, we find that sensitivities of this risk are strongest within the urban centers due to the significantly larger emissions within the urban centers than in the surrounding areas. We also find average individual risks resulting from BC emissions in single grid cells to be upwards of 9.5 in ten million in 2007 for the NY/PHI region, which is larger than the risk from flying.

4.2 Introduction

There is strong evidence from epidemiological studies that prolonged exposure to ambient fine particulate matter ($PM_{2.5}$) results in many adverse health effects, including premature death [Krewski et al., 2009; WHO, 2006; Pope et al., 2002; Katanoda et al., 2011; Lepeule et al., 2012; Kazuhiko et al., 2011; Puett et al., 2009; Gauderman et al., 2002; Cohen et al., 2004; Beelen et al., 2007; Laden et al., 2006]. Recent studies have investigated the possibility that certain species within $PM_{2.5}$ are more harmful to health than $PM_{2.5}$ as a whole, any many have found exposure to black carbon (BC) to be one of the most harmful [Suh and Zanobetti, 2010; Adar et al., 2007; Peng et al., 2009; WHO, 2012; Power et al., 2011; Wilker et al., 2013; Qiao et al., 2014]. Janssen et al. [2011] found that by reducing a unit of BC, life expectancy is extended four to nine times more than a unit reduction of $PM_{2.5}$. In a review of the epidemiological and toxicological literature regarding the health effects of BC, Grahame et al. [2014] suggested that exposure to BC is causally linked to premature death.

While these previously mentioned studies portray the link between exposure of the general population to ambient $PM_{2.5}$ and premature death, other studies have suggested that certain population demographics are at higher risk than others [Flachs et al., 2013; Wilhelm et al., 2009; Neidell, 2004; Finkelstein et al., 2003; Su et al., 2009; Mensah et al., 2005]. Krewski et al. [2009] showed that a decrease in the effect of $PM_{2.5}$ exposure on premature death was correlated with an increase in education level. Mensah et al. [2005] used national surveys to determine risk factors for cardiovascular disease (CVD) by ethnicity, education level, and socioeconomic status. They found that reported cases of heart disease were inversely related to poverty status and education level. Finkelstein et al. [2003] performed an analysis of the effects of air pollution on premature death rates for an area of southern Ontario and found that the relative risk of death from all causes for low income households was up to twice as large as high income households (relative risk for high income, high pollutant

level households of 1.33 and relative risk for low income, high pollutant households of 2.62).

When developing air pollution control policies, many different approaches have been considered to achieve the main objective of protecting the health and welfare of the public. One such approach is using a health effect analysis (e.g., Fann et al. [2012b,a, 2009]; Anenberg et al. [2011]; Muller et al. [2011]) in order to evaluate the costs and benefits of air pollution control policies [Johns et al., 2012; Hubbell, 2012]. However, a concern with using total health effects as a target for air quality policy is the potential unequal treatment of individuals, with more weight given to emissions that impact people in the most populous regions [Tietenberg, 1995]. Alternative approaches include a risk-based analysis and an analysis of the average individual risk (AIR). While previous air quality studies have defined risk-based approaches to include intake fraction [Xu et al., 2013; Zhou et al., 2010; Levy et al., 2002; Humbert et al., 2011] or total incidences [Wesson et al., 2010; Fann et al., 2011], these are both metrics that depend upon the magnitude and spatial distribution of the exposed population. While previous studies have analyzed spatial and sectoral variability in external damages of air pollutant emissions (e.g., Fann et al. [2009, 2012a]; Turner et al. [2015b]; Muller et al. [2011]; Anenberg et al. [2012]), few studies have analyzed the spatial and sectoral variability of average individual risk.

In this paper, we investigate the influences of population, mortality rates, and relative risk factors on the different approaches used in health-based analyses for air quality controls. Using the CMAQ adjoint model, we quantify the number of premature deaths attributed to exposure to BC for four demographic groups in order to determine locations and sources that affect certain populations more than others. For risk-based analysis in this study, we first consider a health impact function that does not include baseline mortality rates and population. This metric is not marginalized for low populations, however it also does not include any information about mortality rates. We next consider AIR, which does not include the population variable. It does, however, includes information about baseline mortality rates and provides an estimate of the risk of an adverse health effect on a per-person basis. This

metric is thus similar to the notion of an individual's risk that is commonplace for hazards such as developing cancer [Howlader et al., 2014; Ahmad et al., 2015; Feuer et al., 1993]. We estimate the impact of emissions on both risk and average individual risk throughout the US and in three specific urban regions.

4.3 Materials and Methods

Simulated annual average BC concentrations were obtained using the CMAQ model v4.7.1 [Byun and Schere, 2006] for 2007. Forward model evaluation, as well as discussion of meteorological and emission inputs can be found in Turner et al. [2015b].

Estimates of premature deaths attributed to exposure to BC for four demographic groups (persons below 50% of the poverty level, above 200% of the poverty level, with less than a high school education, and with a bachelors degree or higher) are calculated using the following health impact function:

$$J_d = \sum_{i=1}^{N} M_{0,i} \cdot P_i^d \cdot (1 - e^{-\beta^d \cdot C_{av,i}}) \tag{4.1}$$

where M_0 is the gridded baseline mortality rate for people age 30 or older (and is constant across all demographic groups), P_i^d is the population for demographic d, $C_{av,i}$ is the gridded annual average BC concentration, i is the grid cell index, N is the number of grid cells, and β^d is the concentration response factor. We used a constant β^d ($\beta^T = 0.005827$, calculated from the relative risk estimate presentey6y yyp6y6lluy u7l;yeFinkelstein:2003tz,Mensah:2005ii,Su:2009hh, these studies analyzed the effects of total suspended particles [Finkelstein et al., 2003], a combination of multiple environmental hazards [Su et al., 2009], or morbidity from specific health outcomes [Mensah et al., 2005]. 'j'[l. Our use of a constant β means that the results are likely biased low for the analysis of persons below 50% of the poverty level, and biased high for the analysis of persons above 200% of the poverty level. We use a varying β^d per Krewski et al. [2009] for different education levels ($\beta^{BHS} = 0.006204$ for below high school education, and $\beta^{AHS} = 0.004018$ for above high school education). Demographic population information was obtained from the NASA Socioeconomic Data and Applications Center [Seirup and Yetman., 2015], and is based on the US Census 2000 TIGER files. While the demographic population information provided populations for persons with a bachelors degree or higher, we used the concentration response factor from Krewski et al. [2009] for greater than a high school education, and refer to this demographic group as persons with above a high school

education. Therefore, our results are possibly biased low for this demographic group, as we are not including the full population of people with above a high school education but without a bachelors degree (e.g., people with an associates degree).

4.3.1 Risk Modification Factor

In addition to simulations that have premature death as the metric of interest, we have also performed simulations where the metric of interest is defined as the national risk modification factor, or risk modification factors for specific urban regions (Equation 4.2). For the regional risk estimate simulations, three regions were considered (New York City and Philadelphia (NY/PHI), Dallas, and San Joaquin Valley). These specific regions were chosen from the analysis in Turner et al. [2015a] because NY/PHI showed the largest number of premature deaths, the San Joaquin Valley showed large per-unit emission damages along a route where a new rail system is to be build, and the Dallas region showed significant impacts from outside of the region. For the risk modification factor simulations, the risk modification factor (the probability of damage to life as a result of a given hazard) is calculated using the following equation

$$R = \sum_{i=1}^{N} (1 - e^{-\beta^T \cdot C_{av,i}}) \tag{4.2}$$

where R is the risk modification factor for the region of interest, β^T is the concentration response factor for all-cause premature deaths for the total population, i is the grid cell index, N is the number of grid cells in the region, and $C_{av,i}$ is the annual average BC concentration in the region.

4.3.2 Average Individual Risk

Lastly, we perform simulations where the metric of interest is the average individual risk for both national and regional simulations (Equation 4.3). As with the risk modification factor simulations, only three regions are considered (NY/PHI, Dallas, and San Joaquin

Valley). The average individual risk is calculated using the following equation

$$AIR = \frac{1}{N} \cdot \sum_{i=1}^{N} M_{0,i} \cdot (1 - e^{-\beta^T \cdot C_{av,i}}) \tag{4.3}$$

where M_0 is the baseline non-accidental mortality rate for grid cell i. We estimate an average individual risk value (as opposed to a sum) in order to account for the fact that emissions in any given grid cell might not have an effect on the entire region. For example, an analysis of the national AIR includes the effects of emissions in both southern California and Maine. However, emissions from southern California do not have a significant effect on AIR in Maine, and vice versa. Therefore, we present the average individual risk calculation instead of the summed individual risk calculation.

4.3.3 Adjoint Sensitivities

We use the CMAQ adjoint to obtain the sensitivities of national premature deaths attributed to exposure to BC with respect to emissions for each demographic, as well as sensitivities of risk and average individual risk with respect to emissions for the nation as a whole and three urban regions. See Turner et al. [2015b] for full details of the development and validation of the CMAQ adjoint model. In order to reduce the computational cost of this analysis, adjoint simulations were run for the first week of each month. The resulting 12 week average has been shown to be an accurate representation of the year as a whole [Turner et al., 2015b]. Semi-normalized health impact sensitivities ($\frac{\partial J_d}{\partial E_{i,k,m}} \cdot E_{i,k,m}$) represent the contributions of BC emissions in grid cell i, sector k, and month m to the number of estimated premature deaths in demographic d attributed to exposure to BC. Semi-normalized sensitivities for average individual risk ($\frac{\partial AIR}{\partial E_{i,k,m}} \cdot E_{i,k,m}$) represent the increased risk that an individual will pass away prematurely as a result of exposure to BC from emissions in grid cell i, sector k, and month m. Absolute sensitivities of risk modification factor ($\frac{\partial R}{\partial E_{i,k,m}}$) with respect to emissions represent the increased risk associated with emissions in grid cell i, sector k, and month m on a per-unit-emission basis. While the other analyses in this

paper present semi-normalized sensitivities, we present absolute sensitivities for the risk modification factor analysis in order to investigate the impact of changes in emissions on risk on a per-unit emission basis.

4.4 Results and Discussion

4.4.1 Demographic Analysis - Nationwide

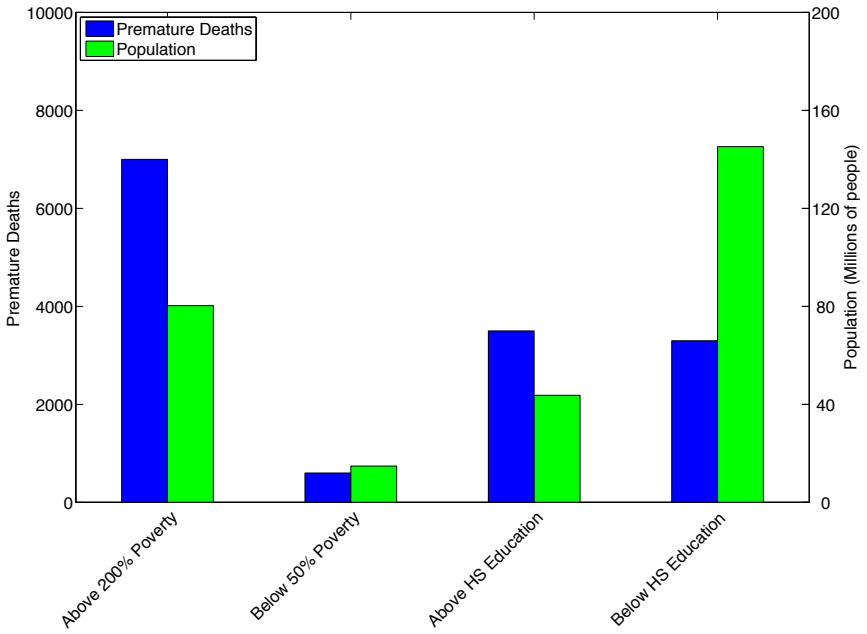

Figure 4.1: Total number of premature deaths from exposure to BC in 2007 and total US populations for each demographic.

Figure 4.1 shows the estimate of premature deaths for each demographic group, and the US population of each demographic group (spatial distributions of each demographic group are shown in Figure 4.13). While there are significantly more people with less than a high school education than any other demographic analyzed (almost double that of the above 200% poverty group, and 10 times that of the below 50% poverty group), there are less premature deaths attributed to exposure to BC for this group than both of the 'above' groups (above 200% poverty level and above high school education). Additionally, the below high school education group has triple the population of the above high school education group, yet has 200 less premature deaths. This is due to the fact that the distribution of the above high school education group is more correlated with high BC concentrations that occur in and near the urban centers, while the below high school education group is more

rural, nationally. The above 200% poverty level group has the most premature deaths, with twice as many premature deaths as the next closest group (above high school education). This is again owing to the large percentage of people from this demographic living in and near the urban regions (see Figure 4.13a). Finally, the below 50% poverty level group has the fewest premature deaths with 600 (420 - 780) and the lowest population.

We first consider the contributions of BC emissions for each demographic group (Figure 4.12). Figure 4.12a shows the number of premature deaths in the above 200% poverty level demographic resulting from emissions in each grid cell. The largest contributions occur within the urban centers throughout the US, with smaller contributions as the distance to urban centers increases. A significant portion of the rural areas in the eastern US are shown to have fractional contributions (between 0.01 and 1), while a majority of the rural regions in the western half of the US show no contributions. This is a result of the larger populations in the rural areas of the eastern US (Figure 4.13a). The below 50% poverty level group has approximately ten times fewer premature deaths (Figure 4.12b) than the above 200% poverty level group. Again, we see the largest contributions coming from the urban centers where populations (Figure 4.13b) and emissions are largest. Contributions from BC emissions to premature deaths for the above high school education (Figure 4.12c) and below high school education (Figure 4.12d) groups appear to be nearly identical, with maximums occurring within the urban centers and fractional contributions from emissions in many of the rural areas in the eastern US. While the spatial maps of the contributions to above high school education and below high school education are very similar (Figure 4.12c-d), the respective population distributions (Figures 4.13c-d) show significantly larger populations in the below high school education demographic in those rural areas.

It is interesting to evaluate the extent to which differences in the maps of contributions of BC emissions to premature deaths in these different demographics are driven by differences in the spatial distribution of these populations. In order to determine this, we next compare contribution percentages to population percentages for each demographic group (Figures 4.2

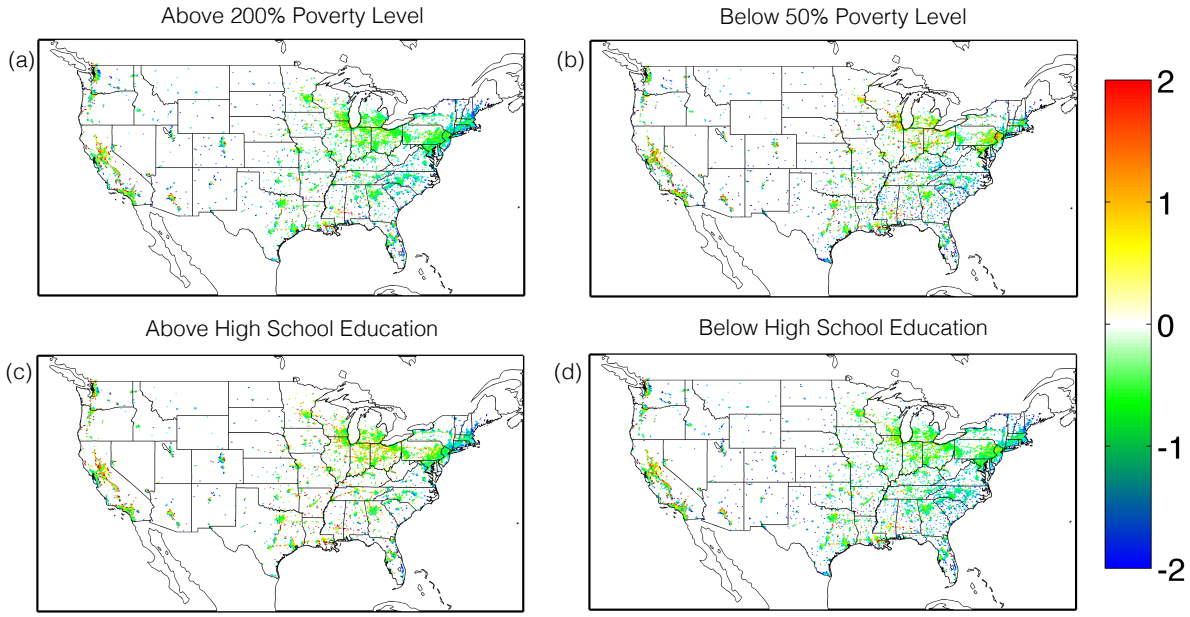

Figure 4.2: Spatial plot of the ratios of contribution percentage to population percentage for (a) persons above 200% poverty level, (b) persons below 50% poverty level, (c) persons with above a high school education, and (d) persons with below a high school education. Data presented on a log scale.

and 4.3). Results in Figure 4.2 are presented as a ratio of the contribution percentage to the population percentage, on a log scale. Similar to the ratio analyses of contributions in Turner et al. [2015b], in order to emphasize the locations with the largest contributions for each demographic group we have included only the grid cells that sum to the top 85% of the numerator and denominator. For example, when plotting the ratio of contributions for people with an education above high school to population for persons with above a high school education, we only plot the grid cells that sum to 85% of contributions for persons with above a high school education and the grid cells that sum to 85% of population for persons with above a high school education. This filtering prevents some large ratios that correspond to locations with negligible contributions from being displayed on the plots. Additionally, we plot ratios of the contribution percentages instead of absolute concentrations in order to account for differences in total contributions for each demographic group.

Figure 4.2a shows the ratio of contribution percentage to population percentage for persons above 200% of the poverty level, with a maximum ratio of 4.7 in southeastern Louisiana. A majority of locations that have a larger contribution percentage than population percentage occur along interstates in the south central US and in California, due to the significant disparity between vehicle emissions along rural interstates and populations within the grid cells that contain the rural interstates. On the other hand, many locations with a larger population percentage than contribution percentage occur on the east coast (with a large number in the northeast), with a maximum in Florida. Figure 4.2b shows the ratio of contribution percentage to population percentage for persons below 50% of the poverty level. Compared to Figure 4.2a, the results for this demographic show more locations with larger contribution percentages, especially in the northeast where Figure 4.2a shows almost no locations with a contribution percentage larger than the corresponding population percentage. Major roadways again stand out as the locations with a larger contribution percentage than population percentage, however, there is a region of large ratios upwind of New York City and Chicago. This is a result of the upwind regions having lower population percentages (Figure 4.13b) for

the 50% poverty level demographic, yet large population percentages in the urban regions downwind of the emissions. Figure 4.2c shows the contribution to population ratio for people with above a high school education. While showing a similar trend to Figure 4.2a, with very few locations in the northeastern US having larger contribution percentages than population percentages, we see much fewer rural locations showing up around the urban centers. This is attributed to the above high school education demographic having a larger percentage of its population in the urban centers (Figure 4.13c), resulting in fewer grid cells being required to sum to 85% of the population. Lastly, Figure 4.2d shows the contribution to population ratio for persons with below a high school education. Similar to Figure 4.2a, many of the locations with higher contribution percentages than population percentages occur in the south central US and in California. The northeastern US and Florida again show much larger population percentages than contribution percentages, resulting from the larger population percentages in the region (Figure 4.13d).

Figure 4.3 shows scatter plots of the contribution percentages versus population percentages for each demographic group. All groups have a strong correlation (correlation coefficients ranging from 0.77 to 0.85) and R^2 values near 0.6 to 0.72. The above 200% poverty level group (Figure 4.3a) shows a larger slope than the above high school education group (Figure 4.3c), which is expected since the above high school education group has a smaller concentration response factor than used for the above 200% poverty level group. Additionally, the below 50% poverty level group (Figure 4.3b) has a smaller slope than the below high school education group (Figure 4.3d), which can again be explained by the larger concentration response factor for the below high school education group.

The above analysis shows that despite effects of transport, there are strong correlations between emission locations and the locations of the population subgroups harmed by BC exposure. It is next of interest to evaluate the extent to which emissions may impact a population subgroup disproportionately compared to other population subgroups. Figure 4.4 shows the ratios of contributions from the various demographic simulations. A trend

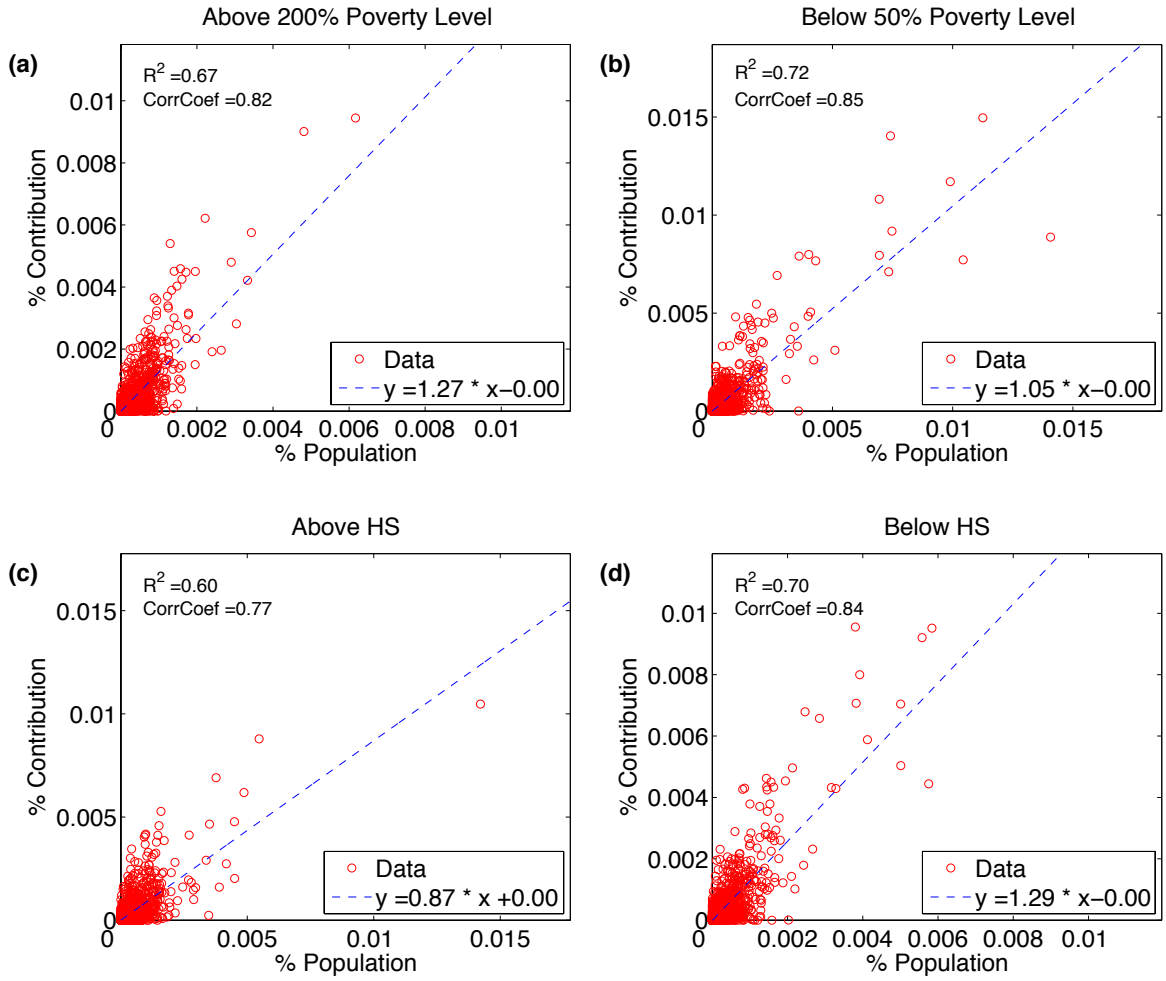

Figure 4.3: Scatter plots of contribution percentages vs. population percentages for (a) persons above 200% poverty level, (b) persons below 50% poverty level, (c) persons with above a high school education, and (d) persons with below a high school education.

that is consistently seen across the various ratios is a difference between contributions in the northern and southern parts of the US, with emissions in the northern part of the US contributing to more premature deaths for the wealthier and more educated demographics. Figure 4.4a shows the ratio of persons with more than a high school education to persons with less than a high school education. While not as pronounced as some of the other panels, there are distinct sections of the US where emissions disproportionally effect persons with different education levels (with a maximum ratio of 1.9 in southeast New Hampshire). On the other hand, the Los Angeles and San Joaquin Valley regions show significantly more contributions (on a percentage basis) for less-educated individuals. In contrast, regions such as Seattle, much of the Northeastern US, and Florida show emissions having a greater impact on more-educated individuals. In order to determine the extent to which these differences can be explained by disparities in the underlying population distributions, Figure 4.5a shows a comparison of the contribution ratios to population ratios. While there are large variations in the population ratios, we see much smaller variations in the contribution ratios ($R^2 = 0.18$). Therefore, a majority of the variability in the contribution ratio is driven by other factors, such as baseline mortality rates and the position of population distributions downwind of emission sources.

Figure 4.4b shows a ratio of contributions to individuals above 200% of the poverty level to individuals below 50% of the poverty level, and shows much larger differences than Figure 4.4a, with a maximum ratio of 3.1 (in southeast New Hampshire) and a minimum ratio of 0.2 (at the southern tip of Texas). The ratio of high income to low income individuals also shows a strong correlation (Figure 4.5b), with higher population ratios resulting in higher contribution ratios. This strong correlation (correlation coefficient of 0.62) is a result of the concentration response factor being constant across varying income levels. Therefore, the population distribution is the most variable input in the analysis. Figure 4.4c shows a ratio of contributions to individuals below 50% of the poverty level to individuals with less than a high school education. Unlike Figures 4.4a-b we do not see a distinct split between the

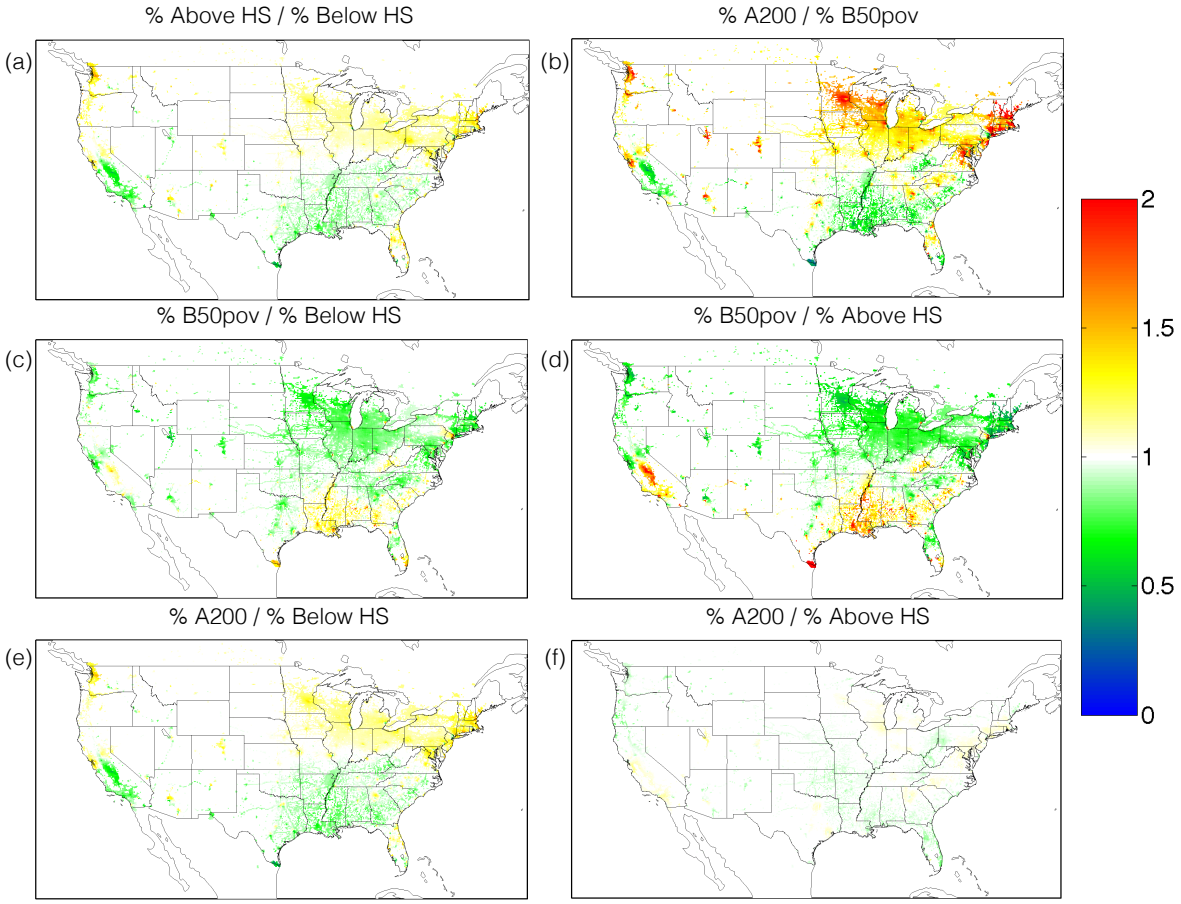

Figure 4.4: Spatial plot of contribution ratios for (a) individuals with above a high school education to individuals with below a high school education, (b) individuals above 200% of the poverty level to individuals below 50% of the poverty level, (c) individuals below 50% of the poverty level to individuals with below a high school education, (d) individuals below 50% of the poverty level to individuals with above a high school education, (e) individuals above 200% of the poverty level to individuals with below a high school education, and (f) individuals above 200% of the poverty level to individuals with above a high school education.

northern and southern US. For this ratio, most of the US shows larger values for individuals with less than a high school education. However, there are still a few regions (southeastern US and the San Joaquin Valley) where individuals below 50% of the poverty level have larger values.

Figure 4.4d shows the ratio of contributions to individuals below 50% of the poverty level to individuals with above a high school education. As with the other figures we again see a distinct split between the northern and southern half of the US, with emissions in the northern US contributing to more premature deaths per person for the above high school education group and emissions in the southern US contributing to more premature deaths per person for the below 50% poverty level group. Figure 4.5d shows the corresponding scatter plot, and shows that the contribution ratios are skewed toward larger values. This skewing in the data is explained by the larger concentration response factor for persons below 50% of the poverty level, which results in a larger number of premature deaths per unit population for the below 50% poverty level group than the above high school education group. A comparison of individuals above 200% of the poverty level to individuals with below a high school education (Figure 4.4e) also shows the trend of emissions in the northern half of the US contributing to a higher fraction of premature deaths to the higher income demographic, with a maximum ratio of 1.7 in southeast New Hampshire. Figure 4.5e shows the correlation between the contribution and population ratios for individuals above 200% of the poverty level to individuals with below a high school education. As with Figure 4.5b, we see a strong correlation between contribution ratio and population ratio with a correlation coefficient of 0.69. Lastly, Figure 4.5f shows the comparison of persons above 200% of the poverty level to persons with above a high school education. Compared to the other panels, this ratio shows very little variation throughout the region. There are still locations where emissions have a larger impact on each demographic group (emissions in the southeast US have a larger impact on persons with above a high school education), however the differences are very small. Figure 4.5f shows the corresponding scatter plot for this relationship. Similarly

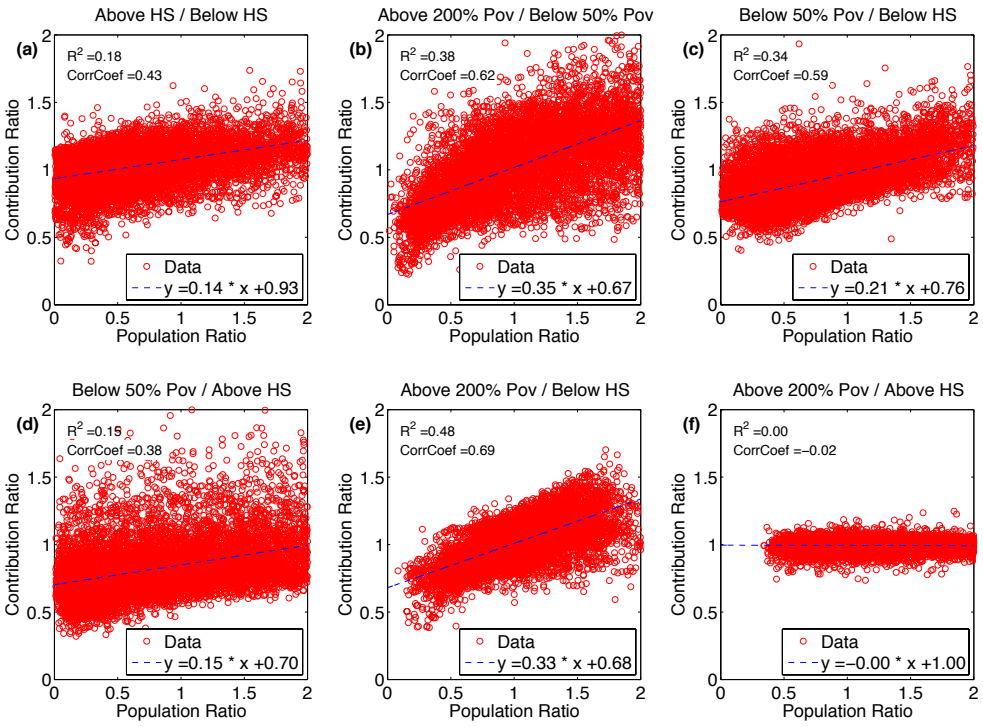

Figure 4.5: Comparisons of contribution ratios to population ratios for ratios of (a) individuals with above a high school education to individuals with below a high school education, (b) individuals above 200% of the poverty level to individuals below 50% of the poverty level, (c) individuals below 50% of the poverty level to individuals with below a high school education, (d) individuals below 50% of the poverty level to individuals with above a high school education, (e) individuals above 200% of the poverty level to individuals with below a high school education, and (f) individuals above 200% of the poverty level to individuals with above a high school education.

to the spatial analysis, we see very little variation in the contribution ratio across varying population ratios. In fact, 0% of the variation in the contribution ratios can be explained by the variation in the population ratios ($R^2 = 0.0$). This is possibly attributed to the different concentration response factor between the demographic groups or the strong correlation between the population distributions of the two demographic groups, however there are likely other factors which require further investigation to understand fully. Overall, the results in Figure 4.5 suggest that BC emissions do not preferentially effect certain demographic groups.

While the previous figures present an analysis of the contributions of total emissions, there is additional interest in identifying potential differences in how certain emission sectors affect different populations. Therefore, we performed an analysis of the impacts of sectoral emissions for each demographic group (Figure 4.6). The results are presented as a percentage of the total contributions in order to more easily determine the relative impacts of each sector. The variability between demographic groups is small for each sector (1-3% differences) for both national (Figure 4.6) and a regional (not shown) analyses of the sensitivities.

4.4.2 Sensitivity of Risk Modification Factor

For the risk modification factor simulations, adjoint sensitivities ($\frac{\partial R}{\partial E_{i,k,m}}$) provide an estimate of the impact of a unit emission in a single grid cell on the nationally summed risk modification factor or regionally summed risk modification factor attributed to exposure to BC. The regions of interest used for the regional simulations are shown in Figure 3.4. It is important to note that the risk modification factor sensitivities do not depend on population density. The results can be interpreted as the potential increased risk associated with adding a unit of emission in each grid cell for any single individual, regardless of the underlying population or mortality rate. Therefore, unlike the sensitivities of premature deaths shown earlier, the distribution of risk modification factor sensitivities is not biased towards urban areas. In contrast, these sensitivities show locations where BC emissions have the potential to most impact any individual's risk regardless of their location.

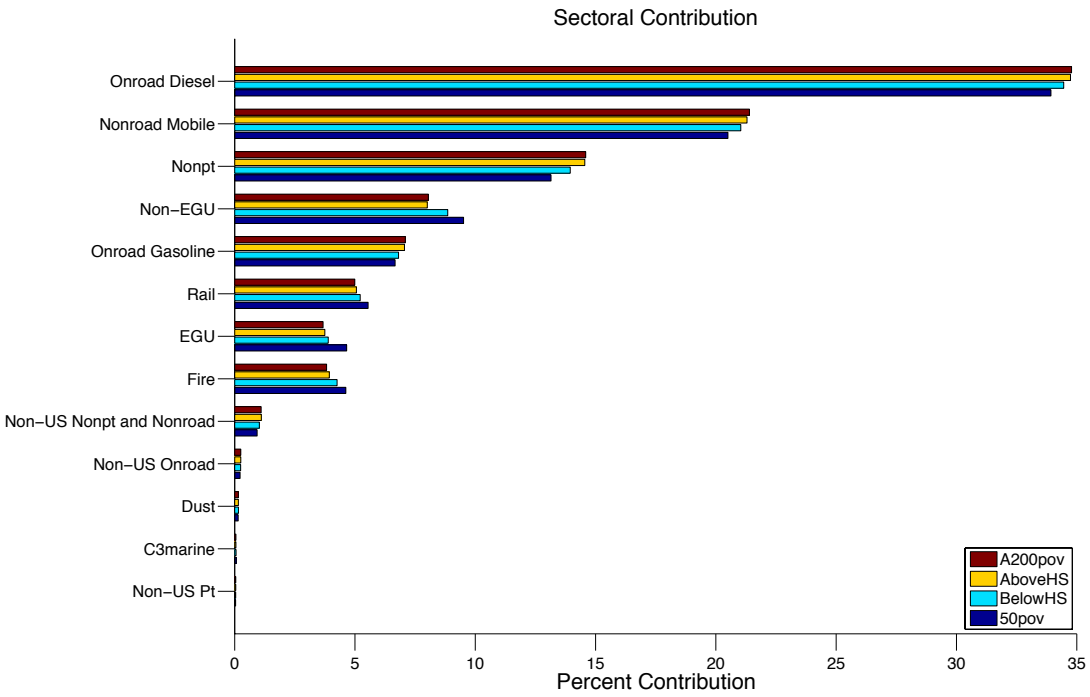

Figure 4.6: Analysis of contributions from sectoral emissions to premature deaths for each demographic group. 50pov corresponds to persons below 50% of the poverty level, A200pov refers to persons above 200% of the poverty level, AboveHS refers to persons with above a high school education, and BelowHS refers to persons with below a high school education.

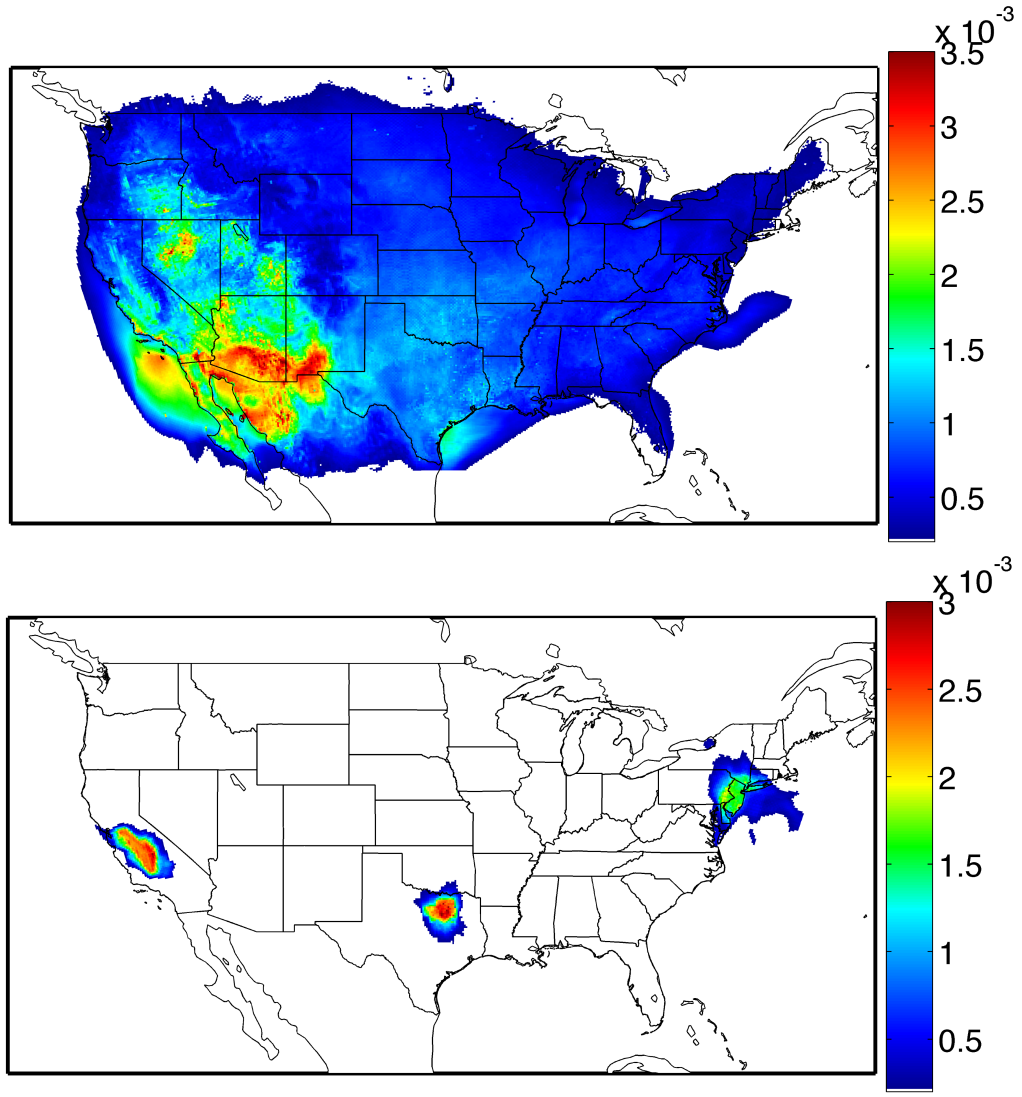

Figure 4.7: Sensitivity of risk modification factor with respect to emissions for national risk (top) and regional risk (bottom). Regional risk modification factor figure combines results from three regions (Dallas, San Joaquin Valley, and NY / PHI region) on the same figure. Results are presented as sensitivity normalized by the number of grid cells within the region of interest.

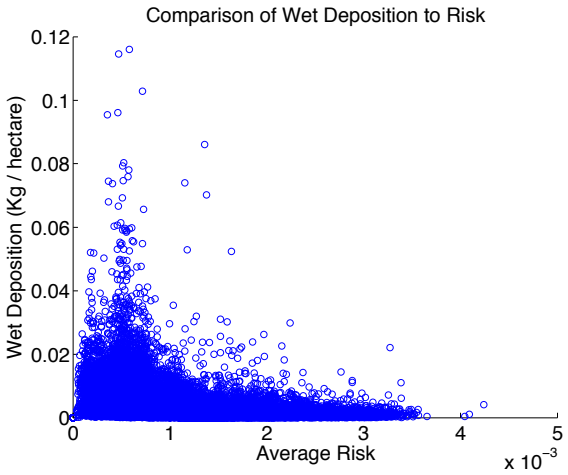

Figure 4.8: Comparison of national risk modification factor estimate (x-axis) to simulated 2007 wet deposition totals for BC (y-axis).

Figure 4.7 (top) shows the sensitivity of national risk modification factor with respect to emissions, normalized by the number of grid cells in the region of interest (to facilitate comparisons between national and regional results). Higher risk values are associated with emissions from drier climates. A majority of the moderate to high sensitivities (warm colors) occur in the southwestern portion of the US, with the highest values occurring in the Sonoran, Mojave, and Great Basin deserts. This is particularly important, as many individuals who are at a higher risk from exposure to air pollution (such as retirees) tend to live in these drier locations. The phenomenon of high risk modification factors being associated with drier climates is most likely attributed to the increased atmospheric lifetime of particles being emitted in drier climates, resulting from less wet removal of particles from the atmosphere. This is further supported by the comparison of risk modification factors to modeled wet deposition values (Figure 4.8). A majority of the large risk modification factor values occur in regions with the lowest 10-20% of wet deposition. Additionally, the grid cells with the most wet deposition have some of the lowest risk modification factor estimates. The smallest sensitivities occur over regions where BC would not be efficiently transported into the national domain, such as most of the oceans and northeastern US.

In addition to the sensitivity analysis of national risk modification factor estimates, simulations were also performed to estimate the sensitivity of risk modification factor within three unique regions (Figure 4.7, bottom). While adjoint simulations were performed separately for each region of interest, all of the results have been plotted on the same figure. In Figure 4.7 (bottom), the results in each region are normalized by the number of grid cells contained within the region of interest. As expected given the short atmospheric lifetime of BC, the largest sensitivities occur within the regions of interest.

For NY/PHI, the largest values occur along the Pennsylvania-Delaware border. Larger sensitivities are observed in Pennsylvania (along the border of the region of interest) than within New Jersey, which lies completely within the region of interest. This suggests that, in order to minimize the BC exposure risk modification factor within the region, new emission sources should be placed within New Jersey (as opposed to Pennsylvania), or existing sources should be preferentially controlled in Pennsylvania. Outside of the region of interest, non-zero sensitivities extend mostly to the southeast, with additional impacts occurring along the coast south of the region.

Of all of the regions analyzed, the largest sensitivity occurs within the Dallas region; however, there are a greater number of large sensitivities in the San Joaquin Valley than any other region. The maximum sensitivity being in Dallas is attributed to the drier climate in the Dallas region. Similar to NY/PHI, a majority of the large sensitivities occur within the region of interest. For the San Joaquin Valley, a majority of the largest sensitivities also occur within the region of interest. The largest values occur along the southeastern portion of the region, with the largest value occurring just east of Bakersfield. Sensitivities outside of the region of interest show that emissions in the San Francisco Bay area are the only emissions that have an impact on risk in the region.

4.4.3 AIR Sensitivity Analysis

While Figure 4.7 presents the absolute sensitivities of risk ($\frac{\partial R}{\partial E_{i,k,m}}$) and are independent of population and emission values, in this section we present semi-normalized sensitivities of AIR ($\frac{\partial AIR}{\partial E_{i,k,m}} \cdot E_{i,k,m}$), which have units of premature deaths per person. Figure 4.9 shows the contribution of emissions to average individual risk in each of the modeled regions.

The national analysis (Figure 4.9a) shows the contributions of emissions in each grid cell to the national average AIR. As might be expected for this type of analysis where the metric of interest is independent of total population, the largest sensitivities occur in the locations with the largest emissions. Additionally, the further away a grid cell is from the urban centers, the smaller the sensitivity (with many rural regions such as central Nevada and southern Utah having sensitivities of 0). The emission with the largest contribution is approximately 4.75 in one hundred million, and occurs in central Idaho where there were significant fires in 2007. Following central Idaho, the emissions with the next largest sensitivities are in Baltimore, MD, Lafayette and Baton Rouge, LA, and many of the major metropolitan areas across the country. Emissions in many of these metropolitan areas (such as Atlanta, Houston, Washington DC, and Minneapolis) have sensitivities of approximately 1 in one hundred million. For comparison the annual average AIR from BC in the continental US is 1.43 in 100,000 people. This is larger than the risk from some common activities, such as bicycling (1.32 in 100,000 [Consumer Product Safety Commission]), flying (4.52 in one hundred million [Sivak et al., 1991]), and skydiving (0.8 in 100,000 [Westman and Björnstig, 2005]).

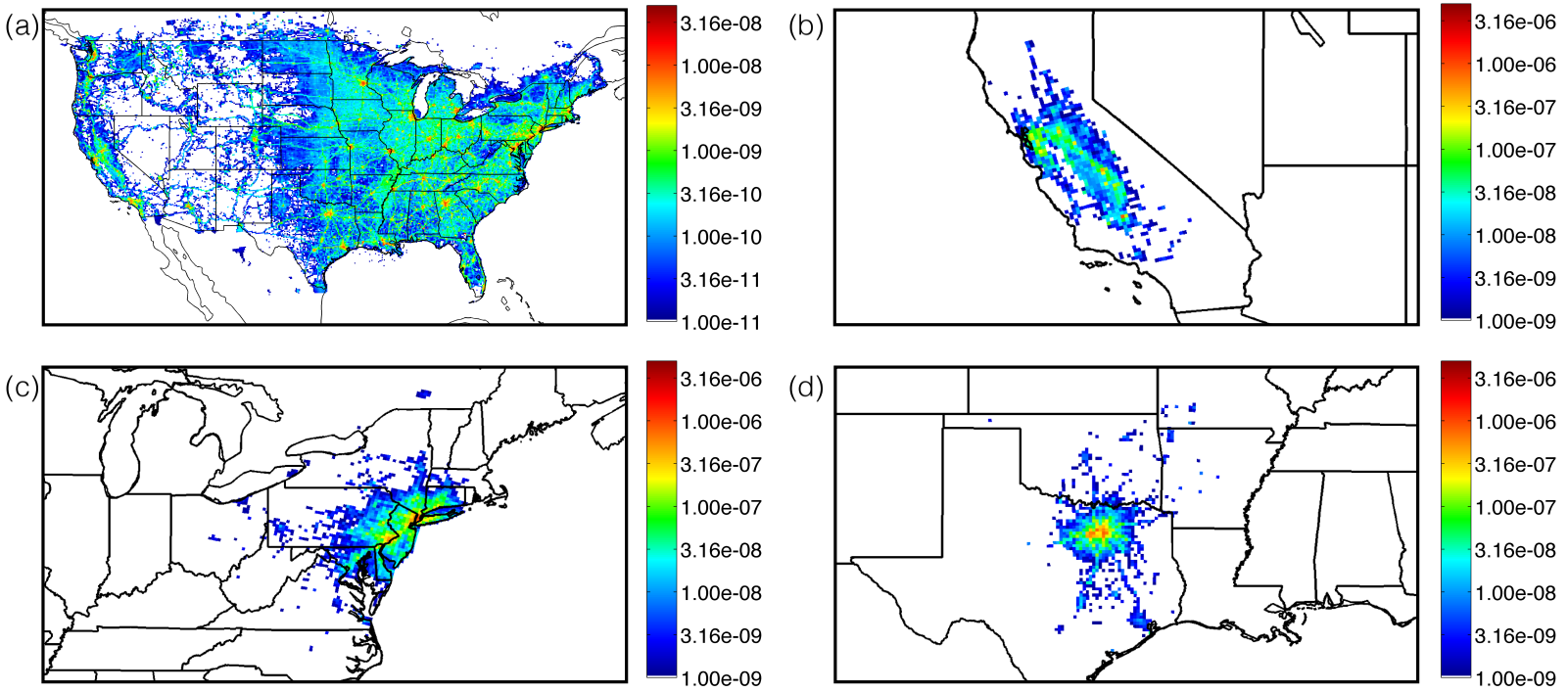

Figure 4.9: Semi-normalized sensitivity of average individual risk with respect to BC emissions in each grid cell for (a) national average individual risk, (b) average individual risk in the San Joaquin Valley, (c) average individual risk in NY/PHI, and (d) average individual risk in Dallas. Plots have units of premature death rate.

An analysis of the AIR sensitivities for the San Joaquin Valley (Figure 4.9b) shows that the sum of contributions of emissions to average AIR in the San Joaquin Valley is 1.35 in 100,000. As in the national analysis, the summed contributions to average AIR in the San Joaquin Valley results in a risk that is larger than the risk from flying, bicycling, and skydiving. Many of the emissions with the largest sensitivities occur along CA-99, with a maximum of 8.7 in 10 million occurring in Bakersfield, CA. Further analysis shows that emissions from within the region pose a AIR sensitivity of 8.56 in a million, and emissions from outside of the region pose a AIR of 5.02 in a million. A majority of the large sensitivities from outside of the region occur within the San Francisco Bay area, which closely borders the region of interest. While previous studies have shown that a large percentage of premature deaths in the region are attributed to emissions from within the region (73% in Turner et al. [2015b]), our analysis shows that the risk of an individual in the region from emissions outside of the region is half of the risk from emissions within the region. This is a result of the AIR analysis being independent of population, and only depending on whether or not emissions in a given location contribute to BC anywhere within the region (not just the populated areas).

Figure 4.9c shows the sensitivities of average AIR for an individual in NY/PHI. Our analysis shows that the annual average AIR in the region is 3.55 in 100,000. The annual AIR for the NY/PHI region is larger than the annual average AIR for the national analysis, due to the averaging in the AIR analysis; the national analysis includes many grid cells within the region that have little or no contributions. On the other hand, the NY/PHI region contains many urban centers, and the resulting average AIR is not diluted by low-emission areas. The maximum sensitivity occurs within the grid cell that encompasses New York City, and has a value of 9.47 in 10 million. Additionally, the AIR in the region from emissions outside of the region is 7.51 in a million while the AIR from emissions inside the region is 2.80 in 100,000. As with the other regions, the largest sensitivities occur within the urban centers. Sensitivities decrease as the distance from the urban centers increases, however

larger sensitivities are observed along the heavily trafficked roadways. Outside of the region, the largest sensitivity occurs within the grid cell that encompasses Baltimore, MD.

Finally, Figure 4.9d shows the AIR sensitivities for the Dallas region, with an annual average AIR in the region of 2.15 in 100,000. The maximum sensitivity values coincide with the largest emission sources within the region, and have values of 6 to 8.1 in 10 million. Analysis of the sensitivities inside and outside of the region shows that emissions from within the region yield an AIR sensitivity of 1.78 in 100,000, while emissions from outside of the region yield an AIR sensitivity of 3.64 in a million.

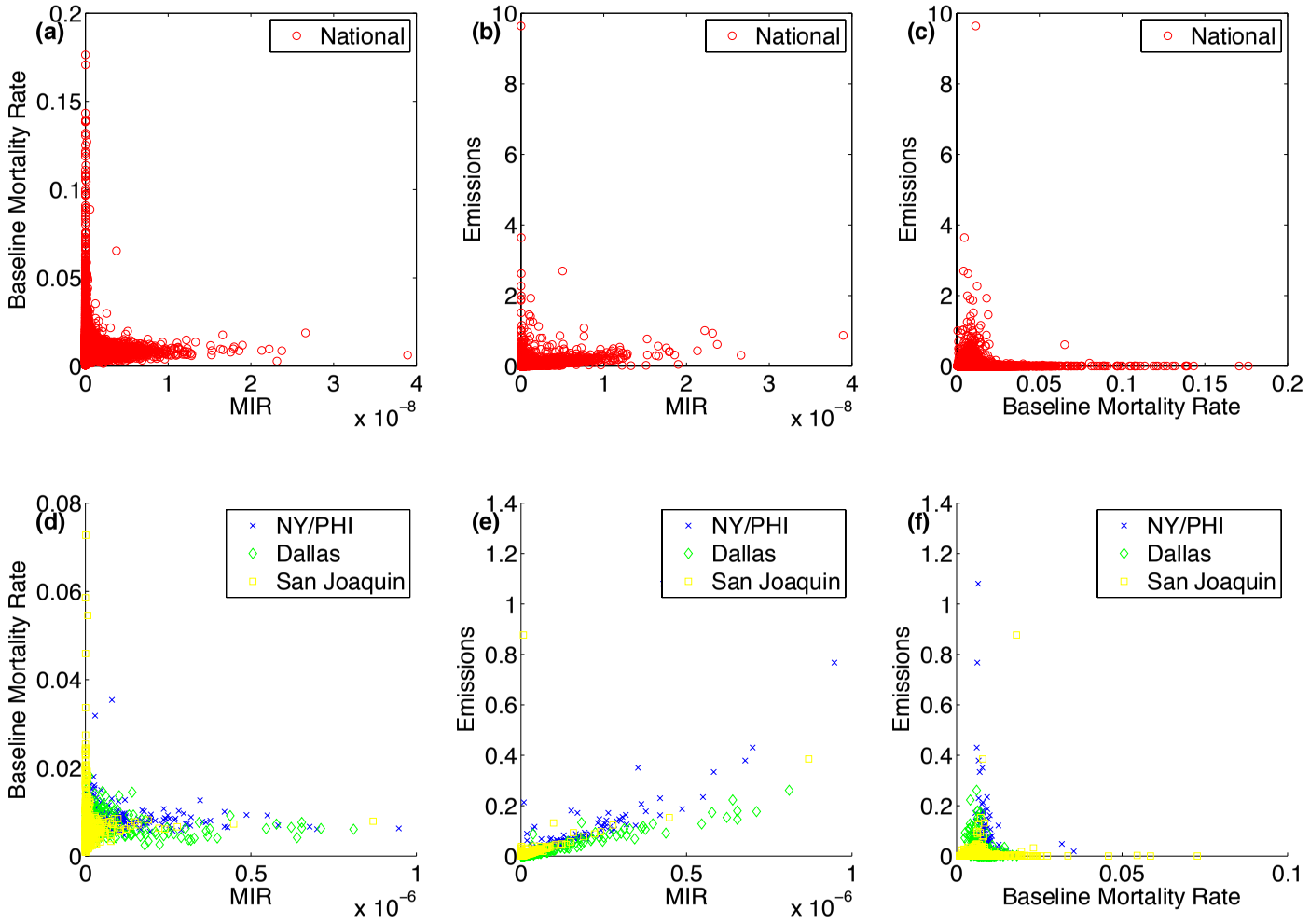

Figure 4.10: Comparisons of AIR sensitivities to baseline mortality rate and emissions for both the national analysis and regional analyses. (a) National baseline mortality rate versus AIR sensitivity, (b) national emissions versus AIR sensitivity, (c) national emissions versus baseline mortality rate, (d) regional baseline mortality rate versus AIR sensitivity, (e) regional emissions versus AIR sensitivity, and (f) regional emissions versus baseline mortality rate.

Since each of the regions show the largest sensitivities in areas that are likely to be the largest emission sources, we compare AIR sensitivities to baseline mortality rates and emissions (Figure 4.10) in order to determine which variables have the strongest correlation to AIR sensitivities. Figures 4.10a-c show the comparisons for the national analysis, while Figures 4.10d-f show the comparisons for the regional analyses. Figures 4.10a and 4.10d are both bimodal for the comparison of baseline mortality rates to AIR sensitivities. This is due to AIR contributions being semi-normalized by the emissions, meaning that large AIR contributions typically correspond to large emissions. On the other hand, baseline mortality rates are independent of emissions; many large baseline mortality rates occur in areas with very low emissions. However, Figure 4.10b shows a similar bimodal distribution of the comparison of AIR contributions to emissions for the national analysis. This is a result of the national analysis including locations where significant emissions occur in areas of low mortality rates (Figure 4.10c). The comparison of baseline mortality rates to AIR contributions for the regional analysis (Figure 4.10d) shows a coefficient of determination (R^2) of 0.0034 for NY/PHI, 0.079 for Dallas, and 0.0052 for the San Joaquin Valley. The greatest correlation is obtained by regressing emissions on AIR contributions (Figure 4.10e) for all regions (NY/PHI: $R^2 = 0.65$, Dallas: $R^2 = 0.93$, San Joaquin Valley: $R^2 = 0.23$). Similar to the national analysis, Figure 4.10f shows a bimodal distribution of the comparison of emissions to baseline mortality rates. However, the regional analyses contain much fewer locations of large baseline mortality rates where there are insignificant emissions. Additionally, the maximum emission for all of the regional analyses is approximately ten times smaller than the maximum emission in the national analysis.

While we have thus far considered the risk associated with total BC emissions, further information about the type of emissions may also be of use for policy development. As such, we have performed a sectoral analysis of the AIR sensitivities for each region (Figure 4.11). Similarly to the results in Turner et al. [2015b] for premature deaths attributed to exposure to BC in the US, the onroad diesel and nonroad mobile sources contribute the most

to AIR, due to the large emissions of BC from these sources. While fires are a significant source of BC emissions, the contribution of fire emissions to AIR in each urban region is small when compared to other sources. However, the contribution of fire emissions to AIR on a national level is much larger (the fourth largest contributor). In the national analysis, there are significant fire emissions within the region, yet these fires occur far from the urban regions that were analyzed and therefore have small contributions to AIR in these particular urban regions in 2007. Even though there are signifiant more fire emissions than non-point emissions (nearly twice as much in 2007), there are larger contributions from non-point emissions due to the fact that most of the fire emissions occur in a small number of grid cells that are near areas with low baseline mortality rates, while non-point emissions tend to occur near the larger baseline mortality rates. Additionally, over half of the contributions in the Dallas region come from onroad diesel emissions; onroad diesel and nonroad mobile emissions combine to account for over 80% of the contributions to AIR in the Dallas region. In contrast, sources such as EGU, non-EGU, and onroad gasoline are much more prominent in NY/PHI; EGU sources in the NY/PHI region have a contribution percentage two to three times larger than in any other region. This is attributed to the large amount of EGU emissions in the NY/PHI region, compared to other regions.

Lastly, a comparison of the sector specific AIR contributions to premature death contributions for both national [Turner et al., 2015b] and regional [Turner et al., 2015a] analyses allows us to quantify the influence of population on health-based analyses. In the national analysis of Turner et al. [2015b] the percent contributions to premature deaths for both onroad diesel and nonroad mobile emissions were approximately 6% larger than the AIR contribution estimates (Figure 4.11). Additionally, while Turner et al. [2015b] estimated approximately 3% of contributions to premature deaths come from fire emissions, the AIR contribution analysis estimates that fire emissions account for approximately 12% of the total contributions. The larger percentage of contributions from fire emissions in the AIR analysis is caused by the fact that the premature death contribution estimates were marginalized for

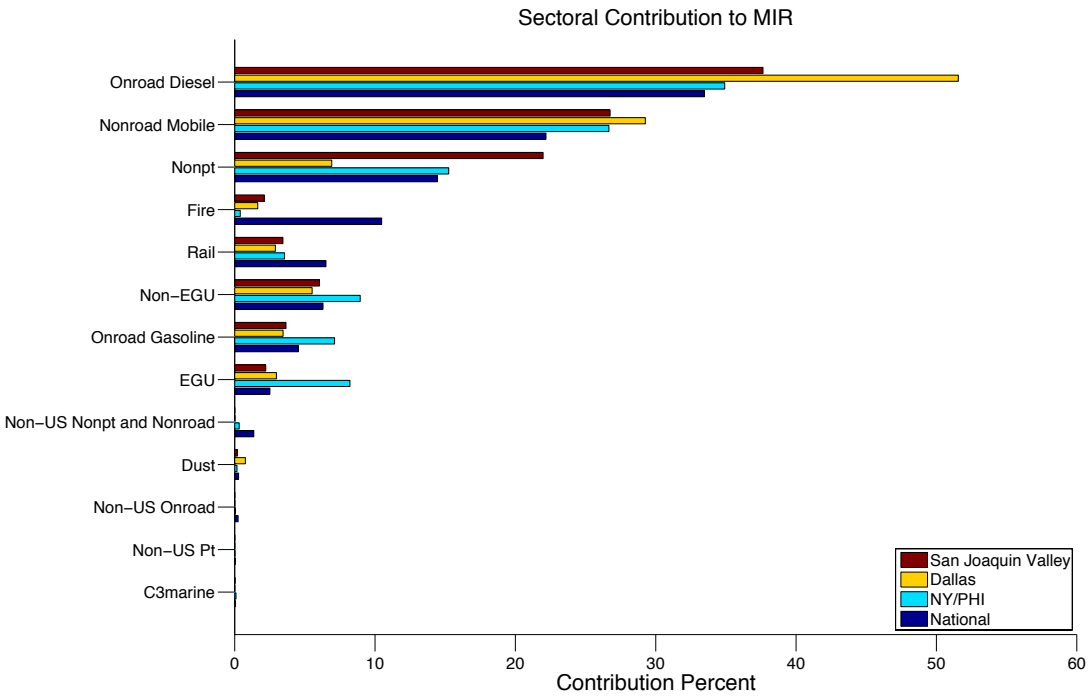

Figure 4.11: Analysis of the sectoral contributions of emissions to AIR in each region.

less-populated rural areas, where a majority of fire emissions occur. Comparing the regional sector-specific AIR contributions to the regional premature death contribution analysis in Turner et al. [2015a] shows that the contribution percentage of both onroad diesel and nonroad mobile are nearly identical for each region. However, nonpoint emissions account for approximately 22% of the AIR contributions in the San Joaquin Valley, yet only account for approximately 5% of the premature death contributions. Additionally, non-EGU and EGU sectors both have AIR contributions approximately two to three times larger than the corresponding premature death contribution percent for each region (EGU AIR contributions for NY/PHI are approximately 10%, yet EGU premature death contributions for NY/PHI account for approximately 5%).

4.5 Conclusions

In this paper we analyze the effects of BC emissions in the US on three different risk-based metrics: premature deaths attributed to BC exposure, average individual risk attributed to pollutant exposure, and a metric independent of population and baseline mortality rates (referred to as risk modification factor). The premature death analysis focuses on specific demographic groups (persons above 200% of the poverty level, persons below 50% of the poverty level, persons with below a high school education, and persons with above a high school education) in order to analyze potential disparities of health impacts of emissions from different sectors and locations on certain demographic groups. We find strong correlations between contribution percentage and population percentage for each demographic group, with correlation coefficients ranging between 0.77 for persons with above a high school education to 0.85 for persons below 50% of the poverty level. However, there were less direct relationships between contributions and population subgroups in areas such as southern Maine, the Florida coasts, and parts of the San Joaquin Valley. Thus, emissions in the southern US contribute to a larger fraction of premature deaths in the groups that include persons below 50% of the poverty level and persons with below a high school education since they have a higher percentage of population in the south.

Comparisons of contribution ratios to population ratios between each demographic group show that there is much less variability in the types of people harmed by BC emissions than there is in the variability of population demographics themselves. A comparison of people with above a high school education to people with below a high school education shows that only 18% of the variability in contribution ratios can be explained by the variability in population ratios. Therefore, a majority of the variability in the contribution ratio is driven by other factors, such as baseline mortality rates and the distribution of populations in areas downwind of emissions. Additionally, a comparison of the contribution ratios to population ratios for people above 200% of the poverty level to people with above a high

school education shows that none of the variability in the contribution ratio is explained by the variability in the population ratio ($R^2 = 0$). Lastly, in terms of national totals, we found vehicle emissions to contribute to more premature deaths (1-3%) for the above high school education and above 200% poverty level groups. On the other hand, non-EGU, EGU, and fire emissions contribute to more premature deaths (1-3%) in the below high school education and below 50% poverty level groups.

Analysis of the effects of BC emissions on national risk modification factor in the US shows that the largest risk modification factors result from emissions in drier climates, such as the Sonoran, Mojave, and Great Basin deserts. This phenomenon of higher risk modification factors occurring in drier climates is likely attributed to the increased atmospheric lifetime of particles being emitted in these climates, resulting from less wet removal of aerosols. Lastly, analysis of the impacts of BC emissions on average individual risk shows that, while the average individual risk analysis is independent of population, the largest sensitivities occur within the urban centers. This is attributed to the significantly larger emissions within the urban centers than in the surrounding areas. We also find average individual risks resulting from emissions in single grid cells to be upwards of 9.47 in ten million in 2007 for the NY/PHI region, which is larger than the risk from flying (4.52 in on hundred million). Finally, we found that non-local emissions have a greater effect on AIR than premature deaths in certain regions. While Turner et al. [2015a] estimated that 73% of premature death contributions are from emissions within the San Joaquin Valley region, our AIR analysis estimates that 62% of the AIR is attributed to emissions within the region. However, both the AIR contribution analysis and the premature death contribution analysis yield similar percentages for the NY/PHI region (78% of premature death contributions come from emissions in the region, 79% of AIR contributions come from emissions in the region) and Dallas regions (84% of premature death contributions come from emissions in the region, 84% of AIR contributions come from emissions in the region). This is a result of the Dallas and NY/PHI regions encompassing urban centers, while the San Joaquin Valley region borders the San Francisco

Bay area. The large emissions from the San Francisco Bay area do not result in a large percentage of premature death contributions because much of the population in the San Joaquin Valley region are further south in the region, and are not exposed to the emissions from the San Francisco Bay area while in the AIR contribution analysis, contributions are independent of the population.

4.6 Supplemental Information

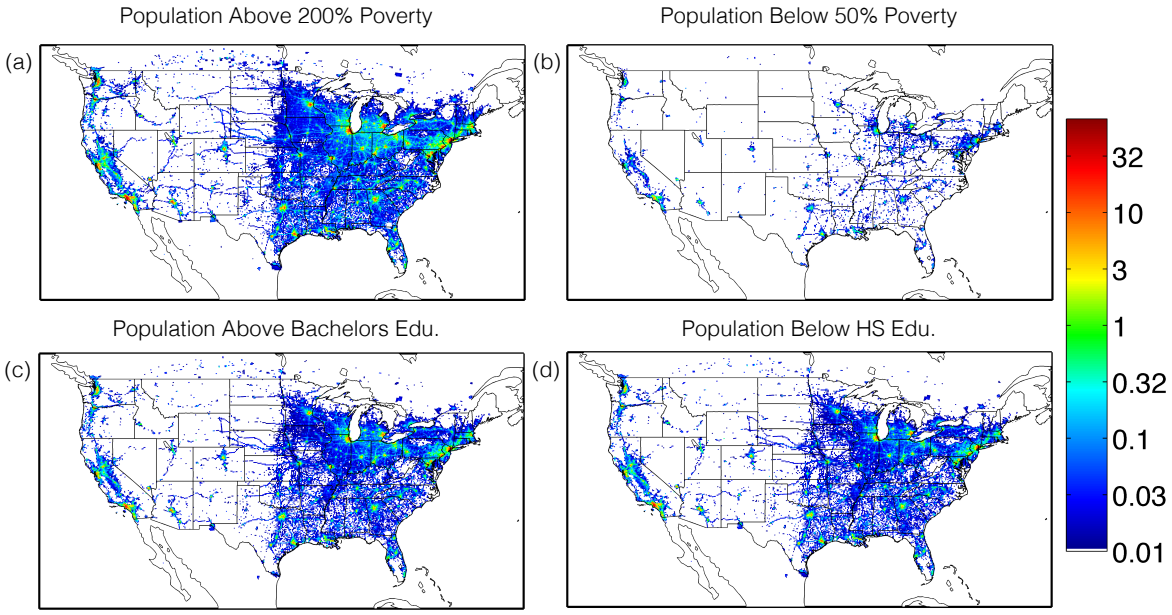

Figure 4.12: Contributions of emissions to premature death for (a) persons above 200% poverty level, (b) persons below 50% poverty level, (c) persons with above a high school education, and (d) persons with below a high school education.

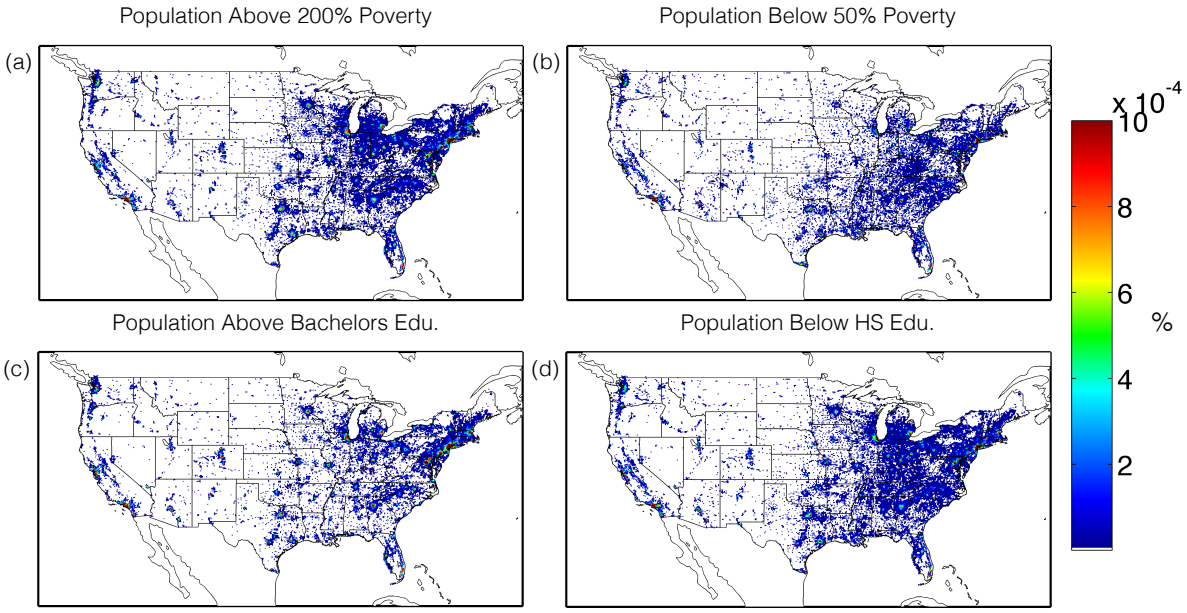

Figure 4.13: Population distributions for (a) persons above 200% poverty level, (b) persons below 50% poverty level, (c) persons with above a high school education, and (d) persons with below a high school education.

4.7 References

SD Adar, DR Gold, BA Coull, J Schwartz, PH Stone, and H Suh. Focused exposures to airborne traffic particles and heart rate variability in the elderly. Epidemiology, 18(1): 95–103, January 2007.

AS Ahmad, N Ormiston-Smith, and PD Sasieni. Trends in the lifetime risk of developing cancer in Great Britain: comparison of risk for those born from 1930 to 1960. British Journal of Cancer, 112(5):943–947, 2015.

SC Anenberg, K Talgo, S Arunachalam, P Dolwick, C Jang, and JJ West. Impacts of global, regional, and sectoral black carbon emission reductions on surface air quality and human mortality. Atmos. Chem. Phys., 11(14):7253–7267, 2011.

SC Anenberg, J Schwartz, D Shindell, M Amann, G Faluvegi, Z Klimont, G Janssens-Maenhout, L Pozzoli, R Van Dingenen, E Vignati, L Emberson, NZ Muller, JJ West, M Williams, V Demkine, WK Hicks, J Kuylenstierna, F Raes, and V Ramanathan. Global air quality and health co-benefits of mitigating near-term climate change through methane and black carbon emission controls. Environ. Health Perspect., 120(6):831–839, June 2012.

R Beelen, G Hoek, PA van den Brandt, RA Goldbohm, P Fischer, LJ Schouten, M Jerrett, E Hughes, B Armstrong, and B Brunekreef. Long-term effects of traffic-related air pollution on mortality in a Dutch cohort (NLCS-AIR study). Environ. Health Perspect., 116 (2):196–202, November 2007.

D Byun and KL Schere. Review of the governing equations, computational algorithms, and other components of the Models-3 Community Multiscale Air Quality (CMAQ) modeling system. Appl. Mech. Rev., 59(1/6):51, 2006.

AJ Cohen, HR Anderson, B Ostro, KD Pandey, M Krzyzanowski, N Kuenzli, K Gutschmidt, CA Pope, I Romieu, JM Samet, and KR Smith. Mortality impacts of urban air pollution. In Majid Ezzati, AD Lopez, A Rodgers, and C Murray, editors, Comparative Quantification of Health Risks: Global and Regional Burden of Disease Due to Selected Major Risk Factors, Vol. 2. World Health Organization, Geneva, 2004.

Consumer Product Safety Commission. An overview of the bicycle study. URL `http://www.cpsc.gov//PageFiles/112701/344.pdf`.

N Fann, CM Fulcher, and BJ Hubbell. The influence of location, source, and emission type in estimates of the human health benefits of reducing a ton of air pollution. Air Qual., Atmos. Health, 2(3):169–176, 2009. doi: 10.1007/s11869-009-0044-0.

N Fann, HA Roman, CM Fulcher, MA Gentile, BJ Hubbell, K Wesson, and JI Levy. Maximizing health benefits and minimizing inequality: Incorporating local-scale data in the design and evaluation of air quality policies. Risk Analysis, 31(6):908–922, June 2011.

N Fann, KR Baker, and CM Fulcher. Characterizing the PM2.5-related health benefits of emission reductions for 17 industrial, area and mobile emission sectors across the U.S. Environ. Int., 49(C):141–151, November 2012a.

N Fann, AD Lamson, SC Anenberg, K Wesson, D Risley, and BJ Hubbell. Estimating the national public health burden associated with exposure to ambient PM2.5 and ozone. Risk Analysis, 32(1):81–95, January 2012b.

EJ Feuer, LM Wun, CC Boring, WD Flanders, MJ Timmel, and T Tong. The lifetime risk of developing breast-cancer. Journal of the National Cancer Institute, 85(11):892–897, 1993.

MM Finkelstein, M Jerrett, P DeLuca, N Finkelstein, DK Verma, K Chapman, and MR Sears. Relation between income, air pollution and mortality: a cohort study. Can. Med. Assoc. J., 169(5):397–402, 2003.

EM Flachs, J Sørensen, J Bønløkke, and H Brønnum-Hansen. Population dynamics and air pollution: the impact of demographics on health impact assessment of air pollution. J. Environ. Public Health., 2013(6):1–12, 2013.

WJ Gauderman, F Gilliland, H Vora, E Avol, and D Stram. Association between air pollution and lung function growth in southern California children: Results from a second cohort. Am. J. Respir. Crit. Care Med., 166:76–84, June 2002.

TJ Grahame, R Klemm, and RB Schlesinger. Public health and components of particulate matter: The changing assessment of black carbon. J. Air Waste Manage., 64(6):620–660, May 2014.

N Howlader, AM Noone, M Krapcho, J Garshell, D Miller, SF Altekruse, CL Kosary, M Yu, J Ruhl, Z Tatalovich, A Mariotto, DR Lewis, HS Chen, EJ Feuer, and KA Cronin, editors. SEER Cancer Statistics Review, 1975-2011. National Cancer Institute, Bethesda, MD, April 2014. URL `http://seer.cancer.gov/csr/1975_2011/`.

B Hubbell. Understanding urban exposure environments: new research directions for informing implementation of us air quality standards. Air Qual., Atmos. Health, 5(2):259–267, June 2012.

S Humbert, JD Marshall, S Shaked, JV Spadaro, Y Nishioka, P Preiss, TE McKone, A Horvath, and O Jolliet. Intake fraction for particulate matter: Recommendations for life cycle impact assessment. Environ. Sci. Technol., 45(11):4808–4816, 2011.

NAH Janssen, G Hoek, M Simic-Lawson, P Fischer, L van Bree, H ten Brink, M Keuken, RW Atkinson, HR Anderson, B Brunekreef, and FR Cassee. Black carbon as an additional indicator of the adverse health effects of airborne particles compared with PM10 and PM2. 5. Environ. Health Perspect., 119(12):1691–1699, August 2011.

DO Johns, LW Stanek, K Walker, S Benromdhane, B Hubbell, M Ross, RB Devlin, DL Costa, and DS Greenbaum. Practical advancement of multipollutant scientific and aisk assessment approaches for ambient air pollution. Environ. Health Perspect., 120(9): 1238–1242, September 2012.

K Katanoda, T Sobue, H Satoh, K Tajima, T Suzuki, H Nakatsuka, T Takezaki, T Nakayama, H Nitta, K Tanabe, and S Tominaga. An association between long-term exposure to ambient air pollution and mortality from lung cancer and respiratory diseases in japan. J. Epidemiol., 21(2):132–143, 2011.

I Kazuhiko, R Mathes, Z Ross, A Nádas, G Thurston, and T Matte. Fine particulate matter constituents associated with cardiovascular hospitalizations and mortality in New York City. Environ. Health Perspect., 119(4):467, April 2011.

D Krewski, M Jerrett, RT Burnett, R Ma, E Hughes, Y Shi, MC Turner, CA Pope, G Thurston, EE Calle, MJ Thun, B Beckerman, P DeLuca, N Finkelstein, K Ito, DK Moore, KB Newbold, T Ramsay, Z Ross, H Shin, and B Tempalski. Extended follow-up and spatial analysis of the American Cancer Society study linking particulate air pollution and mortality. Technical Report HEI Research Report 140, Health Effects Institute, Boston, Mass., USA, 2009. URL `http://ephtracking.cdc.gov/docs/RR140-Krewski.pdf`.

F Laden, J Schwartz, F E Speizer, and D W Dockery. Reduction in fine particulate air pollution and mortality - Extended follow-up of the Harvard six cities study. American Journal Of Respiratory And Critical Care Medicine, 173(6):667–672, 2006.

J Lepeule, F Laden, D Dockery, and J Schwartz. Chronic exposure to fine particles and mortality: an extended follow-up of the Harvard Six Cities study from 1974 to 2009. Environ. Health Perspect., 120(7):965–970, July 2012.

JI Levy, SK Wolff, and JS Evans. A regression-based approach for estimating primary and secondary particulate matter intake fractions. Risk Analysis, 22(5):895–904, October 2002.

GA Mensah, AH Mokdad, ES Ford, KJ Greenlund, and JB Croft. State of disparities in cardiovascular health in the United States. Circulation, 111(10):1233–1241, 2005.

NZ Muller, R Mendelsohn, and W Nordhaus. Environmental accounting for pollution in the United States economy. Am. Econ. Rev., 101(5):1649–1675, August 2011.

MJ Neidell. Air pollution, health, and socio-economic status: the effect of outdoor air quality on childhood asthma. J. Health Econ., 23(6):1209–1236, 2004.

RD Peng, ML Bell, AS Geyh, A McDermott, SL Zeger, JM Samet, and F Dominici. Emergency admissions for cardiovascular and respiratory diseases and the chemical composition of fine particle air pollution. Environ. Health Perspect., 117(6):957–963, February 2009.

CA Pope, RT Burnett, MJ Thun, EE Calle, D Krewski, K Ito, and GD Thurston. Lung cancer, cardiopulmonary mortality, and long-term exposure to fine particulate air pollution. J. Am. Med. Assoc., 287(9):1132–1141, 2002.

MC Power, MG Weisskopf, and SE Alexeeff. Traffic-related air pollution and cognitive function in a cohort of older men. Environ. Health Perspect., 119(5):682–687, 2011.

RC Puett, JE Hart, JD Yanosky, C Paciorek, J Schwartz, H Suh, FE Speizer, and F Laden. Chronic fine and coarse particulate exposure, mortality, and coronary heart disease in the Nurses' Health Study. Environ. Health Perspect., 117(11):1697–1701, June 2009.

L Qiao, J Cai, H Wang, W Wang, M Zhou, S Lou, R Chen, H Dai, C Chen, and H Kan. PM2.5 constituents and hospital emergency-room visits in Shanghai, China. Environ. Sci. Technol., 48(17):10406–10414, 2014.

L. Seirup and G. Yetman. U.S. Census Grids (Summary File 3), 2000, May 2015. URL http://dx.doi.org/10.7927/H42R3PMN.

M Sivak, DJ Weintraub, and M Flannagan. Nonstop flying is safer than driving. Risk Analysis, 11(1):145–148, March 1991.

JG Su, R Morello-Frosch, BM Jesdale, AD Kyle, B Shamasunder, and M Jerrett. An index for assessing demographic inequalities in cumulative environmental hazards with application to Los Angeles, California. Environ. Sci. Technol., 43(20):7626–7634, 2009.

HH Suh and A Zanobetti. Exposure error masks the relationship between traffic-related air pollution and heart rate variability. J. Occup. Environ. Med., 52(7):685–692, July 2010.

T Tietenberg. Tradeable permits for pollution control when emission location matters: What have we learned? Environmental and Resource Economics, 1995.

MD Turner, DK Henze, A Hakami, S Zhao, J Resler, GR Carmichael, CO Stanier, J Baek, A Sandu, AG Russell, A Nenes, G Jeong, SL Capps, PB Percell, RW Pinder, SL Napelenok, JO Bash, and T Chai. Sector-specific health impacts of BC emissions in six urban US regions. In Prep, 2015a.

MD Turner, DK Henze, A Hakami, S Zhao, J Resler, GR Carmichael, CO Stanier, J Baek, A Sandu, AG Russell, A Nenes, GR Jeong, SL Capps, PB Percell, RW Pinder, SL Napelenok, JO Bash, and T Chai. Differences between magnitudes and health impacts of BC emissions across the United States using 12 km scale seasonal source apportionment. Environ. Sci. Technol., 49(7):4362–4371, 2015b. doi: 10.1021/es505968b.

K Wesson, N Fann, M Morris, T Fox, and B Hubbell. A multi-pollutant, risk-based approach to air quality management: Case study for detroit. Atmospheric Pollution Research, 1(4): 296–304, October 2010.

A Westman and U Björnstig. Fatalities in swedish skydiving. Accident Analysis & Prevention, 37(6):1040–1048, November 2005.

WHO. Health risks of particulate matter from long-range transboundary air pollution. Technical report, World Health Organization Regional Office of Europe, Copenhagen, 2006. URL http://www.euro.who.int/__data/assets/pdf_file/0006/78657/E88189.pdf.

WHO. Health effects of black carbon. Technical report, World Health Organization, European Centre for Environment and Health, Bonn Office, April 2012. URL http://www.euro.who.int/__data/assets/pdf_file/0004/162535/e96541.pdf.

M Wilhelm, L Qian, and B Ritz. Outdoor air pollution, family and neighborhood environment, and asthma in LA FANS children. Health Place, 15(1):25–36, March 2009.

EH Wilker, MA Mittleman, BA Coull, A Gryparis, ML Bots, J Schwartz, and D Sparrow. Long-term exposure to black carbon and carotid intima-media thickness: the Normative Aging Study. Environ. Health Perspect., 121(9):1061–1067, September 2013.

Jianhua Xu, Xuesong Wang, and Shiqiu Zhang. Risk-based air pollutants management at regional levels. Environmental Science & Policy, 25:167–175, January 2013.

Y Zhou, JS Fu, G Zhuang, and JI Levy. Risk-based prioritization among air pollution control strategies in the Yangtze River delta, China. Environ. Health Perspect., 118(9):1204–1210, September 2010.

Chapter 5

Conclusions

The adjoint of the Community Multiscale Air Quality (CMAQ) model was developed to facilitate projects that elucidate the sources of aerosols that contribute the most to adverse human health impacts and, eventually, to perform inverse modeling to reduce uncertainty in such sources. After successful development and validation of the adjoint (see section 2.7.1), the model was used in multiple research studies analyzing the impacts of: (1) seasonal and sectoral emissions on premature death associated with exposure to BC in the US, (2) BC emissions on health in multiple urban US regions, (3) disparities in health impacts for different population demographics, and (4) BC emissions on maximum individual risk in the US. This dissertation presents the results of each of these research projects.

In Chapter 2 we used the CMAQ adjoint model to quantify source-receptor relationships of emissions to premature deaths associated with national exposure to BC at highly-resolved sectoral, spatial, and temporal scales. We found that highly populated urban areas account for a larger percentage of national premature deaths than national emissions. Additionally, while damages resulting from anthropogenic emissions of BC are strongly correlated with population and premature death, there is inconsistant correlation between damages and emission magnitude. This suggests that controls on the largest emissions may not be the most efficient means of reducing damages resulting from anthropogenic BC emissions. Rather, the best proxy for locations with damaging BC emissions is locations where premature deaths occur. We next performed a state-level analysis of contributions to national health impacts.

However, the overall differences in emission, damage, and premature death percentage are small at these scales, suggesting that optimal control strategies for BC need to be developed at a state and sector level, given the relatively short lifetime of this pollutant.

In the study presented in Chapter 3, we estimated the extent to which emissions from individual locations and sources throughout the US result in adverse health effects in six urban areas. Onroad gasoline accounts for half as many premature deaths than nonroad mobile and onroad diesel emissions, yet it has the greatest efficiencies. Fugitive dust results in negligible premature deaths, but has large efficiency due to the proximity of the largest dust emissions to the most populous grid cells. Additionally, non-EGU emissions in the NY/PHI and Phoenix regions have efficiencies close to that of onroad gasoline emissions, yet result in a fraction of the premature deaths of onroad gasoline emissions (approximately 10% for Phoenix, approximately 50% for NY/PHI). Contributions from emissions outside of the region account for between 7% and 27% of the premature deaths within each of the six regions. Interestingly, the largest efficiencies in the San Joaquin Valley occur along CA-99, which is the location along which the new California rail system is to be built. This suggests that, in the short term, there will be significantly more premature deaths from nonroad mobile BC emissions in the region while the rail system is being constructed. However, in the long term, the reduction in onroad mobile contributions along CA-99 will likely be greater than the increase in rail contributions from the new rail system. Lastly, recent studies have shown that onroad mobile source emissions of BC have decreased by approximately 66% in the past 30 years and off road mobile engines are estimated to account for 37% of mobile emissions of BC in 2010 [McDonald et al., 2015]. Meanwhile, a majority of the vehicle emission controls that regulate PM emissions focus on diesel emissions [US EPA, 2012, 2001]. However, the greatest benefit per unit emission for reductions of BC emissions occurs for onroad gasoline sources, suggesting that BC emissions from gasoline sources would be the ideal target for stricter controls.

In Chapter 4 we analyzed the effects of BC emissions in the US on three different

risk-based metrics: premature deaths attributed to BC exposure, maximum individual risk attributed to pollutant exposure, and a metric independent of population and mortality rates (referred to as risk). The premature death analysis focuses on specific demographic groups (persons above 200% of the poverty level, persons below 50% of the poverty level, persons with below a high school education, and persons with above a high school education) in order to analyze potential disparities of health impacts of emissions from different sectors and locations on certain demographic groups. We find strong correlations between contribution percentage and population percentage for each demographic group, with correlation coefficients ranging between 0.77 for persons with above a high school education to 0.85 for persons below 50% of the poverty level. However, there were less direct relationships between contributions and population subgroups in areas such as southern Maine, the Florida coasts, and parts of the San Joaquin Valley. Thus, emissions in the southern US contribute to a larger fraction of premature deaths in the groups that include persons below 50% of the poverty level and persons with below a high school education since they mostly live in the south. Comparisons of contribution ratios to population ratios between each demographic group show that there is much less variability in the types of people harmed by BC emissions than there is in the variability of population demographics themselves. Analysis of the effects of BC emissions on national total risk in the US shows that the largest risks result from emissions in drier climates, such as the Sonoran, Mojave, and Great Basin deserts. This phenomenon of higher risks occurring in drier climates is likely attributed to the increased atmospheric lifetime of particles being emitted in these climates, resulting from less wet removal of aerosols. Lastly, analysis of the impacts of BC emissions on maximum individual risk shows that, while the maximum individual risk analysis is independent of population, the largest sensitivities occur within the urban centers. This is attributed to the significantly larger emissions within the urban centers than in the surrounding areas. We also find maximum individual risks resulting from emissions in single grid cells to be upwards of 9.5 in ten million in 2007 for the NY/PHI region, which is larger than the risk from flying (4.52 in one

hundred million).

5.1 References

BC McDonald, AH Goldstein, and RA Harley. Long-term trends in california mobile source emissions and ambient concentrations of black carbon and organic aerosol. Environ. Sci. Technol., 49(8):5178–5188, 2015.

US EPA. Control of air pollution from new motor vehicles: Heavy-duty engine and vehicle standards and highway diesel fuel sulfur control requirements. U.S. Environmental Protection Agency, Washington, DC, 2001. URL `http://www.gpo.gov/fdsys/pkg/FR-2001-01-18/pdf/01-2.pdf`.

US EPA. Second report to congress: Highlights of the diesel emissions reduction program. U.S. Environmental Protection Agency, Washington, DC, 2012. URL `http://www.epa.gov/cleandiesel/documents/420r12031.pdf`.

Chapter 6

Bibliography

- Environmental Benefits and Mapping Program (BenMAP, Version 4.0.67). Abt Associates, Inc., 2013. Bethesda, MD.

- SD Adar, DR Gold, BA Coull, J Schwartz, PH Stone, and H Suh. Focused exposures to airborne traffic particles and heart rate variability in the elderly. Epidemiology, 18(1): 95–103, January 2007.

- AECOM, Cambridge Systematics, and Arellano Associates. 2013 California State Rail Plan. AECOM, Oakland, CA, 2013. URL `http://californiastaterailplan.dot.ca.gov/docs/Final_Copy_2013_CSRP.pdf`.

- AS Ahmad, N Ormiston-Smith, and PD Sasieni. Trends in the lifetime risk of developing cancer in Great Britain: comparison of risk for those born from 1930 to 1960. British Journal of Cancer, 112(5):943–947, 2015.

- BA Albrecht. Aerosols, cloud microphysics, and fractional cloudiness. Science, 245(4923): 1227–1230, 1989.

- SC Anenberg, LW Horowitz, DQ Tong, and JJ West. An estimate of the global burden of anthropogenic ozone and fine particulate matter on premature human mortality using atmospheric modeling. Environ. Health Perspect., 118(9):1189–1195, April 2010.

- SC Anenberg, K Talgo, S Arunachalam, P Dolwick, C Jang, and JJ West. Impacts of global, regional, and sectoral black carbon emission reductions on surface air quality and human mortality. Atmos. Chem. Phys., 11(14):7253–7267, 2011.

- SC Anenberg, J Schwartz, D Shindell, M Amann, G Faluvegi, Z Klimont, G Janssens-Maenhout, L Pozzoli, R Van Dingenen, E Vignati, L Emberson, NZ Muller, JJ West, M Williams, V Demkine, WK Hicks, J Kuylenstierna, F Raes, and V Ramanathan. Global air quality and health co-benefits of mitigating near-term climate change through methane and black carbon emission controls. Environ. Health Perspect., 120(6):831–839, June 2012.

- KW Appel, AB Gilliland, G Sarwar, and RC Gilliam. Evaluation of the Community Multiscale Air Quality (CMAQ) model version 4.5: Sensitivities impacting model performance part I - Ozone. Atmos. Environ., 41(40):9603–9615, 2007.

- SE Bauer and S Menon. Aerosol direct, indirect, semidirect, and surface albedo effects from sector contributions based on the IPCC AR5 emissions for preindustrial and present-day conditions. J. Geophys. Res.: Atmos., 117:D01206, 2012.

- R Beelen, G Hoek, PA van den Brandt, RA Goldbohm, P Fischer, LJ Schouten, M Jerrett, E Hughes, B Armstrong, and B Brunekreef. Long-term effects of traffic-related air pollution on mortality in a Dutch cohort (NLCS-AIR study). Environ. Health Perspect., 116 (2):196–202, November 2007.

- ML Bell and F Dominici. Effect modification by community characteristics on the short-term effects of ozone exposure and mortality in 98 US communities. Am. J. Epidemiol., 167(8): 986–997, 2008.

- ML Bell, K Ebisu, RD Peng, JM Samet, and F Dominici. Hospital admissions and chemical composition of fine particle air pollution. Am. J. Respir. Crit. Care Med., 179(12):1115–1120, June 2009.

- P Bergamaschi, C Frankenberg, JF Meirink, M Krol, MG Villani, S Houweling, F Dentener, EJ Dlugokencky, JB Miller, and LV Gatti. Inverse modeling of global and regional CH4 emissions using SCIAMACHY satellite retrievals. J. Geophys. Res.: Atmos., 114(D22): D22301, 2009.

- FS Binkowski and SJ Roselle. Models-3 Community Multiscale Air Quality (CMAQ) model aerosol component - 1. Model description. J. Geophys. Res.: Atmos., 108:–, 2003.

- TC Bond. Can warming particles enter global climate discussions? Environ. Res. Letters, 2 (4), 2007.

- TC Bond, SJ Doherty, DW Fahey, PM Forster, T Berntsen, BJ DeAngelo, MG Flanner, S Ghan, B Kärcher, and D Koch. Bounding the role of black carbon in the climate system: A scientific assessment. J. Geophys. Res.: Atmos., 118(11):5380–5552, 2013.

- M Brauer, M Amann, RT Burnett, A Cohen, F Dentener, M Ezzati, SB Henderson, M Krzyzanowski, RV Martin, R Van Dingenen, A van Donkelaar, and GD Thurston. Exposure assessment for estimation of the global burden of disease attributable to outdoor air pollution. Environ. Sci. Technol., 46(2):652–660, January 2012.

- D Byun and KL Schere. Review of the governing equations, computational algorithms, and other components of the Models-3 Community Multiscale Air Quality (CMAQ) modeling system. Appl. Mech. Rev., 59(1/6):51, 2006.

- F Caiazzo, A Ashok, IA Waitz, SHL Yim, and SRH Barrett. Air pollution and early deaths in the United States. Part I: Quantifying the impact of major sectors in 2005. Atmos. Environ., 79(198-208), 2013.

- SL Capps, DK Henze, A Hakami, AG Russell, and A Nenes. ANISORROPIA: the adjoint of the aerosol thermodynamic model ISORROPIA. Atmos. Chem. Phys., 11(8):23469–23511, 2011.

- T Chai, GR Carmichael, Y Tang, A Sandu, A Heckel, A Richter, and JP Burrows. Regional NOx emission inversion through a four-dimensional variational approach using SCIAMACHY tropospheric NO2 column observations. Atmos. Environ., 43(32):5046–5055, 2009.

- CJ Coats and MR Houyoux. Fast emissions modeling with the sparse matrix operator kernel emissions modeling system. In The Emissions Inventory: Key to Planning, Permits, Compliance, and Reporting, New Orleans, LA, 1996.

- AJ Cohen, HR Anderson, B Ostro, KD Pandey, M Krzyzanowski, N Kuenzli, K Gutschmidt, CA Pope, I Romieu, JM Samet, and KR Smith. Comparative Quantification of Health Risks, volume 2, chapter 17, pages 1353–1433. World Health Organization, European Centre for Environment and Health, Bonn Office, 2004a. URL `http://www.who.int/publications/cra/chapters/volume2/1353-1434.pdf?ua=1`.

- AJ Cohen, HR Anderson, B Ostro, KD Pandey, M Krzyzanowski, N Kuenzli, K Gutschmidt, CA Pope, I Romieu, JM Samet, and KR Smith. Mortality impacts of urban air pollution. In Majid Ezzati, AD Lopez, A Rodgers, and C Murray, editors, Comparative Quantification of Health Risks: Global and Regional Burden of Disease Due to Selected Major Risk Factors, Vol. 2. World Health Organization, Geneva, 2004b.

- AJ Cohen, HR Anderson, B Ostro, KD Pandey, M Krzyzanowski, N Kunzli, K Gutschmidt, A Pope, I Romieu, JM Samet, and K Smith. The global burden of disease due to outdoor air pollution. J. Toxicol. Environ. Health, 68(13-14):1301–1307, 2005.

- Consumer Product Safety Commission. An overview of the bicycle study. URL `http://www.cpsc.gov//PageFiles/112701/344.pdf`.

- TR Dallmann and RA Harley. Evaluation of mobile source emission trends in the United States. J. Geophys. Res.: Atmos., 115, 2010.

- IC Dedoussi and SRH Barrett. Air pollution and early deaths in the United States. Part II: Attribution of PM2.5 exposure to emissions species, time, location and sector. Atmos. Environ., 99(C):610–617, December 2014.

- O Dubovik, T Lapyonok, YJ Kaufman, M Chin, P Ginoux, RA Kahn, and A Sinyuk. Retrieving global aerosol sources from satellites using inverse modeling. Atmos. Chem. Phys., 8(2):209–250, 2008.

- H Elbern, H Schmidt, O Talagrand, and A Ebel. 4d-variational data assimilation with an adjoint air quality model for emission analysis. Environ. Modell. Softw., 15(6-7):539–548, 2000.

- J Ewer, ER Galea, M Patel, S Taylor, B Knight, and M Petridis. SMARTFIRE: an intelligent CFD based fire model. J. Fire Protect. Eng., 10(1):13–27, 1999.

- N Fann, CM Fulcher, and BJ Hubbell. The influence of location, source, and emission type in estimates of the human health benefits of reducing a ton of air pollution. Air Qual., Atmos. Health, 2(3):169–176, 2009. doi: 10.1007/s11869-009-0044-0.

- N Fann, HA Roman, CM Fulcher, MA Gentile, BJ Hubbell, K Wesson, and JI Levy. Maximizing health benefits and minimizing inequality: Incorporating local-scale data in the design and evaluation of air quality policies. Risk Analysis, 31(6):908–922, June 2011.

- N Fann, KR Baker, and CM Fulcher. Characterizing the PM2.5-related health benefits of emission reductions for 17 industrial, area and mobile emission sectors across the U.S. Environ. Int., 49(C):141–151, November 2012a.

- N Fann, AD Lamson, SC Anenberg, K Wesson, D Risley, and BJ Hubbell. Estimating the national public health burden associated with exposure to ambient PM2.5 and ozone. Risk Analysis, 32(1):81–95, January 2012b.

- N Fann, CM Fulcher, and K Baker. The recent and future health burden of air aollution apportioned across U.S. sectors. Environ. Sci. Technol., 47(8):3580–3589, April 2013.

- EJ Feuer, LM Wun, CC Boring, WD Flanders, MJ Timmel, and T Tong. The lifetime risk of developing breast-cancer. Journal of the National Cancer Institute, 85(11):892–897, 1993.

- M M Finkelstein, M Jerrett, and M R Sears. Traffic air pollution and mortality rate advancement periods. Am. J. Epidemiol., 160(2):173–177, July 2004.

- MM Finkelstein. Environmental inequality and circulatory disease mortality gradients. J. Epidemiol. Commun. H., 59(6):481–487, June 2005.

- MM Finkelstein, M Jerrett, P DeLuca, N Finkelstein, DK Verma, K Chapman, and MR Sears. Relation between income, air pollution and mortality: a cohort study. Can. Med. Assoc. J., 169(5):397–402, 2003.

- EM Flachs, J Sørensen, J Bønløkke, and H Brønnum-Hansen. Population dynamics and air pollution: the impact of demographics on health impact assessment of air pollution. J. Environ. Public Health., 2013(6):1–12, 2013.

- JB Flanagan, RKM Jayanty, EE Rickman, and MR Peterson. PM2.5 speciation trends network: Evaluation of whole-system uncertainties using data from sites with collocated samplers. J. Air Waste Manage., 56(4):492–499, April 2006.

- MG Flanner, CS Zender, JT Randerson, and PJ Rasch. Present-day climate forcing and response from black carbon in snow. J. Geophys. Res.: Atmos., 112(D11), June 2007.

- C Fountoukis and A Nenes. ISORROPIA II: A computationally efficient thermodynamic equilibrium model for K+–Ca 2+–Mg 2+–NH 4+–Na+–SO 4 2–NO 3–Cl–H 2 O aerosols. Atmos. Chem. Phys., 7(17):4639–4659, 2007.

- EM Fujita, DE Campbell, B Zielinska, JC Chow, CE Lindhjem, A DenBleyker, GA Bishop, BG Schuchmann, DH Stedman, and DR Lawson. Comparison of the MOVES2010a, MOBILE6.2, and EMFAC2007 mobile source emission models with on-road traffic tunnel and remote sensing measurements. J. Air Waste Manage., 62(10):1134–1149, October 2012.

- WJ Gauderman, F Gilliland, H Vora, E Avol, and D Stram. Association between air pollution and lung function growth in southern California children: Results from a second cohort. Am. J. Respir. Crit. Care Med., 166:76–84, June 2002.

- U Gehring, J Heinrich, U Krmer, V Grote, M Hochadel, D Sugiri, M Kraft, K Rauchfuss, GH Eberwein, and HE Wichmann. Long-term exposure to ambient air pollution and cardiopulmonary mortality in women. Epidemiology, 17(5):545–551, September 2006.

- TJ Grahame, R Klemm, and RB Schlesinger. Public health and components of particulate matter: The changing assessment of black carbon. J. Air Waste Manage., 64(6):620–660, May 2014.

- A Hakami, DK Henze, JH Seinfeld, T Chai, Y Tang, GR Carmichael, and A Sandu. Adjoint inverse modeling of black carbon during the asian pacific regional aerosol characterization experiment. J. Geophys. Res.: Atmos., 110(D14301), 2005.

- A Hakami, JH Seinfeld, T Chai, Y Tang, GR Carmichael, and A Sandu. Adjoint sensitivity analysis of ozone nonattainment over the continental United States. Environ. Sci. Technol., 40(12):3855–3864, June 2006.

- A Hakami, DK Henze, JH Seinfeld, K Singh, A Sandu, S Kim, D Byun, and Q Li. The adjoint of CMAQ. Environ. Sci. Technol., 41(22):7807–7817, 2007.

- SL Hallmark, R Guensler, and I Fomunung. Characterizing on-road variables that affect passenger vehicle modal operation. Transport. Res. D-Tr. E., 7(2):81–98, 2002.

- J Hansen. Efficacy of climate forcings. J. Geophys. Res.: Atmos., 110(D18):D18104, 2005.

- J Hansen, M Sato, and R Ruedy. Radiative forcing and climate response. J. Geophys. Res.: Atmos., 102(D6):6831, March 1997.

- M He, J Zheng, S Yin, and Y Zhang. Trends, temporal and spatial characteristics, and uncertainties in biomass burning emissions in the Pearl River Delta, China. Atmos. Environ., 45(24):4051–4059, August 2011.

- DK Henze, JH Seinfeld, W Liao, A Sandu, and GR Carmichael. Inverse modeling of aerosol dynamics: Condensational growth. J. Geophys. Res.: Atmos., 109(D14), 2004.

- DK Henze, A Hakami, and JH Seinfeld. Development of the adjoint of GEOS-Chem. Atmos. Chem. Phys., 7(9):2413–2433, 2007.

- DK Henze, JH Seinfeld, and DT Shindell. Inverse modeling and mapping US air quality influences of inorganic PM 2.5 precursor emissions using the adjoint of GEOS-Chem. Atmos. Chem. Phys., 9(16):5877–5903, 2009.

- N Howlader, AM Noone, M Krapcho, J Garshell, D Miller, SF Altekruse, CL Kosary, M Yu, J Ruhl, Z Tatalovich, A Mariotto, DR Lewis, HS Chen, EJ Feuer, and KA Cronin, editors. SEER Cancer Statistics Review, 1975-2011. National Cancer Institute, Bethesda, MD, April 2014. URL `http://seer.cancer.gov/csr/1975_2011/`.

- Y Hu, MT Odman, and AG Russell. Top-down analysis of the elemental carbon emissions inventory in the United States by inverse modeling using Community Multiscale Air Quality model with decoupled direct method (CMAQ-DDM). J. Geophys. Res.: Atmos., 114 (D24), December 2009.

- B Hubbell. Understanding urban exposure environments: new research directions for informing implementation of us air quality standards. Air Qual., Atmos. Health, 5(2):259–267, June 2012.

- S Humbert, JD Marshall, S Shaked, JV Spadaro, Y Nishioka, P Preiss, TE McKone, A Horvath, and O Jolliet. Intake fraction for particulate matter: Recommendations for life cycle impact assessment. Environ. Sci. Technol., 45(11):4808–4816, 2011.

- N Huneeus, O Boucher, and F Chevallier. Simplified aerosol modeling for variational data assimilation. Geosci. Model Dev., 2(2):213–229, 2009.

- MZ Jacobson. Control of fossil-fuel particulate black carbon and organic matter, possibly the most effective method of slowing global warming. J. Geophys. Res.: Atmos., 107(D19): 4410, 2002.

- MZ Jacobson. Short-term effects of controlling fossil-fuel soot, biofuel soot and gases, and methane on climate, Arctic ice, and air pollution health. J. Geophys. Res.: Atmos., 115, 2010.

- NAH Janssen, G Hoek, M Simic-Lawson, P Fischer, L van Bree, H ten Brink, M Keuken, RW Atkinson, HR Anderson, B Brunekreef, and FR Cassee. Black carbon as an additional indicator of the adverse health effects of airborne particles compared with PM10 and PM2. 5. Environ. Health Perspect., 119(12):1691–1699, August 2011.

- DO Johns, LW Stanek, K Walker, S Benromdhane, B Hubbell, M Ross, RB Devlin, DL Costa, and DS Greenbaum. Practical advancement of multipollutant scientific and aisk assessment approaches for ambient air pollution. Environ. Health Perspect., 120(9): 1238–1242, September 2012.

- K Katanoda, T Sobue, H Satoh, K Tajima, T Suzuki, H Nakatsuka, T Takezaki, T Nakayama, H Nitta, K Tanabe, and S Tominaga. An association between long-term exposure to ambient air pollution and mortality from lung cancer and respiratory diseases in japan. J. Epidemiol., 21(2):132–143, 2011.

- I Kazuhiko, R Mathes, Z Ross, A Nádas, G Thurston, and T Matte. Fine particulate matter constituents associated with cardiovascular hospitalizations and mortality in New York City. Environ. Health Perspect., 119(4):467, April 2011.

- D Koch, M Schulz, S Kinne, C McNaughton, JR Spackman, Y Balkanski, S Bauer, T Berntsen, TC Bond, O Boucher, M Chin, A Clarke, N De Luca, F Dentener, T Diehl, O Dubovik, R Easter, D W Fahey, J Feichter, D Fillmore, S Freitag, S Ghan, P Ginoux, S Gong, L Horowitz, T Iversen, A Kirkevag, Z Klimont, Y Kondo, M Krol, X Liu, R Miller, V Montanaro, N Moteki, G Myhre, JE Penner, J Perlwitz, G Pitari, S Reddy, L Sahu, H Sakamoto, G Schuster, JP Schwarz, O Seland, P Stier, N Takegawa, T Takemura, C Textor, JA van Aardenne, and Y Zhao. Evaluation of black carbon estimations in global aerosol models. Atmos. Chem. Phys., 9(22):9001–9026, 2009.

- J Koo, Q Wang, DK Henze, IA Waitz, and SRH Barrett. Spatial sensitivities of human health risk to intercontinental and high-altitude pollution. Atmos. Environ., 71:140–147, June 2013.

- D Krewski, M Jerrett, RT Burnett, R Ma, E Hughes, Y Shi, MC Turner, CA Pope, G Thurston, EE Calle, MJ Thun, B Beckerman, P DeLuca, N Finkelstein, K Ito, DK Moore, KB Newbold, T Ramsay, Z Ross, H Shin, and B Tempalski. Extended follow-up and spatial analysis of the American Cancer Society study linking particulate air pollution and mortality. Technical Report HEI Research Report 140, Health Effects Institute, Boston, Mass., USA, 2009. URL `http://ephtracking.cdc.gov/docs/RR140-Krewski.pdf`.

- J Kurokawa, K Yumimoto, I Uno, and T Ohara. Adjoint inverse modeling of NOx emissions over eastern China using satellite observations of NO2 vertical column densities. Atmos. Environ., 43(11):1878–1887, 2009.

- F Laden, J Schwartz, F E Speizer, and D W Dockery. Reduction in fine particulate air pollution and mortality - Extended follow-up of the Harvard six cities study. American Journal Of Respiratory And Critical Care Medicine, 173(6):667–672, 2006.

- K Lapina, DK Henze, JB Milford, M Huang, M Lin, AM Fiore, GR Carmichael, GG Pfister, and K Bowman. Assessment of source contributions to seasonal vegetative exposure to ozone in the US. J. Geophys. Res.: Atmos., 119(1):324–340, 2014.

- C Lee, R Martin, DK Henze, M Brauer, A Cohen, and A van Donkelaar. Response of global particulate-matter-related mortality to changes in local precursor emissions. Environ. Sci. Technol., 49(7):4335–4344, 2015. doi: 10.1021/acs.est.5b00873.

- J Lepeule, F Laden, D Dockery, and J Schwartz. Chronic exposure to fine particles and mortality: an extended follow-up of the Harvard Six Cities study from 1974 to 2009. Environ. Health Perspect., 120(7):965–970, July 2012.

- JI Levy, SK Wolff, and JS Evans. A regression-based approach for estimating primary and secondary particulate matter intake fractions. Risk Analysis, 22(5):895–904, October 2002.

- JI Levy, LK Baxter, and J Schwartz. Uncertainty and variability in health-related damages from coal-fired power plants in the United States. Risk Analysis, 29(7):1000–1014, 2009.

- Y Li, DK Henze, D Jack, and PL Kinney. The influence of air quality model resolution on health impact assessment for fine particulate matter and its components. Air Qual., Atmos. Health, 2015.

- V Mallet and B Sportisse. Uncertainty in a chemistry-transport model due to physical parameterizations and numerical approximations: An ensemble approach applied to ozone modeling. J. Geophys. Res.: Atmos., 11(1), 2006.

- WC Malm, BA Schichtel, ML Pitchford, LL Ashbaugh, and RA Eldred. Spatial and monthly trends in speciated fine particle concentration in the United States. J. Geophys. Res.: Atmos., 109(D3), 2004.

- PT Martien and RA Harley. Adjoint sensitivity analysis for a three-dimensional photochemical model: Implementation and method comparison. Environ. Sci. Technol., 40(8): 2663–2670, 2006.

- BC McDonald, AH Goldstein, and RA Harley. Long-term trends in california mobile source emissions and ambient concentrations of black carbon and organic aerosol. Environ. Sci. Technol., 49(8):5178–5188, 2015.

- MR Mebust, BK Eder, FS Binkowski, and SJ Roselle. Models-3 Community Multiscale Air Quality (CMAQ) model aerosol component - 2. Model evaluation. J. Geophys. Res.: Atmos., 108:–, 2003.

- GA Mensah, AH Mokdad, ES Ford, KJ Greenlund, and JB Croft. State of disparities in cardiovascular health in the United States. Circulation, 111(10):1233–1241, 2005.

- SM Mesbah, A Hakami, and S Schott. Optimal ozone reduction policy design using adjoint-based NOx marginal damage information. Environ. Sci. Technol., 47(23):13528–13535, 2013.

- NZ Muller and R Mendelsohn. Measuring the damages of air pollution in the United States. J. Environ. Econ. Manage., 54(1):1–14, 2007.

- NZ Muller and R Mendelsohn. Efficient pollution regulation: getting the prices right. Am. Econ. Rev., pages 1714–1739, 2009.

- NZ Muller, R Mendelsohn, and W Nordhaus. Environmental accounting for pollution in the United States economy. Am. Econ. Rev., 101(5):1649–1675, August 2011.

- G Myhre, D Shindell, FM Bréon, W Collins, J. Fuglestvedt, J Huang, D Koch, JF Lamarque, D Lee, B Mendoza, T Nakajima, A Robock, G Stephens, T Takemura, and H Zhang. Climate Change 2013: The Physical Science Basis. Contribution of Working Group I to the Fifth Assessment Report of the Intergovernmental Panel on Climate Change, chapter Anthropogenic and Natural Radiative Forcing. Cambridge University Press, Cambridge, United Kingdom and New York, NY, USA, 2013.

- NAS. Hidden costs of energy: Unpriced consequences of energy production and use. Technical report, National Research Council Committee on Health, Environmental, and Other External Costs and Benefits of Energy Production and Consumption, The National Academies Press, Washington, DC, 2010. URL `http://www.nap.edu/catalog/12794/hidden-costs-of-energy-unpriced-consequences-of-energy-production-and`.

- MJ Neidell. Air pollution, health, and socio-economic status: the effect of outdoor air quality on childhood asthma. J. Health Econ., 23(6):1209–1236, 2004.

- AJ Pappin and A Hakami. Attainment vs exposure: Ozone metric responses to source-specific nox controls using adjoint sensitivity analysis. Environ. Sci. Technol., 47(23): 13519–13527, December 2013a.

- AJ Pappin and A Hakami. Source attribution of health benefits from air pollution abatement in Canada and the United States: an adjoint sensitivity analysis. Environ. Health Perspect., 121(5):572–579, May 2013b.

- RD Peng, ML Bell, AS Geyh, A McDermott, SL Zeger, JM Samet, and F Dominici. Emergency admissions for cardiovascular and respiratory diseases and the chemical composition of fine particle air pollution. Environ. Health Perspect., 117(6):957–963, February 2009.

- TE Pierce and T Waldruff. PC-BEIS: A personal computer version of the biogenic emissions inventory system. J. Air Waste Manage., 41(7):937–941, 1991.

- E Pisoni, C Carnevale, and M Volta. Sensitivity to spatial resolution of modeling systems designing air quality control policies. Environ. Modell. Softw., 25(1):66–73, January 2010.

- JE Pleim. A combined local and nonlocal closure model for the atmospheric boundary layer. Part I: Model description and testing. J. Appl. Meteorol., 46(9):1383–1395, September 2007.

- CA Pope, RT Burnett, MJ Thun, EE Calle, D Krewski, K Ito, and GD Thurston. Lung cancer, cardiopulmonary mortality, and long-term exposure to fine particulate air pollution. J. Am. Med. Assoc., 287(9):1132–1141, 2002.

- CA Pope, RT Burnett, GD Thurston, MJ Thun, EE Calle, D Krewski, and JJ Godleski. Cardiovascular mortality and long-term exposure to particulate air pollution - epidemiological evidence of general pathophysiological pathways of disease. Circulation, 109(1): 71–77, 2004.

- G Pouliot, E Wisner, and D Mobley. Quantification of emission factor uncertainty. J. Air Waste Manage., 62(3):287–298, 2012.

- MC Power, MG Weisskopf, and SE Alexeeff. Traffic-related air pollution and cognitive function in a cohort of older men. Environ. Health Perspect., 119(5):682–687, 2011.

- RC Puett, JE Hart, JD Yanosky, C Paciorek, J Schwartz, H Suh, FE Speizer, and F Laden. Chronic fine and coarse particulate exposure, mortality, and coronary heart disease in the Nurses' Health Study. Environ. Health Perspect., 117(11):1697–1701, June 2009.

- EM Punger and JJ West. The effect of grid resolution on estimates of the burden of ozone and fine particulate matter on premature mortality in the USA. Air Qual., Atmos. Health, 6(3):563–573, May 2013.

- L Qiao, J Cai, H Wang, W Wang, M Zhou, S Lou, R Chen, H Dai, C Chen, and H Kan. PM2.5 constituents and hospital emergency-room visits in Shanghai, China. Environ. Sci. Technol., 48(17):10406–10414, 2014.

- A Sandu, DN Daescu, GR Carmichael, and T Chai. Adjoint sensitivity analysis of regional air quality models. J. Comput. Phys., 204(1):222–252, 2005a.

- A Sandu, W Liao, GR Carmichael, DK Henze, and JH Seinfeld. Inverse modeling of aerosol dynamics using adjoints: Theoretical and numerical considerations. Aerosol Sci. Technol., 39(8):677–694, 2005b.

- W Schroeder, E Prins, L Giglio, I Csiszar, C Schmidt, J Morisette, and D Morton. Validation of GOES and MODIS active fire detection products using ASTER and ETM plus data. Remote Sensing of Environment, 112(5):2711–2726, 2008.

- JH Seinfeld and SN Pandis. Atmospheric Chemistry and Physics: From Air Pollution to Climate Change. John Wiley & Sons, Inc., Hoboken, New Jersey, 2nd edition, 2006.

- L. Seirup and G. Yetman. U.S. Census Grids (Summary File 3), 2000, May 2015. URL `http://dx.doi.org/10.7927/H42R3PMN`.

- D Shindell, JCI Kuylenstierna, E Vignati, R Van Dingenen, M Amann, Z Klimont, SC Anenberg, NZ Muller, G Janssens-Maenhout, F Raes, J Schwartz, G Faluvegi, L Pozzoli, K Kupiainen, L Hoeglund-Isaksson, L Emberson, D Streets, V. Ramanathan, K Hicks, NTK Oanh, G Milly, M Williams, V Demkine, and D Fowler. Simultaneously mitigating near-term climate change and improving human health and food security. Science, 335(6065): 183–189, 2012.

- RA Silva, JJ West, Y Zhang, SC Anenberg, JF Lamarque, DT Shindell, WJ Collins, S Dalsoren, G Faluvegi, G Folberth, LW Horowitz, T Nagashima, V Naik, S Rumbold, R Skeie, K Sudo, T Takemura, D Bergmann, P Cameron-Smith, I Cionni, RM Doherty, V Eyring, B Josse, IA MacKenzie, D Plummer, M Righi, DS Stevenson, S Strode, S Szopa, and G Zeng. Global premature mortality due to anthropogenic outdoor air pollution and the contribution of past climate change. Environ. Res. Lett., 8(3), 2013.

- M Sivak, DJ Weintraub, and M Flannagan. Nonstop flying is safer than driving. Risk Analysis, 11(1):145–148, March 1991.

- WC Skamarock, JB Klemp, J Dudhia, DO Gill, DM Barker, W Wang, and JG Powers. A Description of the Advanced Research WRF Version 2. Technical report, National Center for Atmospheric Research (NCAR), Boulder, CO, USA, 2005. URL `http://www2.mmm.ucar.edu/wrf/users/docs/arw_v2_070111.pdf`.

- W Squire and G Trapp. Using complex variables to estimate derivatives of real functions. Siam Review, 40(1):110–112, March 1998.

- S Stevenson, FJ Dentener, and MG Schultz. Multimodel ensemble simulations of present-day and near-future tropospheric ozone. J. Geophys. Res.: Atmos., 111(D08301), 2006.

- JG Su, R Morello-Frosch, BM Jesdale, AD Kyle, B Shamasunder, and M Jerrett. An index for assessing demographic inequalities in cumulative environmental hazards with application to Los Angeles, California. Environ. Sci. Technol., 43(20):7626–7634, 2009.

- HH Suh and A Zanobetti. Exposure error masks the relationship between traffic-related air pollution and heart rate variability. J. Occup. Environ. Med., 52(7):685–692, July 2010.

- M Tainio, JT Tuomisto, J Pekkanen, N Karvosenoja, K Kupiainen, P Porvari, M Sofiev, A Karppinen, L Kangas, and J Kukkonen. Uncertainty in health risks due to anthropogenic primary fine particulate matter from different source types in Finland. Atmos. Environ., 44(17):2125–2132, June 2010.

- TM Thompson and NE Selin. Influence of air quality model resolution on uncertainty associated with health impacts. Atmos. Chem. Phys., 12(20):9753–9762, 2012.

- T Tietenberg. Tradeable permits for pollution control when emission location matters: What have we learned? Environmental and Resource Economics, 1995.

- MD Turner, DK Henze, A Hakami, S Zhao, J Resler, GR Carmichael, CO Stanier, J Baek, A Sandu, AG Russell, A Nenes, G Jeong, SL Capps, PB Percell, RW Pinder, SL Napelenok, JO Bash, and T Chai. Sector-specific health impacts of BC emissions in six urban US regions. In Prep, 2015a.

- MD Turner, DK Henze, A Hakami, S Zhao, J Resler, GR Carmichael, CO Stanier, J Baek, A Sandu, AG Russell, A Nenes, GR Jeong, SL Capps, PB Percell, RW Pinder, SL Napelenok, JO Bash, and T Chai. Differences between magnitudes and health impacts of BC emissions across the United States using 12 km scale seasonal source apportionment. Environ. Sci. Technol., 49(7):4362–4371, 2015b. doi: 10.1021/es505968b.

- S Twomey. Pollution and planetary albedo. Atmos. Environ., 8(12):1251–1256, 1974.

- US EPA. Control of air pollution from new motor vehicles: Heavy-duty engine and vehicle standards and highway diesel fuel sulfur control requirements. U.S. Environmental Protection Agency, Washington, DC, 2001. URL `http://www.gpo.gov/fdsys/pkg/FR-2001-01-18/pdf/01-2.pdf`.

- US EPA. Integrated Science Assessment for Particulate Matter. Technical report, U.S. Environmental Protection Agency: National Center for Environmental Assessment, Washington, DC, December 2009. URL `http://www.epa.gov/ncea/pdfs/partmatt/Dec2009/PM_ISA_full.pdf`.

- US EPA. Benefits and Costs of the Clean Air Act from 1990 To 2020. Technical report, U.S. Environmental Protection Agency: Office of Air and Radiation, March 2011a. URL http://www.epa.gov/cleanairactbenefits/prospective2.html.

- US EPA. Meteorological model performance for annual 2007 simulations. Technical report, U.S. Environmental Protection Agency: Office of Air Quality Planning and Standards, Research Triangle Park, NC, USA, 2011b. URL http://epa.gov/ttn/scram/reports/EPA-454_R-11-007.pdf.

- US EPA. Report to Congress on Black Carbon. Technical report, U.S. Environmental Protection Agency, Washington, DC, March 2012a. URL http://www.epa.gov/blackcarbon/2012report/fullreport.pdf.

- US EPA. Second report to congress: Highlights of the diesel emissions reduction program. U.S. Environmental Protection Agency, Washington, DC, 2012b. URL http://www.epa.gov/cleandiesel/documents/420r12031.pdf.

- US EPA. Air quality modeling technical support document for the regulatory impact analysis for the revisions to the national ambient air quality standards for particulate matter. Technical report, U.S. Environmental Protection Agency: Office of Air Quality Planning and Standards, Research Triangle Park, NC, USA, December 2012c. URL http://www.epa.gov/ttn/naaqs/standards/pm/data/201212aqm.pdf.

- US EPA. Technical Support Document (TSD): Preparation of Emissions Inventories for the Version 5.0, 2007 Emissions Modeling Platform. Technical report, U.S. Environmental Protection Agency: Office of Air and Radiation, Research Triangle Park, NC, USA, September 2013. URL http://epa.gov/ttn/chief/emch/2007v5/2007v5_2020base_EmisMod_TSD_13dec2012.pdf.

- TPC van Noije, HJ Eskes, FJ Dentener, DS Stevenson, K Ellingsen, MG Schultz, O Wild, M Amann, CS Atherton, DJ Bergmann, I Bey, KF Boersma, T Butler, J Cofala, J Drevet, AM Fiore, M Gauss, DA Hauglustaine, LW Horowitz, ISA Isaksen, MC Krol, JF Lamarque, MG Lawrence, RV Martin, V Montanaro, JF Muller, G Pitari, MJ Prather, JA Pyle, A Richter, JM Rodriguez, NH Savage, SE Strahan, K Sudo, S Szopa, and M van Roozendael. Multi-model ensemble simulations of tropospheric no_2 compared with gome retrievals for the year 2000. Atmos. Chem. Phys., 6(10):2943–2979, 2006.

- K Wesson, N Fann, M Morris, T Fox, and B Hubbell. A multi-pollutant, risk-based approach to air quality management: Case study for detroit. Atmospheric Pollution Research, 1(4): 296–304, October 2010.

- A Westman and U Björnstig. Fatalities in swedish skydiving. Accident Analysis & Prevention, 37(6):1040–1048, November 2005.

- WHO. Health risks of particulate matter from long-range transboundary air pollution. Technical report, World Health Organization Regional Office of Europe, Copenhagen, 2006. URL http://www.euro.who.int/__data/assets/pdf_file/0006/78657/E88189.pdf.

- WHO. Health effects of black carbon. Technical report, World Health Organization, European Centre for Environment and Health, Bonn Office, April 2012. URL `http://www.euro.who.int/__data/assets/pdf_file/0004/162535/e96541.pdf`.

- M Wilhelm, L Qian, and B Ritz. Outdoor air pollution, family and neighborhood environment, and asthma in LA FANS children. Health Place, 15(1):25–36, March 2009.

- EH Wilker, MA Mittleman, BA Coull, A Gryparis, ML Bots, J Schwartz, and D Sparrow. Long-term exposure to black carbon and carotid intima-media thickness: the Normative Aging Study. Environ. Health Perspect., 121(9):1061–1067, September 2013a.

- EH Wilker, E Mostofsky, SH Lue, D Gold, J Schwartz, GA Wellenius, and MA Mittleman. Residential proximity to high-traffic roadways and poststroke mortality. J. Stroke. Cerebrovasc. Dis., 22(8):e366–e372, November 2013b.

- Jianhua Xu, Xuesong Wang, and Shiqiu Zhang. Risk-based air pollutants management at regional levels. Environmental Science & Policy, 25:167–175, January 2013.

- S Zhao, AJ Pappin, SM Mesbah, JYJ Zhang, NL MacDonald, and A Hakami. Adjoint estimation of ozone climate penalties. Geophys. Res. Lett., 40(20):5559–5563, 2013.

- Y Zhou, JS Fu, G Zhuang, and JI Levy. Risk-based prioritization among air pollution control strategies in the Yangtze River delta, China. Environ. Health Perspect., 118(9):1204–1210, September 2010.

- L Zhu, DK Henze, KE Cady Pereira, MW Shephard, M Luo, RW Pinder, JO Bash, and GR Jeong. Constraining US ammonia emissions using TES remote sensing observations and the GEOSChem adjoint model. J. Geophys. Res.: Atmos., 118(8):3355–3368, April 2013. doi: 10.1002/jgrd.50166.